Universidade Nova de Lisboa

Maria Madalena Prazeres Vieira da Cruz Proença

Mestre em Engenharia Química e Bioquímica

PRODUCTION OF POLYHYDROXYALKANOATES FROM OIL-CONTAINING SUBSTRATES

Dissertação para obtenção do Grau de Doutor em Química Sustentável

Orientador: Doutrora Maria Filomena Andrade de Freitas, Investigadora do UCIBIO-REQUIMTE da Faculdade de Ciências e Tecnologia da Universidade Nova de Lisboa

Co-orientador: Prof. Doutora Maria Ascensão C.F. Miranda Reis, Professora Catedrática da Faculdade de Ciências e Tecnologia da Universidade Nova de Lisboa

Juri:

Presidente: Prof. Doutoura Elvira Maria Correia Fortunato

Arguentes: Doutor Bruno Sommer Ferreira

Doutor João Pedro Martins de Almeida Lopes

Vogais: Doutora Maria Catarina Marques Dias de Almeida

Doutora Catarina Silva Simão de Oliveira

Setembro, 2015

PRODUCTION OF POLYHYDROXYALKANOATES FROM OIL-CONTAINING SUBSTRATES

Aos meus amigos, à minha família e a Deus!

"O Homem é criado para louvar, reverenciar e servir a Deus Nosso Senhor, e mediante isso salvar a sua alma; e as outras coisas à face da terra são criadas para o Homem, para que o ajudem a conseguir o fim para que é criado. Donde se segue que há-de usar delas tanto quanto o ajudem a atingir o seu fim e há-de privar-se delas tanto quanto dele o afastem. Pelo que é necessário tornar-nos indiferentes a respeito de todas as coisas criadas em tudo aquilo que depende da escolha do nosso livre-arbítrio, e não lhe é proibido; de tal maneira que, da nossa parte, não queiramos mais saúde que doença, riqueza que pobreza, honra que desonra, vida longa que vida curta, e consequentemente em tudo mais; mas somente desejemos e escolhamos o que mais nos conduz para o fim para que somos criados."

Princípio e Fundamento, Santo Inácio de Loyola

Agradecimentos

Em primeiro lugar gostava de agradecer à minha orientadora Dra. Filomena, por todo o acompanhamento e amizade durante estes anos. Foi um privilégio trabalhar, aprender contigo e ter-te como orientadora. Não há orientadores nem orientandos perfeitos, mas há aqueles que fazem um esforço para cada vez serem e "servir" melhor o mundo da ciência. E tu pertences a esse grupo pessoas. Obrigada por todo o apoio na realização deste trabalho!

Um obrigada muito especial à minha co-orientadora Prof. Ascensão, por todos os conselhos, pela amizade, pelas ideias, por me ouvir e por me ter ajudado sempre a ultrapassar situações menos boas durante o meu doutoramento. Levo comigo muita e boa formação, tanto a nível pessoal como profissional também graças a si. Fui sem dúvida uma privilegiada na orientação que tive. Obrigada!

Queria agradecer também ao Alexandre Paiva, por toda a ajuda que me deu durante estes anos, deixando-me sempre à vontade para me juntar ao seu grupo fosse para trabalhar, fosse para nos divertirmos. São momentos como os que vivemos no nosso "*gang do tupperware* 427" que ficarão para sempre guardados na minha memória e coração.

Agradeço também às Professoras Ana Ramos e Madalena Dionísio e ao Professor Vitor Alves por todos os ensinamentos e ajuda durante estes anos. Foi um prazer colaborar e aprender convosco. Muito obrigada aos três!

Agradeço também ao Dr. João Lopes e Dra. Mafalda Sarraguça pela ajuda e ensinamentos preciosos na área do NIR e por terem facultado todas as ferramentas necessárias na realização deste trabalho. Gostei muito de trabalhar convosco! Obrigada.

Agradeço à cantina do departamento de Química pelo fornecimento do óleo usado, bem como aos fornecedores dos outros óleos com que trabalhei ao longo destes anos.

Um enorme obrigada ao Bioeng. É uma alegria olhar para trás e ver a quantidade de pessoas que me serviram de inspiração e que foram um bom exemplo para mim. Obrigada a todos! Não posso deixar de agradecer em especial, à ajuda da Diana Araújo, Inês Farinha e da Sílvia Antunes pelo "*babysitting*" aos meus ensaios durante estes anos todos.

A todas as pessoas dos meus dois "*gangs do tupperware*", 427 e membranas, um obrigada gigante pelos nossos almoços que foram sempre momentos de risota e descontração. Quantas vezes não recarreguei baterias em momentos como estes.

Um grande obrigada à minha querida e grande amiga, companheira em tudo, Rita. É tão bom ter alguém com quem partilhar as histórias de um doutoramento e que nos percebe a 100%. Obrigada pela tua amizade, ajuda e presença "naqueles" momentos críticos, que tu também conheces.

Às minhas amigas queridas que tantas vezes me ouviram a falar, cheias de paciência das aventuras deste trabalho e que mesmo não percebendo nada, me apoiaram sempre muito. Obrigada.

Á minha CVX, com quem faço caminho na vida cristã e que me ajuda sempre a encontrar Deus em tudo e em todos. Obrigada.

Á minha família e muito particularmente à Teresinha e à mãe Luísa, obrigada por tudo. Enchem-me sempre de força e de coragem. São exemplos muito fortes na minha vida.

Ao meu maridão João, por todo o apoio incondicional que sempre me deu durante estes anos. És um exemplo para mim e eu admiro-te muito.

A Deus, por me acompanhar sempre e por me dar tantas coisa boas nesta vida. Só posso agradecer!

Resumo

Diferentes substratos oleicos, nomeadamente óleo de cozinha usado (UCO), subproduto da produção de biodiesel que contém ácidos gordos (FAB) e deodestilado subproduto da produção de azeite (OODD) foram testados como fontes de carbono de baixo custo para a produção de polihidroxialcanoatos (PHA), utilizando doze estirpes bacterianas, em ensaios em descontínuo. O OODD e o FAB foram explorados pela primeira vez como substratos alternativos na produção de PHA. Entre as estirpes de bactérias testadas, *Cupriavidus necator* e e *Pseudomonas resinovorans* demonstraram os resultados mais promissores produzindo poli-3-hidroxibutirato, P(3HB) a partir de UCO e OODD e um *mcl*-PHA composto maioritariamente por monómeros de 3-hidroxioctanoato (3HO) e 3-hidroxidecanoato (3HD) a partir de OODD, respectivamente. Posteriormente, estas estirpes bacterianas foram cultivadas em biorreactor.

C. necator foi cultivada em biorreator utilizando UCO como fonte de carbono. Foram utilizadas diferentes estratégias de alimentação, ou seja, em descontínuo, alimentação exponencial e DO-stat. A maior produtividade global de PHA (12.6±0.78 g L^{-1} dia^{-1}) foi obtida utilizando o modo DO-stat como estratégia de alimentação. Aparentemente, os diferentes modos de alimentação não tiveram impacto nas propriedades térmicas de polímeros. No entanto, foram observadas diferenças na distribuição da massa molecular do polímero. *C. neactor* também foi testada em descontínuo e em semi-contínuo, usando um tipo diferente de substrato oleico, extraído das borras de café (SCG) com dióxido de carbono em estado super-crítico (sc-CO2). Em modo semi-contínuo (DO-stat), a produtividade global em PHA foi de 4.7 g L^{-1} dia^{-1} com um rendimento em polímero em relação ao óleo de 0.77 g g^{-1}. Os resultados mostraram que o óleo de SCG pode ser um bio-recurso para a produção de PHA com propriedades interessantes.

Além disso, *P. resinovorans* foi cultivada com OODD em biorreator em modo descontínuo (regime de alimentação por pulsos). O polímero era altamente amorfo, como demonstrado pela sua baixa cristalinidade de 6±0.2%, com baixas temperaturas de fusão e de transição vítrea de 36±1.2 e -16±0.8 ° C, respectivamente. Devido ao seu comportamento adesivo pegajoso à temperatura ambiente, também foram estudadas as propriedades mecânicas e de adesividade. A sua resistência à ruptura na madeira (67±9.4 kPa) e no vidro (65±7.3 kPa) sugere que pode ser utilizado para o desenvolvimento de colas com base biológica.

A operação e monitorização de bioreactores com substratos contendo óleos constitui um desafio, uma vez que estes são imiscíveis em água. Posto isto, a técnica de infravermelho próximo (NIR) foi implementada para a monitorização em tempo real da fermentação de *C. necator* com UCO, utilizando uma sonda de transflectância. Foi aplicada uma regressão parcial dos mínimos quadrados (PLS) para relacionar espectros NIR com concentrações de biomassa, UCO e PHA no caldo. As previsões dadas pelo NIR foram comparadas com os valores obtidos *offline* por métodos de referência.

Erros de previsão para estes parâmetros foram 1.18 g L^{-1}, 2.37 g L^{-1} e 1.58 g L^{-1} de biomassa, UCO e PHA, respectivamente, o que indica a conveniência da espectroscopia NIR para a monitorização em tempo real e como um método para auxiliar o controlo do biorreator.

UCO e OODD foram considerados substratos de baixo custo promissores para serem utilizados na produção de PHA em descontínuo e em semi-contínuo. O uso do NIR neste bioprocesso também abriu uma oportunidade para otimização e controle dos processos de produção de PHA.

Palavras-Chave: Polihidroxialcanoatos (PHA), *C. neactor*, *P. resinovorans*, substratos oleicos, PHA de cadeia curta (*scl*-PHA), PHA de cadeia longa (*mcl*-PHA)

Abstract

Different oil-containing substrates, namely, used cooking oil (UCO), fatty acids-byproduct from biodiesel production (FAB) and olive oil deodorizer distillate (OODD) were tested as inexpensive carbon sources for the production of polyhydroxyalkanoates (PHA) using twelve bacterial strains, in batch experiments. The OODD and FAB were exploited for the first time as alternative substrates for PHA production. Among the tested bacterial strains, *Cupriavidus necator* and *Pseudomonas resinovorans* exhibited the most promising results, producing poly-3-hydroxybutyrate, P(3HB), form UCO and OODD and *mcl*-PHA mainly composed of 3-hydroxyoctanoate (3HO) and 3-hydroxydecanoate (3HD) monomers from OODD, respectively. Afterwards, these bacterial strains were cultivated in bioreactor.

C. necator were cultivated in bioreactor using UCO as carbon source. Different feeding strategies were tested for the bioreactor cultivation of *C. necator*, namely, batch, exponential feeding and DO-stat mode. The highest overall PHA productivity (12.6±0.78 g L^{-1} day^{-1}) was obtained using DO-stat mode. Apparently, the different feeding regimes had no impact on polymer thermal properties. However, differences in polymer's molecular mass distribution were observed. *C. necator* was also tested in batch and fed-batch modes using a different type of oil-containing substrate, extracted from spent coffee grounds (SCG) by super critical carbon dioxide (sc-CO_2). Under fed-batch mode (DO-stat), the overall PHA productivity were 4.7 g L^{-1} day^{-1} with a storage yield of 0.77 g g^{-1}. Results showed that SCG can be a bioresource for production of PHA with interesting properties.

Furthermore, *P. resinovorans* was cultivated using OODD as substrate in bioreactor under fed-batch mode (pulse feeding regime). The polymer was highly amorphous, as shown by its low crystallinity of 6±0.2%, with low melting and glass transition temperatures of 36±1.2 and -16±0.8 ºC, respectively. Due to its sticky behavior at room temperature, adhesiveness and mechanical properties were also studied. Its shear bond strength for wood (67±9.4 kPa) and glass (65±7.3 kPa) suggests it may be used for the development of biobased glues.

Bioreactor operation and monitoring with oil-containing substrates is very challenging, since this substrate is water immiscible. Thus, near-infrared spectroscopy (NIR) was implemented for online monitoring of the *C. necator* cultivation with UCO, using a transflectance probe. Partial least squares (PLS) regression was applied to relate NIR spectra with biomass, UCO and PHA concentrations in the broth. The NIR predictions were compared with values obtained by offline reference methods. Prediction errors to these parameters were 1.18 g L^{-1}, 2.37 g L^{-1} and 1.58 g L^{-1} for biomass, UCO and PHA, respectively, which indicates the suitability of the NIR spectroscopy method for online monitoring and as a method to assist bioreactor control**.**

UCO and OODD are low cost substrates with potential to be used in PHA batch and fed-batch production. The use of NIR in this bioprocess also opened an opportunity for optimization and control of PHA production process.

Key words: Polyhydroxyalkanoates (PHA), *C. neactor*, *P. resinovorans*, oil-containing substrates, short chain length PHA (*scl*-PHA), medium chain length PHA (*mcl*-PHA)

Nomenclature

Abbreviations

AF - Animal Fats

BHT - Butylhydroxytoluene

CO - Canola Oil

DO - Dissolved Oxygen

DSC - Differential Scanning Calorimetry

DSMZ - German Collection of Microorganisms and Cell Cultures

EPO - Emulsified Palm Oil

FAB - Fatty Acids-byproduct from Biodiesel

FAME - Fatty-Acids Methyl Esters

FAT - Margarine Fat Waste

FFA - Free Fatty Acids

FIB-SEM - Focused Ion Beam-Scanning Electron Microscope

FID - Flame Ionization Detector

GC - Gas Chromatography

HPO - Hydrolyzed Pollock Oil

lcl-PHA - long-chain length Polyhydroxyalkanoates

LV - Latent Variables

LVopt - Optimal Number of Latent Variables

mcl-PHA - medium-chain length Polyhydroxyalkanoates

NIR - Near-Infrared Spectroscopy

NRRL - Agricultural Research Service Culture Collection

OO - Virgin Olive Oil

OODD - Olive Oil Deodorizer Distillate

P(3HB) - Poly-3-Hydroxybutyrtate

P(3HB-*co*-3HHx) - Poly-(3-Hydroxybutyrate-co-3-Hydryhexanoate)

P(3HB-*co*-3HO) - Poly-(3-Hydroxyhexanoate-co-3-Hydroxyoctanoate)

P(3HB-*co*-3HV) - Poly-(3-Hydroxybutyrate-co-3-Hydroxyvalerate)

P(3HP) - Poly-(3-Hydroxypropionate)

P(3HHp) - Poly-(3-Hydroxyheptanoate)

P(3HHx) - Poly-(3-Hydroxyhexanoate)

P(3HD) - Poly-(3-Hydroxydecanoate)

P(3HDD) - Poly-(3-Hydroxydodecanoate)

P(3HN) - Poly-(3-Hydroxynonanoate)

P(3HO) - Poly-(3-Hydroxyoctanoate)

P(3HO-*co*-3HD-*co*-3HDd)-Poly-(3-Hydroxyoctanoate-co-3-Hydroxydecanoate-co-Hydroxydecanoate)

P(3HTd) - Poly-(3-Hydroxytetradecanoate)

P(3HV) - Poly-(3-Hydroxyvalerate)

PA - Polyamides

PBAT - Poly(butylene adipate-co-terephtalate)

PBS - Polybutylene succinate

PC - Principal component

PCA - Principal component analysis

PCL - Polycaprolactone

PDI - Polydispersity index

PE - Polyethylene

PET- Polyethylene terephtalate

PFAD - Palm Fatty Acid Distillate

PHA - Polyhydroxyalkanoate

PLA - Polylactic acid

PLS - Partial least squares

PP - Polypropylene

PS - Polystyrene

PTT - Polytrimethylene terephtalate

ROR - Residual oil from rhamnose production

RMSECP -Root-mean-square error of prediction

RMSECV- Root-mean-square error of cross-validation

sc-CO_2 - supercritical carbon dioxide

scl-PHA - short chain length Polyhydroxyalkanoates

SCG - Spent coffee grounds

SEC - Size exclusion chromatography

SFE - Supercritical fluid extraction

SOY - Soybean oil

TG - Triglycerides

UCO - Used cooking oil

VO - Vegetable Oils

WRO - Waste rapeseed oil

Variables

A (m^2) - Superficial area

A_{Cx} - Area of the peak of the methanolized monomers

A_i - Area of detected peak i (methyl ester) in GC

A_{IS} - Area of the peak of the internal standard

C_{NaOH} (mol L^{-1}) - Concentration of the alkali solution

CDM (g L^{-1}) - Cell dry mass

C_x (mol mL^{-1}) - Molar concentration of the methanolized monomers

F (kN) - Maximum load at break

FFA as oleic acid (%) - Free fatty acids content

F_s (g UCO h^{-1} L^{-1}) - Feeding rate

IS (mol mL^{-1}) - Molar concentration of the internal standard

K (mL g^{-1}) and *a* - Mark-Houwink constants

m_0 (g) - Mass of the picnometer

m_2 (g) - Mass of the picnometer filled with water

m_b (mg) - Mass of biomass

M_{Cx} - Molar mass of the monomeric units

m_i - Mass of the picnometer filled with oil

m_i (g) - Weighted mass of the substrate (oil)

$\overline{M}_n$ (g mol) - Number average molecular mass distribution

m_{PHA} (mg) - PHA mass

$\overline{M}_w$ (g mol) - Weight average molecular mass distribution

N - Dimensionless parameter

n - Exponent of the power law

P (g L^{-1}) - Concentration of the PHA

q_p (gPHA gX^{-1} h^{-1}) - Biomass specific product formation

q_s (gS gX^{-1} h^{-1}) - Biomass specific substrate uptake rate

r_p (g L^{-1} day^{-1}) - Volumetric productivity

S (g L^{-1}) - Substrate

t (h) - Initial time of feeding

T_c (ºC) - Crystallization temperature

t_f (h) - End of batch time

T_g (ºC) - Glass transition temperature

T_m (ºC) - Melting temperature

V (mL) - Volume of chloroform solution

V_{NaOH} (mL) - Volume of sodium hydroxide titrated

X - Methanolysis conversion factor

X (g L^{-1}) - Active biomass concentration

X_c (%) - Crystallinity of the PHA sample

$Y_{P/S}$ ($g^{-1}g^{-1}$) - Yields of product on substrate

$Y_{X/S}$ ($g^{-1}g^{-1}$) - Yields of biomass on substrate

ΔH_c (J g^{-1}) - Crystallization enthalpy

ΔH_m (J g^{-1}) - Melting enthalpy

Δt (h) - Period of time

Greek letters

μ_{max} (h^{-1}) - Maximum specific growth rate

β_{Cx} - Efficiency factor of the methanolized monomers

β_{IS} - Efficiency factor of the internal standard

ρ_i (g cm^{-3}) - Density of the oil-containing substrate

ρ_{H2O} (g cm^{-3}) - The density of the water at 20ºC

[η] - Viscosity number limit

ε (%) - Elongation at break

τ (MPa) - Tensile stress at break

E (GPa) - Young's modulus

τ_1 (kPa) - Shear bond stress

η (Pas) - Polymer's viscosity

η_0 (Pas) - Viscosity of the first Newtonian plateau

$\dot{\gamma}$ (s^{-1}) - Shear rate

λ - Time constant

Table of Contents

List of Figures

List of Tables

1. CHAPTER 1

Background and motivation

1.1. Background

Conventional oil based plastics have been growing at almost 5% per year over the past 20 years. Due to the global recession, the plastic production slowed significantly from 2010 to 2013. However, during the last year, production achieved 270 million tonnes, in which Europe was responsible for 23.5% of the overall production (Lunt, 2014). Total plastics consumption is expected to continue increasing at an average growth rate of 5-6% year, and is projected to reach 297 million tonnes by 2015 (Lunt, 2014).

Plastic production is highly dependent on petroleum resources and plastic disposal constitutes serious environmental and public health problems, there is a need for new alternative, more sustainable, eco-efficent and environmentally friendly resources and materials, such as biobased and biodegradable plastics (e.g bioplastics) (Akaraonye, Keshavarz and Roy 2010; Choi and Lee, 1999; Keshavarz and Roy, 2010; Pandey, 2015; Reddy, Reddy and Gupta, 2013; Siracusa et al., 2008; Sukan, Roy and Keshavarz, 2014). The replacement of conventional plastics by bioplastics has many advantages, namely: reduction of carbon dioxide emissions (1 metric ton of bioplastics generates between 0.8 and 3.2 fewer metric tons of carbon dioxide than 1 metric ton of fossil fuel-based plastics); competing price, i.e. bioplastics are becoming more viable with oil prices' volatility; reduction in waste, since the toxicity of bioplastics is much lower than that of conventional fossil fuel-based plastics and reduction in carbon footprint (Reddy et al., 2013). Competing with large volume commodities, demand for bioplastics is strongly influenced by its price. Although their prices are currently 80% lower than ten years ago according to the European Bioplastics Association (http://en.european-bioplastics.org/market/), on the range 1.3-4 euro/kg, they are still not competitive. However, the global bioplastics market is expected to expand from 7.2 billion € (2014) to 39.9 billion € by 2020 (http://www.futuremarketinsights.com/press-release/bio-plastics-market).

Due to the plastic industry demand, to the trend in research and development and to the economic and environmental issues several new polymers are being developed in the last decades. According to their origin and biodegradability, they can be divided in biobased, i.e. obtained from renewable resources, or fossil fuel based, and/or biodegradable and non-biodegradable polymers (Figure 1.1) (Lunt, 2014; Rydz et al., 2014). Considerable efforts have been made in the development of biobased plastics, such as polylactic acid (PLA) (Jamshidian et al., 2010), biobased polyethylene terephtalate (PET) (http://www.soci.org/chemistry-and-industry/cni-data/2012/9/bio-based-pet-project-on-track), starch blends (http://www.bio-plastics.org/en/information--knowledge-a-market-know-how/bioplastic-types/starch-blends-a-derivates) and polyhydroxyalkanoates (PHA) (Tan et al., 2014). It is expected the production capacity of biobased bioplastics will triplicate from 5.1 (value of 2013) to 17 million tonnes in 2020, being PLA and PHA (biobased and biodegradable plastics) great contributors for market growth (Aeschelmann and Carus, 2015). However, the market forecast until 2020 is clearly dominated by biobased and non-biodegradable plastics, such as biobased PET and

biobased polyethylene (PE), which are partially derived from biomass (Aeschelmann and Carus, 2015). Though this type of plastics are biobased, they are non-biodegradable, meaning they are still contributing for large disposal environmental issues. On the other hand, biobased and biodegradable plastics, such as PHA and PLA, may be more eco-efficient and sustainable alternatives in which more research and development have to be invested.

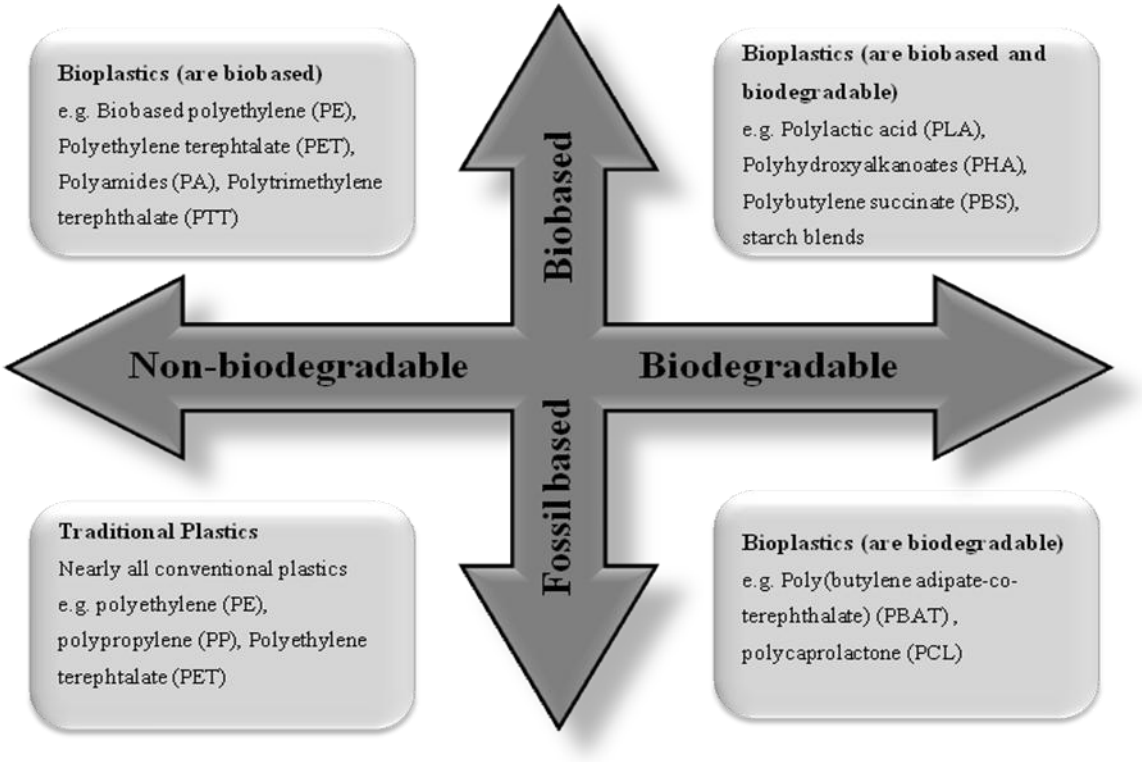

Figure 1.1: European bioplastics classification based on biodegradability (adapted from Lunt, 2014) .

PHA is biobased and biodegradable thus, being a promising alternative to other bioplastics.

1.2. Polyhydroxyalkanoates (PHA)

PHA belong to a family of naturally-occurring polyesters synthesized by various microorganisms as carbon and energetic intracellular reserves (Pandey, 2015). This type of bioplastic was first discovered by Lemoigne in 1926 and is within the group of the biobased and biodegradable bioplastics (Figure 1.1). PHA is a potential substitute of petroleum-based polymers (e.g. polypropylene, polyethylene), that has been attracted intensive research in several fields, such as medicine, pharmaceutical industry, agriculture, packaging industry, biotechnology, polymer waste management, etc. (Philip, Keshavarz and Roy, 2007; Rydz et al., 2015). Furthermore, PHA has a chemical-diversity, is manufactured from renewable carbon and has the advantage of being fully biodegradable and biocompatible, allowing a sustainable life cycle (Rydz et al., 2014; Tan et al., 2014).

PHA molecules are typically composed of 600 to 35000 (R)-hydroxy fatty acid monomer units, with a side chain group (R) which is usually a saturated alkyl group (Figure 1.2) (Tan et al., 2014). However, they can also have unsaturated alkyl groups, branched alkyl groups, and substituted alkyl groups, although these forms are less common (Lu, Tappel and Nomura 2009). PHA can be classified in three classes depending on the total number of carbon atoms within a monomer, namely short chain length PHA (*scl*-PHA), composed of 3 to 5 carbon atoms, medium-chain length PHA (*mcl*-PHA), composed of 6 to 14 atoms, and long chain length PHA (*lcl*-PHA) with more than 15 carbon atoms (Tan et al., 2014).

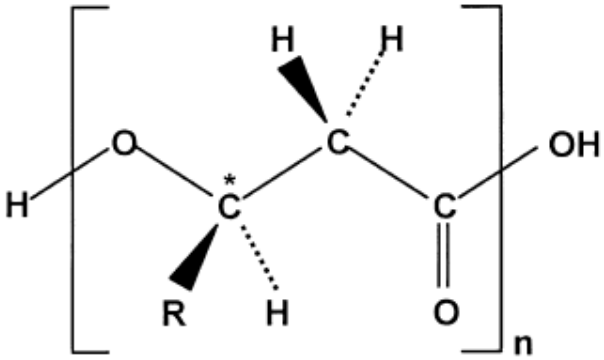

Figure 1.2: PHA general structure. For n=1 and R=H - Poly-(3-hydroxypropionate), P(3HP), R=methyl - Poly(3-hydroxybutyrate), P(3HB), R=ethyl - Poly(3-hydroxyvalerate P(3HV) belonging to *scl*-PHA; for n=1 and R=propyl - Poly(3-hydroxyhexanoate), P(3HHx), R=pentyl - Poly(3-hydroxyoctanoate), P(3HO), R=hexyl - Poly(3-hydroxydecanoate), P(3HD) and R=nonyl- Poly(3-hydroxydodecanoate), P(3HDD) belonging to *mcl*-PHA (adapted from Zinn , Witholt and Egli, 2001).

PHAs may also be classified as homopolymers and copolymers. Homopolymers contain only one type of monomer unit [e.g. poly-3-hydroxybutyrtate, P(3HB)], while copolymers are composed of more than one type of monomer unit, being either a combination of only *scl*-PHA units [e.g. poly-(3-hydroxybutyrate-*co*-3-hydroxyvalerate), P(3HB-*co*-3HV)] or *mcl*-PHA monomers [e.g. poly-(3-hydroxyhexanoate-*co*-3-hydroxyoctanoate), P(3HB-co-3HO)], or consisting of both *scl*- and *mcl*-PHA units [e.g. poly-(3-hydroxybutyrate-*co*-3-hydryhexanoate), P(3HB-*co*-3HHx)]. Of all PHAs, *scl*-PHA, such as P(3HB), have been the most widely explored (Kaur and Roy, 2015).

PHA can be produced through a fermentation process by several different bacteria. Depending on the fermentation process and the selected bacterial strain, different types of PHA are synthesised. Many different companies are involved in the pilot and industrial scale production of different types of PHA, including: the homopolymer poly-3-hydroxybutyrate, P(3HB) (e.g. Biomer Inc., Germany; Mitsubishi Gas Chemical Company Inc., Japan; PHB Industrial Brazil S.A., Brazil), the co-polymer poly-3-hydroxybutyrate-*co*-3-hydroxyvalerate, P(3HB-*co*-3HV), mainly sold for packaging and drug delivery applications (e.g. Tianan Biologic Ningbo, China) and poly-3-hydroxybutyrate-*co*-3-

hydroxyhexanoate, P(3HB-*co*-3HHx) (e.g. Kaneka Corporation, Japan; Meredian Inc., USA; P&G, USA; Kaneka Corporation, Japan) (Chanprateep, 2010; Chen, 2009; Endres and Siebert-Raths, 2011). Depending on the country policies, producing facilities, type of bioprocess, bacterial strain, carbon source (feedstock), downstream process, etc., the prices of PHA can vary between 1.5-5.0 € Kg^{-1} (Chanprateep, 2010) (Table 1.1).

Table 1.1: Prices of different types of PHA currently produced by worldwide manufactures (adapted from Chanprateep, 2010).

Company	**PHA trade name/type**	**Price (€ Kg^{-1})** (values of 2010)
Mitsubishi Gas Chemical Inc. (Japan)	Biogreen® / P(3HB)	2.5-3.0
Telles (USA)	Mirel™/ P(3HB)	1.50
PHB Industrial Company (Brazil)	Biocycle®/ P(3HB)	n.a.
Biomer Inc. (Germany)	Biomer®/ P(3HB); P(3HB-*co*-3HV)	3.0-5.0
Tianan Biologic, Ningbo (China)	Enmat®/ P(3HB-*co*-3HV)	3.26
P&G (USA)	Nodax™/ P(3HB-*co*-3HHx)	2.50
Lianyi Biotech (China)	Nodax™/ P(3HB-*co*-3HHx)	3.70
Kaneka Corporation (Japan)	Kaneka PHBH/ P(3HB-*co*-3HHx)	n.a.
Tianjin Gree Bio-Science Co/DSM	Green Bio/ P(3HB-co4HB)	n.a.
Meredian (USA)	Meredian/Different types PHA	n.a.

n.a. - not available

1.3. Biosynthesis of PHA

The biochemical pathways involved in PHA biosynthesis have been well studied over the past years (Chen, 2010; Kim et al., 2007; Sudesh, Abe and Doi 2000; Verlinden et al., 2007; Zinn, Witholt and Egli, 2001).

Synthesis of *scl*-and *mcl*-PHA have different pathways. The metabolic pathways for the synthesis of P(3HB) is shown in Figure 1.3. It occurs in a three-step reaction, involving 2 acetyl-coenzyme-A (acetyl-*Co*A) molecules produced in the tricarboxylic acid (TCA) cycle.

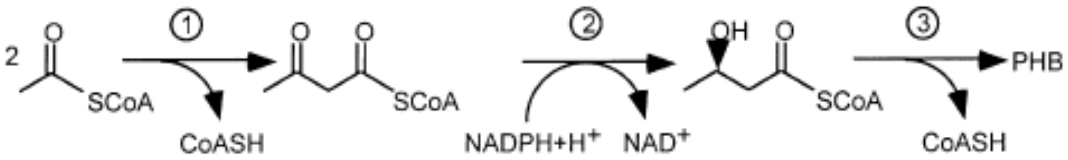

Figure 1.3: Biosynthesis of P(3HB) in three-step reaction (adapted from Zinn, Witholt and Egli, 2001).

Firstly, the enzyme *β*-thiolase (enconded by *phbA*) condenses the acetyl-*Co*A to acetoacetyl-*Co*A. Afterwards, the reduction of acetoacetyl-CoA to (R)-3-hydroxybutyryl-*Co*A by an NADPH-dependent acetoacetyl-CoA dehydrogenase (encoded by *phbB*) takes place. And in the third reaction, the (R)-3-hydroxybutyryl-CoA monomers are polymerized into poly-(3-hydroxybutyrate) by P(3HB) polymerase (encoded by *phbC*) (Chen, 2010; Verlinden et al., 2007; Zinn, Witholt and Egli, 2001).

On the other hand, *mcl*-PHA biosynthesis is linked to three different metabolic routes (Figure 1.4), namely: (1) de *novo* fatty acid biosynthesis pathway, which produces (R)-3-hydroxyacyl-*Co*A precursors from non-related carbon sources (e.g. glucose and gluconate); (2) fatty acid degradation by *β*-oxidation, which is the main metabolic route of fatty acids and (3) chain elongation in which acyl-*Co*A is extended with acetyl-*Co*A (Kim et al., 2007). In the final step of *mcl*-PHA production, the PhaC enzyme catalyzes the conversion of (R)-3-hydroxyacyl-CoA molecules into *mcl*-PHA with simultaneous release of CoA.

PHA synthases can be grouped into four classes based on their *in vivo* substrate specificities, primary amino acid sequences and subunit composition (Jain and Tiwari, 2014). Class I synthases belonging to *Cupriavidus necator* (a.k.a. *Wautersia eutropha*, *Ralstonia eutropha*) and *Alcaligenes latus* are active towards *scl*-(R)-hydroxyacyl-CoA consisting of three to five carbon atoms, as discussed before. Class II synthases primarily utilizes *mcl*-(R)-3-hydroxyacyl-CoA that contain six to fourteen carbon atoms and is represented by *Pseudomonas* species. Class III PHA synthases, is enclosed by *Allochromatium vinosum* and Class IV PHA synthases by *Bacillus megaterium* which have a similar subunit composition to class III PHA synthases (Jain and Tiwari, 2014).

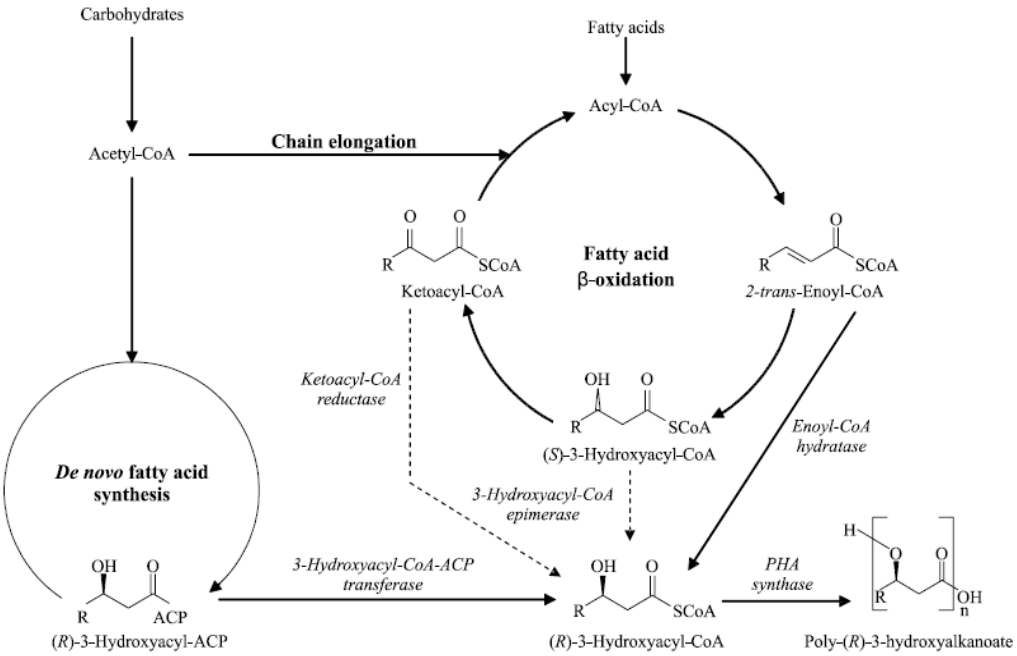

Figure 1.4: *Mcl*-PHA biosynthesis which is linked to three different metabolic routes (adapted from Kim et al., 2007).

1.4. Bacterial strains

A big wide range of Gram-positive and Gram negative bacteria (> 300 species) have the capability to synthesize PHA (Keshavarz and Roy, 2010), including strains belonging to *Pseudomonads* gender (*P. aeruginosa*, *P. putida*, *P. oleovorans, P. resinovorans*), *C. necator, Alcaligenes latus, Comomonas testosteroni*, *Azotobacter vinelandii*, etc. *scl*- and *mcl*-PHA can be synthesized by several different bacterial strains, and the majority of them are only able to produce either *scl*- or *mcl*-PHA homopolymers or copolymers. However, some of them (e.g. *C. necator*, *P. oleovorans*) can produce both *scl*- and *mcl*-PHA copolymers (Ashby, Solaiman and Foglia 2002; López-Cuellar et al., 2011; Rathinasabapathy et al., 2014).

Several *C. necator* strains (e.g. *C. neactor* 437-540 and DSM 545) have been widely studied because of its ability to produce P(3HB) from simple carbon sources, such as glucose (Atlić et al., 2011; Park et al., 2015), fructose (Fukui, Abe and Doi, 2002) and sucrose (Park et al., 2015). Many researchers developed mathematical models to improve P(3HB) production conditions (Chanprateep et al., 2002, Chanprateep et al. 2001; Wang and Lee, 1997). For example, optimal feeding profiles of glucose and ammonium hydroxide were modelled and *C. necator* NCIMB 11599 achieved high cell density of 141 g L^{-1} and P(3HB) concentration of 105 g L^{-1}, resulting in a high volumetric productivity of 2.63 g L^{-1} h^{-1} (Lee, Hong and Lim, 1997). The highest P(3HB) volumetric productivity was recorded (5.13 g L^{-1} h^{-1}) for fed-batch cultivation of *A. latus* DSM 1123 using sucrose (Chanprateep, 2010; Wang and Lee, 1997).

Among the *mcl*-PHA producers, *P. oleovorans* and *P. putida* (Huijberts and Eggink, 1996; Le Meur et al., 2012) are the most studied bacterial species. Typically, *Pseudomonas* species can be grown on both 'related' and 'unrelated' carbon sources. 'Related' carbon sources, are for example alkanes, alkenes and aldehydes which have structures related to the constituents of *mcl*-PHA. Unrelated carbon sources, i.e. glucose and glucanoate have non-similar structure to the *mcl*-PHA (Rai et al., 2011a). For example, when *P. putida* KT 2442 was cultivated in glucose, it was capable to produce a *mcl*-PHA enriched in 3-hydroxydecanoate (3HD) monomers, with minor contents of 3-hydroxyhexanoate (3HHx), 3-hydroxyocatnoate (3HO) and 3-hydroxydodecanoate (3HDD) (Kim et al., 2007; Rai et al., 2011a). When grown in substrates with an even number of carbon atoms, i.e., C_6, C_8, C_{10}, C_{12}, C_{14}, etc., *Pseudomonas* sp. produce polymers mainly composed of 3HO monomers and, when cultivated in substrates with odd number of carbon atoms, i.e., C_7, C_9 and C_{11}, etc., they produce polymers enriched in poly-3-hydroxynonanoate P(3HN) (Rai et al., 2011a).

Sugars such as glucose, sucrose and fructose are among the simplest substrates that are usually used for PHA production. Sucrose and glucose are the most suitable carbon sources for large scale production due to their availability in the market (Chanprateep, 2010; Chen, 2009). Also, starch (Shamala et al., 2012) and alcohols (Yamane, Chen and Ueda 1996) have been proposed as carbon sources for PHA production.

PHA production cost is highly dependent on the carbon source, as well as on other factors, including the microorganism's capability to utilize inexpensive carbon sources, the cost of the medium, the growth rate, the polymer synthesis rate, the quality and quantity of PHAs, and the cost of downstream processes (Chanprateep, 2010; Lee and Choi, 2001). The economic analysis for PHA production indicated that carbon substrates alone can contribute from 30 to 50% of the overall production cost (Ashby and Solaiman, 2008; Hassan et al., 2013; Kaur and Roy, 2015). Table 1.2 presents the typical prices for usual carbon sources used in industry.

Table 1.2: Price of some carbon sources used in PHA (adapted from Chanpantree, 2010).

Carbon source	Price (€ Kg^{-1})	Storage yield g g^{-1}	Cost of C-source per Kg of PHA
Sucrose	0.35	0.40	0.87
Glucose	0.41	0.38	1.07
Ethanol	0.31	0.50	0.63
Cassava starch	0.19	0.20	0.94
Cane molasses	0.10	0.42	0.24

Due to high impact of the feedstocks on the final polymer price, cheaper or inexpensive carbon sources, such as glycerol byproduct (Cavalheiro et al., 2009), lignocellulosic materials (Obruca et al., 2015) and vegetable oils (da Cruz Pradella et al., 2012; Lee et al., 2008) have been studied as possible candidates for PHA production.

1.5. Oil-containing substrates as alternative feedstock in PHA production

Due to their availability, vegetable oils, fats and wastes and/or industrial byproducts containing oils can be very interesting feedstock for PHAs production at a large scale. Fats and oils are mainly composed by triglyceride structures resulting from the combination of one unit of glycerol and three units of fatty acids (Strayer et al., 2006). They can have minor component such as monoglycerides, diglycerides and free fatty acids, i.e. unattached fatty acids from the main glycerol structure, phosphatides, sterols, fat-soluble vitamins, tocopherols, pigments, waxes, and fatty alcohols (Strayer et al., 2006). Fatty acids can be saturated, i.e. having carbon-to-carbon single bonds (e.g. myristic, palmitic and stearic acids), or unsaturated, i.e. composed by carbon-to-carbon double bonds (e.g. oleic, linoleic, linolenic acids).

Oils are immiscible with water but soluble in most organic solvents (e.g. *n*-hexane, ethanol, chloroform, etc.) and have lower densities than water. Fats have solid appearance and oils are liquid at room temperature.

Several substrates containing oils can be grouped taking into account their nature and origin, namely:

- Used cooking oils (UCO), mainly composed by triglycerides with lower amounts of di- and monoglycerides. 35% of UCO are collected in the EU, of which 90% are used for biodiesel production. However, biodiesel production is always dependent of the UCO composition (Hillairet and Borovska, 2011);

- Animal fats (e.g. tallow and lard) are also mainly composed by triglycerides. Europe has approximately 3.2 million tonnes of animal fats available per year out of which 1.7 million ton are used industrially (Hillairet and Borovska, 2011);

- Byproducts from the food industry, namely, from vegetable oil refining [e.g. palm fatty acid distillate (PFAD), olive oil deodorizer distillate (OODD)]. Around 10-40 kg of PFAD are generated per tonne of oil produced. PFAD is used in animal feed and detergent industries and as a raw material for the oleochemicals industry (Top, 2010); OODD represents 0.05-0.1 % of the total processed oil and is mainly composed by FFA (> 50 wt.%) (Bondioli et al., 1993). The significant content of squalene, (10-30 wt.%) a valuable antioxidant makes this byproduct interesting.

Oils are carbon enriched nutrients, very suitable to be used as microbial feedstocks. Theoretically, the PHA yield from vegetable oils can be as high as 1 g g^{-1} (Park and Kim, 2011). Yields around 0.6 to 0.8 g g^{-1} were reported for oil substrates, while lower values (0.3 to 0.4 g g^{-1}) have been reported for sugars (Chee et al., 2010). The lower storage yield in these type of substrate have high impact on the final price of the carbon source per Kg of polymer produced (Table 1.2). However, for low cost substrates allowing high product conversion yields, the final price of carbon source per Kg of PHA can be lowered. For this reason, fatty acids-containing substrates, such as vegetable oils (Lee et al., 2008; Ng et al., 2010), used cooking oils (Obruca et al., 2010; Verlinden et al., 2011) industrial wastes/byproducts containing oils (Ashby, Solaiman and Foglia 2004; Morais et al., 2014), animal fats (Muhr et al., 2013) and saponified oils (Allen et al., 2010) or pure fatty acids (Fukui and Doi, 1998) have been the focus of several studies in the latter years (Table 1.3). Among the bacterial strains able to utilize oil-containing substrates, *Cupriavidus necator* and several *Pseudomonas* species are widely reported. When *C. necator* was cultivated in spent coffee ground oil, a high polymer content was obtained (up to 90%) (Obruca et al., 2014a). *mcl*-PHA are commonly accumulated in lower cell contents (~50 wt.%). However, *Pseudomonas resinovorans* was able to accumulate 65 wt.% when cultivated in coconut oil (Ashby et al., 2001).

Several authors also reported on high cell density (30-138 g L^{-1}) cultivations in batch and fed-bioreactor, reaching high PHA productivities (up to 1.5 g L h^{-1}) (Park and Kim, 2010; Obruca et al., 2010; Obruca et al., 2014a, 2014b; Muhr et al., 2013).

Due to the different oil composition (medium and long fatty acids units) and type of bacterial strains, different polymers and co-polymers can be obtained. As referred before, the different monomer composition in the polymer have strong impact on polymer's properties and, thus, its final commercial application. Since oils are composed by different fatty acids, that can act as different PHA monomers precursors, they can be considered very good alternatives for tailor-made PHA production.

In the latter, process conditions (e.g. cultivation conditions, operation mode, carbon source concentration, bacterial strain, downstream process, etc.) have to be tuned in order to build a robust PHA process.

Table 1.3: Utilization of oil-containing substrates as carbon sources for PHA production using different bacterial strains.

Strain	Carbon Source	Operation Mode	CDM ($g\ L^{-1}$)	PHA ($g\ L^{-1}$)	PHA content (%)	Productivity ($g\ L^{-1}\ h^{-1}$)	PHA Composition	References
	Vegetable virgin oils							
***Cupriavidus necator* H16**	Jatropha Oil	Fed-Batch bioreactor	65.2	49.6	76	1.36	P(3HB)	Ng et al., 2010
***C. necator* H16**	Olive oil	Shake Flask	4.9	3.9	80	0.05	P(3HB)	Lee et al., 2008
	Sunflower oil	Shake Flask	4.7	3.4	72	0.05	P(3HB)	
	Coconut oil	Shake Flask	4.4	3.3	76	0.05	P(3HB)	
	Soybean oil	Shake Flask	3.6	3.0	82	0.04	P(3HB)	
***C. necator* H16**	Sesame oil	Shake Flask	6.1	4.1	68	0.06	P(3HB)	Taniguchi , Kagotani and Kimura 2003
***C. necator* H16**	Olive Oil	Shake flask	4.3	3.4	79	0.05	P(3HB)	Fukui et al., 1998
***C. necator* H16**	Corn Oil	Shake flask	3.6	2.9	81	0.04	P(3HB)	
***C. necator* H16**	Soybean oil	Batch and Fed-batch	15-32	n.a.	78-83	n.a.	P(3HB)	Park and Kim, 2010
***Pseudomonas resinovorans* NRRL B-2649**	Coconut oil	Shake flask	6.6	4.6	65	0.07	P(3HHx-co-3HO-co-3HD-co-3HDD-co-3HTD)	Ashby et al., 2001
	Soybean oil	Shake Flask	5.5	3.1	56	0.06		
***Comomonas testosteroni* IMI No. 375313**	Castor oil, coconut oil, mustard oil, groundnut oil, cottonseed oil, sesame oil, olive oil	Shake flask	n.a.	n.a.	78.6-87.5	n.a.	P(3HHx-co-3HO-co-3HD-co-3HDD-co-3HTD)	Thakor, Trivedi and Patel, 2005
	Used cooking oils							
***C. necator* H16**	Waste Sesame oil	Shake Flask	4.8	3.1	63	0.04	P(3HB)	Taniguchi , Kagotani and Kimura 2003
***C. necator* H16**	Waste rapeseed oil/Propanol	Batch bioreactor	138	105	76	1.46	P(3HB-co-3HV)	Obruca et al., 2010
C. necator H16	Waste rapeseed oil	Batch bioreactor	25-31	20-28	79-90	0.69-0.96	P(3HB)	Obruca et al., 2014a
***C. necator* H16**	Waste rapeseed oil	Shake flask	3.7	1.2	32	n.a.	P(3HB)	Verlinden et al., 2011
***C. necator* DSM 428**	Used cooking oil	Batch bioreactor	10.7	3.8	37	0.14	P(3HB)	Martino et al., 2014

Table 1.3: (Continuation) Utilization of oil-containing substrates as carbon sources for PHA production using different bacterial strains.

Strain	Carbon Source	Operation Mode	CDM ($g\ L^{-1}$)	PHA ($g\ L^{-1}$)	PHA content (%)	Productivity ($g\ L^{-1}\ h^{-1}$)	PHA Composition	References
	Industrial wastes/byproducts							
***P. oleovorans* NRRLB-14682**	Biodiesel co-product (containing glycerol, fatty acid soaps, and residual fatty acid methyl esters)	Shake flask	1.3	n.a.	13-27	n.a.	P(3HB)	Ashby, Solaiman and Foglia, 2004
Pseudomonas corrugata 388		Shake flask	2.1	n.a.	42	n.a.	P(3HHx-co-3HO-co-3HD-co-3HDD-co-3HTD)	
***C. necator* H16**	Spent coffee grounds oil	Batch and Fed-batch bioreactor	29-55	26-49	89-90	1.33	P(3HB)	Obruca et al., 2014b
***C. necator* DSM 428**	Margarine waste	Batch bioreactor	11.2	6.4	52-69	0.33	P(3HB)	Morais et al., 2014
	Animal fats							
***P. citronellolis* DSM 50332**	Tallow-based fatty acids methyl esters (FAME)	Fed-batch Bioreactor	30-42	2.1-3.7	6.8-9.2	0.04-0.1	P(3HHx-co-3HHp-co-3HO-co-3HN-co-3HD-co-3HHD)	Muhr et al., 2013
	Others							
***C. necator* H16**	Oleic Acid	Shake flask	4.1	3.4	82	0.05	P(3HB)	Fukui et al., 1998
***C. necator* H16**	Emulsified Palm oil	Batch bioreactor	10	7.9	79	0.11	P(3HB)	Budde et al., 2011a
***Pseudomonas oleovorans* ATCC 29347**	Saponified Jatropha oil	Shake flask	n.a.	n.a.	26	n.a.	P(3HB-co-3HV)	Allen et al., 2010

One of the key factors in PHA production is to reach high PHA yields and productivities, which is related to bioprocess feeding strategies. Several strategies can be employed, namely, batch, fed-batch with different feeding regimes (e.g. pulse, exponential, DO-stat, pH-stat, etc.), continuous cultivation and two or multi-step cultivation in batch systems (Kaur and Roy, 2015). In Table 1.3 is also display the common operation mode studied in PHA production using oil-containing substrates. Typically, studies of this bioprocess are performed in batch mode either in shake flasks (Ashby et al., 2004; Fukui and Doi, 1998; Lee et al., 2008; Taniguchi , Kagotani and Kimura 2003) or in bioreactor (Budde et al., 2011a; Martino et al., 2014; Morais et al., 2014; Obruca et al., 2014a). However, some authors have studied the PHA production from oil-containing substrates on fed-batch operation mode (Muhr et al., 2013; Ng et al., 2010; Obruca et al., 2014a; Park and Kim, 2011), which allows high polymer production, depending on the feeding strategy. Regarding the feeding strategies, pulse feeding is the most common technique to feed oil-containing substrates to the cultures (Kahar et al., 2004; Obruca et al., 2014a). Further alternative feeding strategies, such as exponential and DO-stat should be explored.

Batch experiments are very useful to determine kinetic parameters (e.g. biomass growth, product formation, substrate consumption) of a specific culture using efficient monitoring techniques.

Monitoring of PHA process performance (e.g. evaluation of cell growth and PHA production during the fermentation) is usually done offline, applying time consuming analytical methods (e.g. residual oil removal with solvents, lyophilisation, gas chromatography, etc.), reducing the effectiveness of fermentation control. To enable fast and reliable development of the fermentation process, new approaches to process monitoring are needed. Methods for reliable online measurement of process variables, like the concentrations of substrates, products and cell concentration, are often lacking. To advance scientific process understanding and speed up process development, new methods for the fast and accurate determination of these important variables are needed. In view of this, near infrared (NIR) spectroscopy technique can be very useful to monitor nutrients concentration, biomass concentration and PHA cell content during the fermentation (Lourenço et al., 2012). NIR may also be useful to characterize the waste-derived feedstocks in terms of their composition (e.g. fatty acids).

1.6. Extraction techniques for the isolation and purification of PHA from microbial cells

The most common extraction methods of PHA are solvent-based. They are routinely used in the laboratory because they are simple and fast. They are performed in two steps: membrane disruption and product solubilization (Kunasundari and Sudesh, 2011). Afterwards,

the polymer is precipitated in a non-solvent (e.g. methanol or ethanol) to be purified. Common solvents used to extract PHA are chloroform (Ramsay et al., 1994; Shawaphun and Manangan, 2009), 1,2-dichloroethane (Ramsay et al., 1994; Shawaphun and Manangan, 2009) or some cyclic carbonate, such as ethylene carbonate and 1,2-propylene carbonate (Fiorese et al., 2009). Acetone is also used for extraction of *mcl*-PHA (Elbahloul and Steinbüchel, 2009). With chlorinated solvents, such as chloroform, it is possible to obtain extraction high yields, >90%, and product purity, >95% (Kunasundari and Sudesh, 2011). However, due the large volume requirement of these solvents and their toxicity, non-solvent alternatives, in which non-polymer, i.e., cellular material, is digested, have been proposed. Among those are sodium hypochlorite (Heinrich et al., 2012), sodium hydroxide (Mohammadi et al., 2012), enzymes and detergents (Martino et al., 2014). The disadvantage of using the chemical digestion methods is the reduction in polymer's molecular mass due to low resistance of chain polymer to chemical attack and low extraction yields and purity. However, strong efforts have been made in investigation of PHA extraction in order to overcome these issues, lowering the toxicity of the process, as well as the costs.

1.7. PHA properties and application

PHAs are produced intracellularly and accumulated in the form of granules. Depending on the PHA composition in terms of monomers, i.e., *scl*- or *mcl*-PHA, granules can be of different sizes and structures. Generally, PHA granules consist of PHA polymer, a lipid monolayer, and integrated proteins consisting of PHA polymerase, PHA depolymerase, structural proteins (phasins), and proteins of unknown function (Figure 1.5) (Pandey, 2015; Zinn, Witholt and Egli 2001). The granules have a typical diameter of 0.2 to 0.7 μm and are composed by 97.7 % of polyester and 1.8% of protein and 0.5 % lipids and they can be observed under the light microscope with Nile Blue Staining (Koller et al., 2010; Ostle and Holt, 1982; Pandey, 2015).

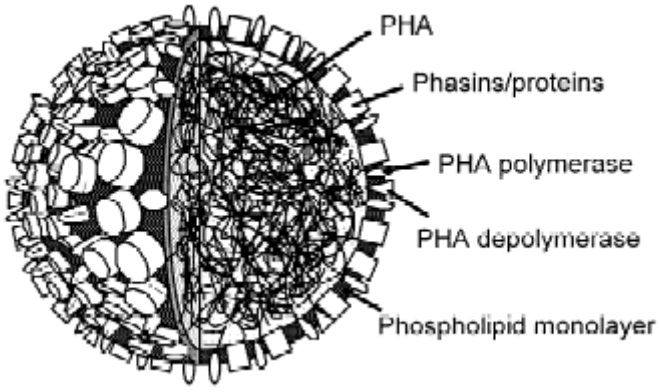

Figure 1.5: Structure of PHA granule (adapted from Zinn, Witholt and Egli 2001).

All type of PHA (*scl*-, *mcl*- and *lcl*-PHA) independent of their composition share some properties, namely (Koller et al., 2010):

- they are thermoplastic and/or elastomeric compounds, which can be processed with the apparatus used by the plastic manufacturing industry;
- they are water insoluble;
- exhibit a rather high molecular weight ranging from 10^5 to almost 10^7 Da;
- they are enantiomerically pure chemicals consisting, in general, only of the R-stereoisomer;
- they are non-toxic and biocompatible;
- they exhibit piezoelectric properties as revealed (at least) for P(3HB) and P(3HB-*co*-3HV);
- PHAs are biodegradable, since they can be hydrolysed by extracellular PHA depolymerases, and the cleavage products are subsequently utilized as sources of carbon and energy by many bacteria and fungi.

The physical-chemical, thermal and mechanical properties of the *scl*- and *mcl*-PHA varied depending on the structure, monomer composition, content and distribution in the polymer, as well as their molecular mass distribution (Liu et al., 2011). The *scl*-PHA, such as P(3HB) and copolymer of P(3HB-*co*-3HV) with low HV content, are highly crystalline, stiff and brittle with poor impact strength, while *mcl*-PHA are typically sticky, elastic and amorphous materials (Laycock et al., 2013; Wong et al., 2012). Table 1.4 summarizes the main *scl*- and *mcl*-PHA properties. These properties depend not only on the bacterial strain and carbon source used during cultivation but also on the process control parameters, extraction and purification procedures (Laycock et al., 2013).

The molecular mass distribution is a key factor which determines the PHA end-use and it depends on several factors: type of PHA synthase, the availability of precursors for PHA synthesis, the availability of enzymes that hydrolyze PHA and the expression level of PHA synthases (Wong et al., 2012). P(3HB) is the type of PHA with higher molecular mass (< 3 x 10^6 g mol^{-1}) (Table 1.4). Low molecular mass polymer is obtained if the PHA accumulated are produced by a high PHA synthase concentration in the cells (Wong et al., 2012). Commonly, co-polymers of *scl*-PHA and *mcl*-PHA have lower molecular masses. The molecular mass reported in literature for *mcl*-PHA with both saturated and unsaturated side chain groups is between 0.6 to 4 x 10^5 g mol^{-1} (Rai et al., 2011a). Extraction and purification methods can be determinant in the polymer's molecular mass, since some of extraction solvents (e.g. sodium hypochlorite) causes scission in the polymer chains.

Also, thermal and mechanical properties are crucial in PHA processing. *scl*-PHA exhibit high melting temperatures around 170 ºC, for P(3HB), and low glass transition temperatures, i.e. -5 to 15 ºC and high crystallinity, 55-80 % (Jain, Kosta and Tiwari 2010; Laycock et al., 2013) (Table 2). The melting temperature of a copolymer P(3HB-*co*-3HV) can be reduced from 172 to 64 ºC when 3HV is incorporated in the polymer's structure. , the glass transition temperature of the copolymer is lower (-13 to 10 ºC). On the other hand, polymers composed of *mcl*-PHA can exhibit very low melting (39-53 ºC) and glass transition temperatures (-49 to -25ºC), and crystallinity (1-19%) when compared to *scl*-PHA. These properties can constitute an advantage for some biomedical applications (e.g. soft tissue engineering, skin tissue engineering, wound healing and controlled drug delivery), since *mcl*-PHA have more elasticity and due to their variability in monomeric composition, provide more flexibility in tailoring the physical and mechanical properties to meet the application requirements (Rai et al., 2011a).

However, the degradation rate of *mcl*-PHA is higher than that of *scl*-PHA, since the degradation of the polymer decreases with the increase of highly ordered structure, i.e. crystallinity (Rai et al., 2011a). At temperatures close or above to the *mcl*-PHA's melting temperature, the polymer is completely amorphous and sticky. For *mcl*-PHA, the glass transition temperature decreases with increasing of the side chain structures in the polymer due their increased mobility (Rai et al., 2011a).

Mechanical properties, such as tensile strength (the stress required to break a sample), elongation at break (ratio between changed length and initial length after breakage of a sample) and Young modulus or modulus of elasticity (the slope of the stress-strain curve), are also very important parameters that should be determined for different types of PHA. Depending on the chain length, these properties may be completely different. P(3HB) tensile strength can range between 8 and 40 MPa, but typical values are within 30-40 MPa (Muhr et al., 2013). The average value for elongation at break for P(3HB) is usually around 6%. However, it can vary between 1 and 8% (Table 1.4) (Laycock et al., 2013; Muhr et al., 2013). P(3HB-co-3HHx) is a combination of *scl*- and *mcl*-PHA, and depending on the 3HHx monomers content, the mechanical properties vary. Polymers with high content of HHx (32-70 %mol) can exhibit an elongation at break from 368 to 1075 %. In this case, the tensile strength is lower, <1-8, than that reported for P(3HB). On the other hand, *mcl*-PHA copolymers of different contents of 3HHx and 3HO monomers can have different mechanical behavior. Young modulus and elongation to break vary according to the content of 3HHx in a copolymer of P(3HHx-*co*-3HO). Polymer with high content in 3HHx monomer, have high elongation at break and lower Young modulus (Rai et al., 2011a).

Table 1.4: Physical-chemical, thermal and mechanical properties of different types of *scl*- and *mcl*-PHA.

PHA composition	Mass average molecular mass x 10^5 ($\bar{M}_w$, g mol^{-1})	Number average molecular mass x 10^5 ($\bar{M}_n$,g mol^{-1})	Polidispertity Index ($\bar{M}_w/\bar{M}_n$)	Melting Temperature (T_m, C°)	Glass transition temperature (T_g, C°)	Crystallinity (%)	Tensile Strength (MPa)	Elongation at break (%)	Young modulus (GPa)	Reference
P(3HB)	2-30	n.a.	1.5-2.0	162-178	-4 -15	55-80	8-40	1-8	1.2-3.6	Jain. Kosta and Tiwari , 2010; Laycock et al.,
P(3HB-co-HV) HV content range (0.1-71 %mol)	n.a.	n.a.	n.a.	64-172	-13-10	45-65	1.8-50.5	0.2->1200	0.1-8.7	Laycock et al.,
P(3HB-co-3HHx) HHx content range (2.5-17 %mol)	n.a.	n.a.	n.a.	96.2-142	-1.8-0	n.a.	4.5-26	3-850	0.1-1.0	Laycock et al.,
HHx content range (32-70 %mol)	1.7-3.5	0.7-2.2	1.5-1.8	86-88	-12 to -1	n.a.	<1-8	368-1075	$0.27x10^{-3}$-0.1	Wong et al., 20
P(3HO)	2.3-6.0	1.2-2.8	1.8-2.3	39.2-49.5	-36.2 to -34.5	5-11[3]	n.a.	n.a.	n.a.	Rai et al., 2011
P(3HHx-co-3HHp[1]-3HO-co-3HN[2]-co-3HD-co-HDD) Monomer content range (5.1-6.5 %mol;1.5-1.7 %mol; 40.0-46.5 %mol; 2.4-4.7 %mol; 35.8-39.8 %mol; 6.9-9.0 %mol)	0.7-2.0	0.4-0.8	1.9-2.5	48.6-53.6	-46.9 to -43.5	10.4-12.3	n.a.	n.a.	n.a.	Muhr et al., 201
Various *mcl*-PHA	0.8-3.4	0.4-1.8	1.7-4.4	38.1-58.5	-49.3 to -25.8	1-19[3]	n.a.	n.a.	n.a.	Rai et al., 2011

[1] 3-hydroxyheptanoate; [2] 3-hydroxynonenoate; [3] Calculated as the ratio of melting enthalpy of the polymer to melting enthalpy of P(3HB) as reference (146.3 J mol^{-1})

The stiff and brittleness of P(3HB) has been reported as an obstacle to some applications in industry, and for this reason some efforts have been made to manipulate the mechanical properties of this polymer (Laycock et al., 2013). As discussed before one of the strategies to improve mechanical properties of PHA is to use copolymeric materials, such as P(3HB-*co*-3HV) and P(3HB-*co*-3HHx). Compared to P(3HB), these copolymers have decreased stiffness and brittleness, increased flexibility (higher elongation to break), and increased tensile strength and toughness. Also the glass transition temperature and even mechanical properties of a polymer can be altered mixing additives, such as plasticizers and/or nucleating agents (Laycock et al., 2013). In Figure 1.6 are presented some of the possible applications of PHA copolymers depending on their co-monomer content and molecular mass.

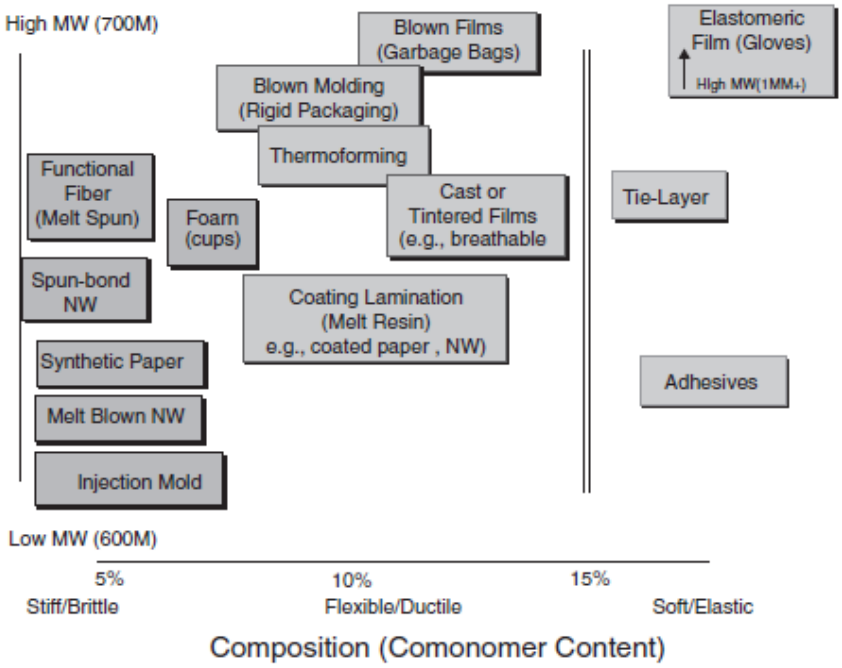

Figure 1.6: PHA possible applications depending in co-monomer content and molecular mass (adapted from Noda, Lindsey and Caraway, 2010).

1.8. Motivation

Due to the high cost of common carbon sources used in the PHA production process, alternative feedstocks have been the focus of intensive scientific research in the last years. In this sense, one of the main goals and motivation of this thesis was to produce different types of PHA through the bioconversion of low cost or inexpensive carbon sources, namely oil-containing wastes and/or byproducts. Although some of these carbon rich materials have already been tested as substrates for PHA production, there are still many that were still not explored, including spent coffee grounds oil (SCG), olive oil deodorizer distillate (OODD) and fatty acids from biodiesel production (FAB). Besides the impact of these substrates on production costs of PHA production it is also important to look to the process yields and polymer composition.

PHA production using oil-containing substrates has been studied in bioreactor systems as referred in state of the art. However, fed-batch systems with different feeding regimes, are still rarely explored with oil-containing substrates. Thus, alternative process conditions have to be tested in order to evaluate culture performance and polymer's properties. Also, one of the main advantages of these type of carbon sources is their composition, since the different fatty acids units can act as precursors of different PHA monomers. Thus, "novel" polymers with unique properties can be produced allowing their application in several different commercial areas.

One of the big disadvantages of using oil-containing substrates is their water immiscibility. This can constitutes a drawback in process optimization and polymer recovery, since the offline analysis of metabolites (e.g. biomass and PHA) are very time consuming involving hazardous chemicals. In this sense, it is very challenging to overcome this process issues in order to have a robust process. The use of monitoring techniques can constitute a great advantage once implemented in the biosystem. Taking this into account, and among different monitoring tools, near infrared spectroscopy (NIRS) is able to follow the course of cultivation run, predicting the concentration of biomass, substrate and product in each step of the process. This is a novel research approach in PHA production process, constituting a strong motivation in this work. With this technique implementation, it is possible to have fast response, quality control and optimization of PHA production from oil-containing substrates.

1.9. Thesis outline

This thesis was structured taking some milestones into account, namely: selection of microbial strains and oil-containing substrates for PHA production; testing of different oil feeding regimes in bioreactor production; extraction and purification of PHAs and their characterization; to develop a monitoring model able to quantify the metabolites, i.e. biomass, substrate and product during bioreactor production.

This work originated three publications in international peer reviewed journals. It is organized according to the following chapters:

- **Chapter 1:** Describes the background (state of the art) and motivation of the thesis;

  Chapter 2: Reports the selection of the suitable microorganisms capable to convert efficiently the tested oil-containing substrates into PHA. This work was published as Cruz, M.V., Freitas F., Paiva, A., Mano, F., Dionisio, M., Ramos, A.M., Reis, M.A.M. (2015) Valorization of fatty acids-containing wastes and byproducts into short- and medium-chain length polyhydroxyalkanoates. 2015. 33-1, 206-215;

- **Chapter 3:** Encompasses two sub-chapters, namely the batch and fed-batch production of scl-PHA by *Cupriavidus necator* DSM 428 with different used cooking oil (UCO) feeding regimes (**Chapter 3.A)** and with spent coffee grounds oil (SCG) (**Chapter 3.B).** The latter was published as Cruz, M.V., Paiva, A., Lisboa, P., Freitas F., Alves, V.D., Simões, P., Barreiros S., Reisa, M.A.M. Production of polyhydroxyalkanoates from spent coffee grounds oil obtained by supercritical fluid extraction technology. 2014 Bioresource Technology, 157, 360–363;

- **Chapter 4:** Reports on the production, characterization and application of *mcl*-PHA synthesized by *Pseudomonas resinovorans* using olive oil deodorizer distillate (OODD) as carbon source. This work was published as Cruz M.V., Araújo D., Alves V.D., Freitas F., Reis M.A.M. Characterization of medium chain length polyhydroxyalkanoate produced from olive oil deodorizer distillate. 2015 Int J Biol Macromol, 82, 243-248.

- **Chapter 5:** Describes the use of a spectroscopy technique to monitor the production of PHA by *Cupriavidus necator* cultivated with UCO. This study was published as Cruz, M.V., Sarraguça, M.C., Freitas, F., Lopes, J.A., Reis, M.A.M. Online monitoring of P(3HB) produced from used cooking oil with near-infrared spectroscopy. 2015. Journal of Biotechnology, 194, 1-9.

- **Chapter 6:** Conclusions and Future work

This work also originated two more publication associated to this project subject. However, those publications are only referenced in this work as:

Morais, C., Freitas, F., Cruz, M.V., Paiva, A., Dionísio, M., Reis, M.A.M, Conversion of fat-containing waste from the margarine manufacturing process into bacterial polyhydroxyalkanoates.2014. International Journal of Biological Macromolecules 71, 68–73.

Martino, L., Cruz M.V., Scoma A., Freitas F., Bertin, L., Scandolaa, M., Reis, M.A.M. Recovery of amorphous polyhydroxybutyrate granules from *Cupriavidus necator* cells grown on used cooking oil. 2014. International Journal of Biological Macromolecules 71, 117–123.

2. CHAPTER 2

Valorisation of fatty acids-containing wastes and byproducts into short- (*scl*-) and medium-chain length (*mcl*-) polyhydroxyalkanoates

The results presented in this chapter were published in one peer reviewed paper:

Cruz, M.V., Freitas F., Paiva, A., Mano, F., Dionisio, M., Ramos, A.M., Reis, M.A.M. (2015) Valorization of fatty acids-containing wastes and byproducts into short- and medium-chain length polyhydroxyalkanoates. 2015. 33-1, 206-215.

2.1. Summary

Olive oil deodorizer distillate (OODD), biodiesel fatty acids-byproduct (FAB) and used cooking oil (UCO) were tested as inexpensive carbon sources for the production of polyhydroxyalkanoates (PHA) with different composition using twelve bacterial strains. OODD and FAB were exploited for the first time as alternative substrates for PHA production. UCO, OODD and FAB were used by *Cupriavidus necator* and *Pseudomonas oleovorans* to synthesise the homopolymer poly-3-hydroxybutyrate, while *Pseudomonas resinovorans* and *Pseudomonas citronellolis* produced *mcl*-PHA polymers mainly composed of hydroxyoctanoate and hydroxydecanoate monomers. The highest polymer content in the biomass were obtained for *C. necator* (62 wt.%) cultivated on OODD. Relatively high *mcl*-PHA content (28-31 wt.%) was reached by *P. resinovorans* cultivated in OODD. This study shows, for the first time, that OODD is a promising substrate for PHA production since it gives high polymer yields and allows for the synthesis of different polymers (*scl*- or *mcl*-PHA) by selection of the adequate strains.

2.2. Introduction

As referred before (Chapter 1) the production cost of PHA is still high, mainly due to the expensive feedstocks involved in this type of bioprocess (e.g. glucose, sucrose). Taking this into account, alternative inexpensive and/or low cost feedstocks have to be explored in order to lower the overall production cost of PHA. In this study, fatty acids-containing substrates are being proposed as alternative feedstocks for PHA production.

Three different fatty acids-containing industrial wastes and/or byproducts were selected based in their availability, price, appearance (liquid and/or solid) and composition. Those selected were: used cooking oil (UCO), olive oil deodorizer distillate (OODD) and fatty acids-byproduct from the biodiesel industry (FAB).

Used cooking oil (UCO) is a food industry waste mainly composed by triglycerides (TG), containing long chain fatty acids (e.g. palmitic, oleic and linoleic acids) with saturated and/or unsaturated bonds. In the European Union, the generation of UCO (e.g. food manufactures, domestic sources, catering industry, etc.) is estimated to be 3.55 million tons per year, which is equivalent to 8 liters of UCO per capita (Toop et al., 2013). The price of UCO naturally increases along the supply chain from the generating source to the final collectors. Commonly, restaurants sell UCO for a maximum of 0.30 €/kg, which is lower than the selling price of sugars (0.35-0.41 €/Kg) (Chanprateep, 2010). Although, UCO is usually valorized by its conversion into biodiesel, there is surplus of this waste that can be efficiently converted into PHA.

Some bacterial strains are not capable to convert the complex TG structure into simpler units composed by fatty acids, since they do not have strong lipolytic activity (Cromwick, Foglia and Lenz, 1996). For this cases, prior hydrolyses or saponification of the TG structures are required (Allen et al., 2010), which increase the overall production costs. Moreover, free fatty acids (FFAs) are more water-miscible than the hydrophobic structures of TG, thus facilitating the homogeneity of the cultivation broth and facilitating the transport phenomena. For this reason, FFA-enriched wastes and/or byproducts should also be considered.

Olive oil deodorizer distillate (OODD) is a byproduct from the olive oil refining industry with low market value (0.24-0.39 US$/Kg). This byproduct represents 0.05-0.1 % of the total processed oil (Bondioli et al., 1993) and is mainly composed by FFA (> 50 wt.%) followed by squalene (10-30 wt.%) and smaller amounts of tocopherols and sterols (Bondioli et al., 1993; Rocha et al., 2014). Commonly, this byproduct is valorized by the recovery of the antioxidant compounds for different food, pharmaceutical and cosmetic industries (Akgün, 2011; El-shami et al., 2013). As far as the authors know, OODD has not been explored as carbon source for PHA production.

Fatty acids-byproduct (FAB) from the biodiesel industry is generated during glycerol purification and it contains large amounts of soap FFA and minor amounts of other unused reactants (Nanda et al. 2015). Thus, FAB can also be considered as a good substrate for PHA production. However, as far as the authors know this byproduct as not been explored as sole carbon source for PHA production.

Among the known PHA-accumulating bacterial strains, C*upriavidus necator* (Martino et al., 2014, da Cruz Pradella et al., 2012) and several *Pseudomonas* species (e.g. *P. resinovorans* (Follonier et al., 2014), *P. citronellolis* (Cromwick, Foglia and Lenz, 1996), *P. oleovorans* (Allen et al., 2010) and *Comomonas testosteroni* (Thakor et al., 2005) have been reported as capable to convert oil-containing substrates (e.g. soybean, UCO, FFA, saponified *Jatropha curcas* oil) into PHA.

The main goal of this study was to valorize the fatty acids-containing wastes and byproducts (UCO, OODD and FAB) by their conversion into different types of PHA using the twelve different PHA-accumulating strains, including *Cupriavidus necator*, several *Pseudomonas species* (*P. resinovorans*, *P. citronellolis* and *P. oleovorans*), *Comamonas testosteroni* and *Azotobacter vinelandii*. Significant relevance was given to the characterization of the carbon source to better correlate their composition with bacterial strain metabolic activity and performance for PHA production. The final product properties (composition, molecular mass distribution and thermal properties) were also accessed in this chapter.

2.3. Material and Methods

2.3.1. Characterization of the fatty acids-containing substrates

UCO was supplied by the University's cantina; OODD was supplied by Sovena Group SA, Portugal, which is a vegetable oil-refining and packaging industry; fatty-acids methyl esters (FAME), FAB and neutralized soybean oil (SOY) were supplied by SGC Energia SA, Portugal. SOY (high triglyceride content oil) and FAME (transesterified oil, enriched in methyl esters) were tested as control substrates. SOY was a non-edible oil resulting from the neutralization step of the biodiesel production process.

2.3.1.1. Acylglycerides, squalene, and fatty acids content

The acylglycerides content, namely, mono-, di- and triglycerides of the five substrates were determined by gas chromatography (GC) (Trace GC Ultra), according to the European norm EN 14105 (Thermo Fisher Scientific Inc.). Standard solutions (Biodiesel Consumables Kit EN), containing glycerin, monolein, diolein, triolein, butanetriol (IS1) and tricaprin (IS2) were used at the concentration specified in the EN. IS1 (80 µL), IS2 (100 µL) and of N-methyl-N-(trimethylsilyl) triluoroacetamide (MSTFA reagent) (100 µL) were added to 100 mg of the FA-containing substrate and the mixture was vigorously shaken. After 15 min, 8 mL of n-heptane were added, and the mixture was used for GC analysis. Squalene content was also determined using the method described above. Known standards of squalene (Sigma-Aldrich) were used to built the calibration curve.

Total free fatty acids (FFA) content was quantified by titration, according to the AOCS official method Ca 5a-40. A sample of the fatty acids-containing substrate was weighted between 0.1 to 10 g (according to the expected acid value) in a glass vial and dissolved in at least 50 mL of (95% v/v ethanol) with 1% of phenolphtalein as indicator. Afterwards, the solution was titrated with 0.1 M NaOH until turned pink at least for 10s (end point of the indicator). The free fatty acids content, expressed as oleic acid, was calculated using equation (1):

$$FFA_{asoleicacid},\% = \frac{V_{NaOH} \times C_{NaOH} \times 28.2}{m_i} \qquad \text{Equation (1)}$$

where V_{NaOH} (mL) is the volume of sodium hydroxide titrated, C_{NaOH} (mol L^{-1}) is the concentration of the alkali solution and m_i (g) the weighted mass of the substrate (oil). The analysis were performed in duplicate.

The fatty acid composition of the oils was determined by direct transesterification of the lipids to the corresponding methyl esters (FAME), according to a modified (Lepage and Roy, 1986) method.

Briefly, 25 mg of the fatty acids-containing substrate were mixed with 2 mL of methanol containing 5% (v/v) of acetyl chloride and heated at 80 ºC, for 1 hour. Afterwards, the samples were cooled to room temperature and 1 mL of hexane and 1 mL of deionized water were added. The samples were stirred in the vortex for 30 seconds and approximately, 600 µL of methyl esters was transferred to an encapsulated glass vial containing molecular sieves to absorb the residual water. Methylheptadecanoate (10 mg mL^{-1}) was used as internal standard. A sample of 1 µL was injected by means of an automatic injector Triplus. Peak identification was carried out using known standards (FAME mixture). FAME quantification and identification was performed by GC according to the EN14103, and follow the equation (2):

$$MethylEsters,\% = \frac{\frac{A_i}{A_{IS}}}{\sum \frac{A_i}{A_{IS}}} \times 100 \qquad \text{Equation (2)}$$

where A_i is the area of detected peak i (methyl ester) and A_{IS} is the area of internal standard.

The analysis was done using a Thermo Biodiesel (F) column 30 m (L) X 0.25 mm (ID) X 0.25 µm (film thickness) and a programmed temperature vaporizing (PTV) injector. The carrier-gas was helium at a constant flow rate of 2 mL min^{-1}; the oven temperature program was 230 ºC for 15 min; the injector program was 90 ºC to 260 ºC at 10 ºC s^{-1}, a split flow of 100 mL min^{-1}, transfer time of 3 min, cleaning at 360 ºC and a split flow of 250 mL min^{-1} for 20 min. The FID detector temperature was set at 280 ºC. All the data was processed with software Chrom-Card. All analyses were performed in duplicate.

2.3.1.2. Water, inorganic salts and elemental analysis

The water content of the FA-containing substrates was determined by a Karl Fisher system (Metrohm AG, Model 831KF coulometer), as described by Teixeira et al., 2011. Water content determination was conducted with Hydranal-Coulomat CG, as catholyte reagent free of halogenated hydrocarbons, for a coulometric KF titrator with a diaphragm and with Hydranal-Coulomat oil as anolyte reagent for a coulometric Karl Fisher titrator, as well as working medium. Samples were previously weighed (~100 µg) and injected into the KF titrator. The analyses were performed in triplicate.

The content in inorganic salts was determined according to ISO 2098:1972, with slight modifications. Approximately 1 mL of the oil-containing substrate was weighted in a porcelain plate and placed in the oven at 500 ºC for 2 hours, in order to degrade the organic matter. Afterwards, the sample was cooled in a desiccator and the residual inorganic matter was weighted.

The carbon, hydrogen, nitrogen and sulphur content of each oil-containing substrate were analysed using the elemental Analyser Thermo Finnigan – CE Instruments (Italy), model Flash EA 1112 CHNS. Duplicate analyses were performed for each sample.

2.3.1.3. Density

The density (g cm^{-3}) of each oil-containing substrate was determined in a 5 mL picnometer (nr.8) as described by equation (3):

$$\rho_i = \rho_{H_2O}(20^{o}C) \times \frac{m_i - m_0}{m_2 - m_0} \quad \text{Equation (3)}$$

where ρ_i is the density (g cm^{-3}) of the oil-containing substrate and ρ_{H2O} the density (g cm^{-3}) of the water at 20ºC. The mass (g) of the picnometer is given by m_0 and the mass (g) of the picnometer filled with water and oil is given by m_2 and m_i, respectively.

2.3.2. PHA production

2.3.2.1. Microorganisms and media

Pseudomonas oleovorans NRRL B-14682, NRRL B-778, NRRL B-14683 and NRRL B-3429, *P. citronellolis* NRRL B-2504, *P. resinovorans* NRRL B-2649, *P. stutzeri* NRRL B-775, *Cupriavidus necator* NRRL B-4383, *Comamonas testosteroni* NRRL B-2611 and *Azotobacter vinelandii* NRRL B-14641 were kindly offered by the Agricultural Research Service Culture (NRRL) Collection, USA. *C. necator* DSM 428 was purchased from the German Collection of Microorganisms and Cell cultures (DSMZ), Germany, and *Pseudomonas corrugata* 388 was kindly offered by Dr. Daniel Solaiman from the United States Department of Agriculture (USDA). All bacterial strains were kept in frozen stocks (-80 ºC) in LB (Luria-Bertani) medium (pH=6.8), with the following composition (per liter): bacto-triptone, 10 g; yeast extract, 5 g; sodium chloride, 10 g. Glycerol (20% v/v) was added as a cryoprotectant. Reactivation from the stock culture was performed by inoculation in solid LB medium (15 g L^{-1} of agar). Inocula for batch cultivations were prepared by inoculation of a single colony into liquid LB medium and incubation in an orbital shaker, at 30 ºC and 200 rpm, for 24 hours. Afterwards, the culture was transferred into mineral medium with the following composition (per liter): $(NH_4)_2HPO_4$, 3.3 g; K_2HPO_4, 5.8 g; KH_2PO_4, 3.7g; 10 mL of a 100 mM $MgSO_4$ solution and 10 mL of a micronutrient solution. The micronutrient solution had the following composition (per liter of 1N HCl): $FeSO_4.7H_2O$, 2.78 g; $MnCl_2.4H_2O$, 1.98 g; $CoSO_4.7H_2O$, 2.81 g; $CaCl_2.2H_2O$, 1.67 g; $CuCl_2.2H_2O$, 0.17 g; $ZnSO_4.7H_2O$, 0.29 g) (Freitas et al. 2009). The medium was supplemented with 20 g L^{-1} of fatty acids-containing substrate as the sole carbon source.

2.3.2.2. Screening for oil-utilizing and PHA-producing bacteria

The twelve bacterial strains were tested by cultivation on mineral medium supplemented with each of the fatty acids-containing substrates (UCO, OODD and FAB) (20 g L^{-1}). SOY and FAME were used as control experiments for cultivations in UCO and FAB, respectively. The experiments were performed in SeptaVent™ HTS (50 mL) flasks, at 30 ºC and 200 rpm, with an initial pH-value of 6.8±0.2. All experiments took 96 hours. A 10% (v/v) inoculum was used in each experiment. Daily samples were taken for evaluation of the cell growth by measurement of the broth's optical density (at 600 nm). The cells were visualized under the optical microscope (Olympus BX51), in phase contrast, and polymer accumulation was qualitatively evaluated by Nile blue A staining, as described by Ostle and Holt (1982), with slight modifications. Briefly, 500 µL broth sample were centrifuged (15777×*g*, 2 min), the supernatant was removed and the pellet was washed with deionized water and centrifuged again. The pellet was then re-suspended in 500 µL water with 50 µL Nile blue A stain solution (1 g L^{-1}) and placed at 70 ºC, for 15 min. The cells were then observed under fluorescence light.

2.3.2.3. Batch cultivation

The selected strains, *Pseudomonas oleovorans* NRRL B-14682, *P. citronellolis* NRRL B-2504, *P. resinovorans* NRRL B-2649, *Cupriavidus necator* NRRL B-4383 and DSM 428 were cultivated in UCO, OODD and FAB in batch shake flasks (100 mL) for PHA production. The experiments were performed under the cultivation conditions described on section 2.3.2.2. Samples (2 mL) were withdrawn every 24 hours to evaluate bacterial cell growth, through the measurement of the optical absorbance (at 600 nm). At the end of the cultivation runs (48 hours), the broth was collected for quantification of the cell dry mass (CDM), oil and PHA concentrations, as well as polymer composition. All analyses were performed in duplicate.

2.3.2.4. Analytical techniques

For CDM, residual oil and PHA quantification, 100 mL of the cultivation broth were mixed with n-hexane (1:1 v/v) and centrifuged (7012×*g*, 20 min). Three different fractions were obtained: a biomass pellet, an aqueous cell-free supernatant and an upper layer containing the residual oil. The biomass pellet was washed twice with deionized water, and lyophilized to gravimetrically quantify the CDM. For quantification of the residual oil, 10 mL of the upper hexane layer containing the residual oil were transferred to pre-weighted and placed in a fume hood at room temperature for 72 h, for solvent evaporation (Kahar et al., 2004). The residual oil was gravimetrically quantified and its fatty acids profile was analyzed as described on section 2.3.1.1.

PHA quantification was based on the methanolysis method described by (Lageveen et al., 1988), with slight modifications. Briefly, 2-5 mg dried cells were weighted and hydrolyzed with 1 mL 20% (v/v) sulphuric acid in methanol solution (Sigma-Aldrich, HPLC grade) and 1 mL methyl benzoate in chloroform (1 mg mL^{-1}) (Sigma-Aldrich, HPLC grade), at 100 ºC, during 3.5 hours, under vigorous magnetic stirring. Afterwards, the samples were cooled, 500 µL of deionised water was added and the solution was stirred in vortex for 30 seconds. Approximately, 800 µL of methyl esters was transferred to an encapsulated glass vial containing molecular sieves to absorb the residual water. Methyl benzoate acted as internal standard. Pure copolymer solutions, containing poly(3-hydroxybutyrate-*co*-3-hydroxyvalerate), P(3HB-*co*-3HV) (Sigma-Aldrich),poly(3-hydroxyhexanoate-*co*-3-hydroxyocatnoate), P(3HHx-*co*-HO), and poly(3-hydroxyocatonate-*co*-3-decanoate-*co*-3-dodecanoate), P(3HO-*co*-3HD-*co*-3HDd), were used as standards in concentrations ranging from 0.325 to 5 mg mL^{-1}. The resulting methyl esters were analysed by gas chromatography (Varian CP-3800) coupled with a flame ionization detector (FID) (CTC Analytics, Switzerland), in a BR89342 WCOT fused silica column (60m × 0.53mm). Helium was used as carrier gas with a flow rate of 1 mL min^{-1}. Split injection was used at 280ºC with split ration of 10. The oven temperature program was as follows: 40ºC; 20ºC min^{-1}, until 100ºC; 3ºC, until 175ºC and, finally, 20ºC, until 220ºC. The detector temperature was set at 250ºC (Abuquerque et al, 2010). All analysis were performed in duplicate.

2.3.2.5. Calculations

The active biomass was determined by equation (4):

$$X_{(t)} = CDM_{(t)} - P_{(t)} \qquad \text{Equation (4)}$$

where $CDM_{(t)}$ (g L^{-1}) is the cell dry mass and P (g L^{-1}) is the concentration of the $PHA_{(t)}$ in the broth at the same time t. This concentration is given by the percentage of polymer accumulated in the cells (calculated on dry basis).

The PHA content (%) in biomass was calculated based in GC analysis described in section 2.3.2.4. Using the molar concentration of the internal standard (IS, mol mL^{-1}), one can calculate the molar concentration of any of the mathanolized monomers (C_x, mol mL^{-1}) follow equation (5):

$$[C_x] = \frac{A_{C_x}}{A_{C_{IS}}} \times \frac{\beta_{IS}}{\beta_{C_c}} \times [IS] \quad \text{Equation (5)}$$

where A is the area of the peak and β is an efficiency factor (number of C atoms - 0.5 x number of O atoms) calculated based on the monomeric units of 3-hydroxy-alkanoate. The mass of PHA (m_{PHA}, mg) in the sample can be calculated following equation (6):

$$m_{PHA} = V \times \sum [C_x] \times M_{C_x} \quad \text{Equation (6)}$$

where V (mL) is the volume of chloroform solution and M_{Cx} is the molar mass of the monomeric units. Since the methanolysis is never complete, the polymer standards can provide information about the methanolysis conversion factor (*X*), which is the ratio between m_{PHA} and known mass of PHA originally present in standard (mg). Finally, the PHA content can be calculated following equation 7:

$$PHA,\% = \frac{m_{PHA}}{m_b \times X} \times 100 \quad \text{Equation (7)}$$

where the m_b is the mass of biomass (mg).

The yields of product ($Y_{P/S}$) and biomass ($Y_{X/S}$) generation on substrate *S* (g L^{-1}) were calculated for the same period of time (Δt) following equations 8 and 9, respectively:

$$Y_{P/S} = \frac{\Delta P}{\Delta S} \quad \text{Equation (8)}$$

$$Y_{X/S} = \frac{\Delta X}{\Delta S} \quad \text{Equation (9)}$$

The volumetric productivity (r_p) was obtained by dividing the final PHA concentration for the total fermentation time (g L^{-1} day^{-1}).

2.3.3. PHA extraction and characterization

PHA was recovered from the biomass by solvent extraction with chloroform. The lyophilized cells were mixed with chloroform (20 g L^{-1}) and kept at 30ºC, during 24 hours, with constant stirring. Afterwards, the solution was filtered with syringe filters with a pore size of 0.45 µm (GxF, GHP membrane, PALL), to remove cell debris. The filtered solution containing the polymer was placed at a fume hood for solvent evaporation. Due to low content on PHA the polymer was not further purified. The resulting PHA samples were characterized in terms of their composition by GC analysis, as described on section 2.3.2.4., average molecular mass and thermal properties.

2.3.3.1. Average molecular mass distribution

Weight average ($\bar{M}_w$) and number average ($\bar{M}_n$) molecular mass distribution were determined using a Size Exclusion Chromatography (SEC) apparatus (Waters), equipped with a solvent delivery system composed of a model 510 pump, a Rheodyne injector and a refractive index detector (Waters 2410). The polymer extracted from the biomass was re-dissolved in chloroform (Sigma, HPLC Grade) to a final concentration of 0.2-0.3% (w/v). Before analysis by SEC the polymer solution was filtered through a 0.2 mm membrane filter. Butylhydroxytoluene (BHT) was added as internal standard to the filtered solution. A universal calibration was performed and the calibration curve was generated with monodisperse polystyrene (PS) standards (in the range $2x10^3$ to $4x10^6$; Waters and Polymer Laboratories). The calibration curve was correlated with PHA using the Mark-Houwink-Sakurada relationship, described by equation (10):

$$[\eta] = K \times M^a \qquad \text{Equation (10)}$$

where [η] is the viscosity number limit and K and *a* are the Mark-Houwink constants, for each polymer/solvent/temperature system. The values of these constants used for the pairs PHA-chloroform and PS-chloroform, were respectively K=0.0118 mL g^{-1}, *a*=0.794 and K=0.0049 mL g^{-1}, a=0.78. The sample injection volume was 150 µL and analysis were performed in duplicate.

2.3.3.2. Thermal analysis

Thermal analysis was performed by differential scanning calorimetry (DSC) with a DSC Q2000 from TA Instruments inter-faced with a cooling accessory (RCS). The DSC runs covered a temperature

range from −90 to 200 ºC with heating and cooling rate of 10ºC min^{-1}. The samples (2–3 mg) were placed in aluminium hermetic pans. Measurements were performed under dry high-purity nitrogen gas (at a flow rate of 50 mL min^{-1}). The baseline was calibrated scanning the temperature range of the experiments with two empty pans. Calibration was carried out using high purity Indium for temperature transitions and the heats of fusion (Morais et al., 2014a). The glass transition temperatures (T_g, ºC) were taken as the midpoint of the step-transition; melting (T_m, ºC) and crystallization (T_c, ºC) temperatures were estimated from, respectively, the endothermic and exothermic peaks. Melting (ΔH_m, J g^{-1}) and crystallization (ΔH_c, J g^{-1}) enthalpies were also determined. The crystallinity (X_c, %) of the PHA samples was estimated as the ratio between ΔH_m associated with the detected melting peak and the melting enthalpy of 100% crystalline poly-3-hydroxybutyrate, P(3HB), estimated as 146 J g^{-1} (Barham et al., 1984).

2.4. Results and Discussion

2.4.1. Fatty acids-containing substrates selection and characterization

Used cooking oil (UCO), olive oil deodorizer distillate (OODD) and fatty acids-byproduct from biodiesel industry (FAB) were selected based on their low commercial value, stock availability and potential for use as carbon source for microbial growth and PHA production. OODD and FAB were also selected based in their significant content on free fatty acids. In fact, FFA-enriched substrates are usually preferred substrates for microbial fermentation, since prior saponification and/or triglyceride saponification is not required. All substrates were characterized in order to correlate the composition of the feedstocks with the output of PHA production process. Soybean oil (SOY) and fatty acids methyl esters (FAME) were also included in the study for PHA production as triglycerides and methyl esters rich-substrates, as control experiments to compare with UCO and of FAB, respectively.

All FA-containing substrates were characterized in terms of their physical-chemical properties (Tables 2.1 and 2.2).

Table 2.1: Physical-chemical characterization of the FA-containing wastes and byproducts tested as substrates for PHA production

	Fatty acids-containing byproducts			**Control**	
Composition (wt. %)	**UCO**	**OODD**	**FAB**	**FAME**	**SOY**
Tryglycerides	83.4±9.13	2.4±0.06	n.d.	N/D	86.5±8.5
Diglycerides	6.7±0.39	2.2±0.07	0.3±0.01	0.1±0.01	5.0±0.44
Monoglycerides	0.4±0.10	0.8±0.05	n.d.	0.5±0.01	1.1±0.20
FFA[a]	1.0±0.35	64.0±0.02	34.6±1.98	0.1±0.02	0.1±0.01
Methyl esters	n.d.	9.1±0.04	65.3±2.10	88.0±2.21	n.d.
Squalene	n.d.	0.6±0.01	n.d.	n.d.	n.d.
Total	***91.5±9.97***	***79.1±0.25***	***100±4.09***	***88.7±2.25***	***92.7±9.15***
Inorganic compounds	n.d.	n.d.	n.d.	n.d.	n.d.
Water	0.15±0.01	0.37±0.07	0.43±0.03	0.18±0.00	0.11±0.00
Density at 25ºC (g cm^{-3})	0.920±0.00	0.885±0.00	0.886±0.00	0.878±0.00	0.918±0.00

[a] Expressed as g oleic acid per 100 g
n.d. – not detected

Table 2.2: Fatty acids profile of the byproducts selected as substrates for PHA production.

	Fatty acids-containing byproducts			Control		Literature		
Fatty acids profile (wt. %)	**UCO**	**OODD**	**FAB**	**FAME**	**SOY**	**UCO**	**OODD**	**OO**
Saturated Fatty Acids								
Myritic acid ($C_{14:0}$)	n.d.	n.d.	n.d.	n.d.	n.d.	n.d.	2	n.d.
Palmitic acid ($C_{16:0}$)	9.0±0.1	10.3±0.1	6.1±0.1	6.2±0.1	10.8±0.1	14	12	11
Stearic acid ($C_{18:0}$)	3.4±0.6	10.1±1.6	2.2±0.4	2.4±0.1	3.2±0.1	6	10	1
Total	12.4±0.7	20.4±1.7	8.3±0.5	8.6±0.2	14.0±0.2	20	24	12
Unsaturated fatty Acids								
Oleic acid ($C_{18:1}$)	37.5±0.6	69.9±1.0	55.2±0.3	54.0±0.1	27.2±0.2	59	60	74
Linoleic acid ($C_{18:2}$)	49.8±0.5	8.0±0.8	27.2±0.5	29.0±0.1	52.8±0.3	21	13	10
Linolenic acid ($C_{18:3}$)	0.1±0.0	0.9±0.1	9.1±0.1	7.6±0.5	5.8±0.1	n.d.	2	2
Total	87.4±1.1	78.8±1.9	91.5±0.9	92±0.7	85.8±0.6	80	75	86
References	This study	This study	This study	This study	This study	Verlinden et al., 2011	Rocha et al., 2014	Hazer et al., 1998

n.d. – not detected; (OO-olive oil)

UCO was mainly composed of triglycerides (83.4±9.13 wt.%), with minor amounts of other acylglycerides, such as diglycerides (6.7±0.39 wt.%) and monoglycerides (0.4±0.10 wt.%) (Table 2.1). SOY and UCO had identical fatty acid profile, being mainly composed of unsaturated fatty acids (85.8±0.6 - 87.4±1.1 wt.%), with lower content on saturated units (12.4±0.7 – 14.0±0.2 wt.%) (Table 2.2). Oleic and linoleic acids were the major constituents of UCO (37.5±0.6 and 49.8±0.5 wt.%, respectively) and SOY (27.2±0.2 wt.% and 52.8±0.3 wt.%, respectively) (Table 2.2).

In contrast with UCO, OODD was mainly composed of FFA (64.0±0.02 wt.%), with considerably lower content in triglycerides (2.4±0.06 wt.%), diglycerides (2.2±0.07 wt.%) and monoglycerides (0.8±0.05 wt.%). Depending on the process refining conditions and vegetable oil characteristics, deodorizers distillates can exhibit from 32 to 81 wt.% (expressed as oleic acid) of FFA in its total content (Verleyen et al., 2001). OODD was mainly composed of unsaturated fatty acids (78.8±1.9 wt.%), but its content in saturated fatty acids (20.4±1.7 wt.%) was higher than that of UCO. In OODD, oleic acid was the major fatty acid (69.9±1.0 wt.%), followed by palmitic (10.3±0.1 wt.%), stearic (10.1±1.6 wt.%), linoleic (8.0±0.8 wt.%) and linolenic acids (0.9±0.1 wt.%) (Table 2.2). This fatty acid profile is similar to those reported for OODD (Rocha et al., 2014) and olive oil (Hazer et al., 1998) (Table 2.2). Squalene was also detected in OODD, accounting for 0.6±0.01 wt.% of its weight (Table 2.1). It is worth noting that composition of these byproducts has a significant degree of variability, since it depended on the original vegetable oil composition and on the operation conditions used in the steam-stripping distillation procedure, which is the last step of the refining process of vegetable oils (Teixeira et al., 2011).

Although it was expected that FAB would be mainly composed of FFA (34.6±1.98 wt.%), results show that the highest content was for methyl esters (65.3±2.10 wt.%). FAB exhibited very similar fatty acid profile (8.3±0.5 and 91.5±0.9 wt.%) of saturated and unsaturated fatty acids, respectively, to FAME (Table 2.2). This was to be expected, since both substrates are provided from the same biodiesel production process by transesterification of neutralized virgin oil. Given the high methyl esters content (88.0±2.21 wt.%), FAME was selected as substrate to infer on the impact of methyl-esters in PHA microbial metabolic activity.

Further characterization of the oils included their content in water and inorganic compounds, as well as their elemental analysis (C, N, H, S). No inorganic compounds were detected in any of the analysed oils, by their pyrolysis at 550 ºC (Table 2.2). However, trace amounts of water (< 0.5 wt.%) were detected (Table 2.2). Elemental analysis revealed a similar composition for all oils, namely, carbon, hydrogen and oxygen contents of 78±1.5, 12±0.5 and 10±1.7 wt.%, respectively. No nitrogen or sulphur were detected. The density of UCO (0.920 g cm^{-3}) and SOY (0.918 g cm^{-3}) were very similar to each other and to values reported in literature for vegetable oils, such as rapeseed, corn and soybean oils (0.907 to 0.919 g cm^{-3}, at 24ºC) (Noureddini et al., 1992). Waste lipids, such as UCO, commonly have slightly higher densities (0.924 -0.925 g cm^{-3}) (Azócar et al., 2010), which can be related to the absorption of some food compounds during frying procedures.

Taking into account the composition and some chemical properties of those oil-substrates, they were considered to be used as potential carbon sources on microbial fermentation.

2.4.2. PHA Production

2.4.2.1. Screening for oil-utilizing PHA-producing bacteria

Given the composition of the oil-containing substrates (section 2.4.1.), four *scl*-PHA and eight *mcl*-PHA producing strains were selected based on their known ability for use of fatty acids-enriched substrates. The selected *scl*-PHA producers were *P. oleovorans* NRRL B-14682, *Cupriavidus necator* NRRL B-4383 and DSM 428 and *Azotobacter vinelandii* NRRL B-14641, and the *mcl*-PHA producers were *P. oleovorans* NRRL B-778, NRRL B-14683 and NRRL B-3429 and *P. citronellolis* NRRL B-2504, *P. corrugata* 388, *P. resinovorans* NRRL B-2649, *P. stutzeri* NRRL B-775 and *Comamonas testosteroni* NRRL B-2611.

To the best of our knowledge, Azotobacter vinelandii NRRL B-14641, which is a PHA-accumulating strain, was not tested before for growth on oil-substrates. Although several *Cupriavidus necator* strains have been reported for PHA production from oil-substrate (Koller et al., 2014, Koller and Braunegg., 2015), there are no reports on the ability of strain *C. necator* NRRL B-4383 to grow on such substrates. Among the tested bacterial strains, some were reported before as non-capable to produce PHA from triglyceride structures due to low lipase activity (e.g. *Pseudomonas oleovorans*

NRRL B-14682, NRRL B-778 and NRRL B-14683, *P. citronellolis*) (Ashby and Solaiman, 2008; Cromwick, Foglia and Lenz, 1996). Thus, in this study those strains were not tested in triglycerides-enriched substrates, such as UCO and SOY.

Table 2.3 shows qualitative results on bacterial growth and PHA accumulation for each oil-containing substrate and bacterial strain. In the first set of experiments, a preliminary assessment of the performance of each strain was made, based on the final absorbance obtained within 4 days of cultivation and the detection of intracellular granules by Nile Blue staining.

P. oleovorans NRRL B-778, *P. corrugata* and *Azotobacter vinelandii* did not grow when cultivated on any of the tested oils. Among those strains, *P. oleovorans* NRRL B-778 has been reported as only capable to convert simpler sugars (e.g. glucose) and fatty acids and/or saponified oil into PHAs (Ashby and Solaiman, 2008; Ashby, Solaiman and Foglia, 2002) and *P. corrugata* was reported as consuming glycerol byproduct from biodiesel production (Ashby, Solaiman and Foglia, 2004). However, those strains were not previously tested in the FFA-enriched wastes (OODD and FAB) used in this work.

OODD and FAB were considered to be good substrates for the majority of the tested strains (*P. oleovorans* NRRL B-14682, NRRL B-14683 and NRRL B-3429, *P. citronellolis*, *P. resinovorans*, *C. necator* DSM 428 and NRRL B-4383) since the cells grew and accumulated PHA (Table 2.3). When UCO was used as sole carbon sources, only *P. resinovorans*, *C. necator* DSM 428 and NRRL B-4383 were capable to grow and accumulate PHA (Table 2.3).

Both OODD and FAB substrates had high FFA contents (>34.6±1.98 wt.%), whose assimilation by bacteria is considerably easier since no lipase activity is required. Hence, those substrates are preferred for cultivation of bacterial strains with low or no lipolytic activity since avoids the prior saponification/hydrogenation step of the oils required for the hydrolysis of triglycerides (Allen et al., 2010; Ashby and Solaiman, 2008; Cromwick, Foglia and Lenz, 1996).

The ability of the cultures to grow on methyl esters-enriched substrates and accumulate PHA was accessed by cultivating the selected strains in FAB and FAME. FAME, which was mainly composed of methyl-esters (Table 2.1), did not support significant cell growth (Table 2.3). On the other hand, most of the tested strains were able to grow and accumulate PHA on FAB, which was probably due to the substrate's content in FFA.

Based on the results obtained in the first set of experiments, *P. citronellolis*, *P. resinovorans*, *P. oleovorans* NRRL B-14682 and the two *C. necator* strains were considered the most promising strains for further testing of their PHA production capacity from UCO, OODD and/or FAB.

Table 2.3: Qualitative evaluation of cell growth and PHA production by the tested strains, when cultivated in UCO, OODD, FAB, FAME and SOY as sole substrates.

Microorganism	Fatty acids-containing byproducts						Control			
	UCO		OODD		FAB		FAME		SOY	
	Growth[a]	PHA[b]	Growth[a]	PHA[b]	Growth[a]	PHA[b]	Growth[a]	PHA[b]	Growth[a]	PHA[b]
***P. oleovorans* NRRL B-14682**	NT	NT	++	Yes	++	Yes	-	Yes	NT	NT
***P. oleovorans* NRRL B-778**	NT	NT	n.d.	No	n.d.	No	n.d.	No	NT	NT
***P. oleovorans* NRRL B-14683**	NT	NT	++	Yes	++	Yes	++	No	NT	NT
***P. oleovorans* NRRL B-3429**	+	No	++	Yes	++	Yes	+	No	+	No
***P. corrugata* 388**	n.d.	No	n.d.	No	n.d.	No	n.d.	No	n.d.	No
***P. citronellolis* NRRL B-2504**	NT	NT	+	Yes	+	Yes	-	No	NT	NT
***P. resinovorans* NRRL B-2649**	+	Yes	++	Yes	++	Yes	n.d.	No	-	Yes
***P. stutzeri* NRRL B-775**	-	No	+	No	+	No	n.d.	No	n.d.	No
***C. necator* DSM 428**	++	Yes	++	Yes	++	Yes	-	Yes	+	Yes
***C.necator* NRRL B-4383**	+	Yes	++	Yes	++	Yes	-	No	-	No
***Comamonas testosteroni* NRRL B-2611**	-	No	-	Yes	-	No	-	No	-	No
***Azotobacter vinelandii* NRRL B-14641**	n.d.	No	n.d.	No	n.d.	No	n.d.	No	n.d.	No

[a] Based on the absorbance at 600 nm. Evaluation of cell growth is given as: no growth (n.d.), week (-), satisfactory (+) and good (++). NT - not tested in this substrate.

[b] Evaluation by Nile blue staining: visualization of intracellular PHA granules fluorescence (Yes) and no detectable fluorescence (No).

2.4.2.2. Evaluation of selected strain performance in batch cultivation

Taking into account the preliminary bacterial strain and substrate selection, batch cultivation runs were performed, in duplicate experiments, over 48 hours. *scl*- and *mcl*-PHA producing bacterial strains were cultivated in 20 g L^{-1} of fatty acids-containing substrate as sole carbon sources. Results obtained are depicted in Table 2.4.

P. citronellolis was cultivated in OODD and in FAB, reaching CDM of 4.8±0.9 and 3.5±0.3 g L^{-1} with low PHA contents of 10±1.4 and 3±1.0 wt.%, respectively. These values are similar to those reported in literature for cultivation on FFA (1.7±0.1 g L^{-1} and 3±1.0 wt.%) (Cromwick, Foglia and Lenz 1996) and fat-containing waste from the margarine manufacturing FAT (6.3±2.5 g L^{-1} and 8±0.2 wt.%) (Morais et al., 2014a). The results indicate that neither OODD nor FAB are suitable substrates for PHA synthesis by *P. citronellolis*.

P. resinovorans had poor cell growth when cultivated on UCO (3.2±0.4 g L^{-1}) or FAB (2.6±1.2 g L^{-1}). However, while no significant PHA was produced from UCO, a polymer content in the biomass of 28 wt.% was reached on FAB (Table 2.4). OODD was the best substrate for *P. resinovorans* cultivation, with high CDM (7.1±0.1 g L^{-1}) and PHA content (31 wt.%). The presence of non-acylglyceride compounds in OODD (e.g. sterols and tocopherols) might have contributed to enhance cell growth. Such compounds were not analyzed in OODD, but they might correspond to the unidentified components that accounted for ~20 wt% of the substrate's composition (Table 2.1). In fact, Bondioli et al. (1993) reported considerable sterols and tocopherols contents (<10.2 wt.%) in olive oil distillate. However, the impact of such compounds on bacterial growth was not studied. Although higher PHA content was obtained by Ashby and Foglia (1998) by cultivation of *P. resinovorans* on pure olive oil (43±2.2 wt.%), the overall PHA production (1.5±0.2 g L^{-1}) was lower than that obtained in this study using OODD (2.2±0.01 g L^{-1}) (Table 2.4). On the other hand, in contrast to virgin olive oil, OODD is not food grade, so its use for PHA production does not compete with food applications.

P. oleovorans was cultivated on OODD and FAB, reaching CDM values of 4.7±0.3 g L^{-1} and 3.6±0.1 g L^{-1}, respectively, with PHA contents of 19±4.6 wt.% and 17±1.7 wt.%, respectively (Table 2.4).

Table 2.4: Quantitative evaluation of PHA batch shake flask production by *P. citronellolis* NRRL B-2504, *P. oleovorans* NRRL B-14682, *P. resinovorans* NRRL B-2649, *C. necator* NRRL B-4383 and *C. necator* DSM 428, using UCO, OODD and FAB as sole substrates, and comparison with other carbon sources reported in the literature.

	Microorganism	Substrate	CDM[a] ($g\ L^{-1}$)	PHA (wt. %)	PHA ($g\ L^{-1}$)	X ($g\ L^{-1}$)	$Y_{X/S}$ ($g\ g^{-1}$)	$Y_{P/S}$ ($g\ g^{-1}$)	r_p ($g\ L^{-1}\ day^{-1}$)	Reference
***mcl*-PHA producing strains**	***P. citronellolis* NRRL B-2504**	**OODD**	4.8±0.9	10±1.4	0.5±0.01	4.3±0.9	0.73±0.19	0.08±0.01	0.2±0.01	This study
		FAB	3.5±0.3	3±1.0	0.1±0.04	3.4±0.3	0.69±0.01	0.02±0.01	0.1±0.02	This study
		FFA	1.7±0.1	3±1.0	n.a.	n.a.	n.a.	n.a.	n.a.	Cromwick, Foglia and Lenz, 1996
		FAT	6.3±2.5	8±0.2	n.a.	n.a.	n.a.	n.a.	n.a.	Morais et al., 2014
	***P. resinovorans* NRRL B-2649**	**UCO**	3.2±0.4	28±8.4	0.9±0.2	2.4±0.6	0.74±0.20	0.24±0.11	0.5±0.1	This study
		OODD	7.1±0.1	31±0.1	2.2±0.01	4.9±0.0	0.65±0.10	0.29±0.05	1.1±0.1	This study
		FAB	2.6±1.2	>2	0	2.6±1.1	0.51±0.10	0	0	This study
		FAT	3.9±0.8	0	n.a.	n.a.	n.a.	n.a.	n.a.	Morais et al., 2014
		OO	3.4±0.2	43±2.2	1.5±0.2	n.a.	n.a.	n.a.	0.8±0.14	Ashby and Foglia, 1998
	***P. oleovorans* NRRL B-14682**	**OODD**	4.7±0.3	19±4.6	0.9±0.3	3.8±0.0	0.46±0,05	0.11±0.05	0.5±0.1	This study
		FAB	3.6±0.1	17±1.7	0.6±0.1	3.0±0.0	0.41±0.05	0.08±0.02	0.3±0.03	This study
		HPO	1.7	6	0.1	n.a.	n.a.	n.a.	0.03	Ashby and Solaiman, 2008
***scl*-PHA producing strains**	***C. necator* DSM 428**	**UCO**	8.4±0.6	55±10.3	4.6±1.2	3.8±0.6	0,61±0,25	0.68±0.13	2.3±0.6	This study
		UCO	12.8	60	7.7	n.a.	n.a.	n.a.	2.6	Obruca et al., 2010
		UCO	2	30	1.2	n.a.	n.a.	n.a.	0.4	Verlinden et al., 2011
		OODD	9.0±0.4	62±5.2	5.5±0.7	3.4±0.3	0.58±0.28	0.90±0.25	2.8±0.3	This study
		FAB	5.9±0.3	31±8.8	1.8±0.4	4.1±0.8	0.59±0.13	0.28±0.17	1.0±0.1	This study
		PFAD	1.9±0.5	47±1	n.a.	n.a.	n.a.	n.a.	n.a.	Chee et al., 2010
	***C. necator* NRRL B-4383**	**UCO**	3.5±0.9	8±4.0	0.3±0.1	3.2±1.0	0.52±0.10	0.08±0.03	0.1±0.03	This study
		OODD	4.1±0.7	52±2.4	2.1±0.4	1.9±0.2	0.22±0,03	0.24±0.01	1.0±0.2	This study
		FAB	3.2±0.3	6±0.2	0.2±0.1	3.0±0.3	0.44±0.18	0.03±0.01	0.1±0.01	This study

n.a.- data not available

[a] CDM, PHA and X are represented as mean value ± standard deviation (n=4) (this study). Cultivation broth was colected at 48h.

(FFA – free fatty acids; FAT - margarine fat waste; OO - virgin olive oil; HPO - Hydrolyzed Pollock oil; PFAD-Palm fatty acid distillate)

These values, though low, are considerably higher than those reported for other carbon sources, such as hydrolyzed pollock oil (Ashby and Solaiman, 2008). This strain of *P. oleovorans* is also reported to produce 13 to 27 wt.% of PHA from crude co-stream biodiesel byproduct, enriched in glycerol (Ashby, Solaiman and Foglia, 2004).

C. necator DSM 428 was the most versatile strain, being able to grow in all tested substrates (Table 2.4). Cultivation on UCO and OODD resulted in high CDM (8.4±0.6 and 9.0±0.4 g L^{-1}, respectively) and high PHA contents (55±10.3 and 62±5.5 wt.%, respectively). Lower CDM (5.9±0.3 g L^{-1}) and PHA content (31±8.8 wt.%) were obtained for cultivation of FAB.

These results are within the values reported in literature for cultivation of this strain on other oil-substrates, such as UCO or PFAD (palm fatty acids distillate): CDM within 1.9 - 12.8 g L^{-1}, and PHA contents of 30 – 60 wt.% (Verlinden et al., 2011). *C. necator* NRRL B-4383, which was not previously reported as a PHA producer, had poor cell growth and PHA accumulation on UCO and FAB (Table 2.4). On the other hand, OODD was found to be a suitable substrate, with a CDM of 4.1±0.7 g L^{-1} and a PHA content of 52±2.4 wt.%. Nevertheless, these values are lower than those obtained for *C. necator* DSM 428 on the same substrate.

At the end of the cultivation runs, the residual oil concentration and fatty acids composition were determined (Figure 2.1).

Total fatty acids consumption was concomitant with cell growth in all experiments. The highest oil consumption was observed for the experiments with *C. necator* NRRL B-4383 and *P. oleovorans*, in which 8.9±0.5 and 8.3±1.0 g L^{-1} of OODD were consumed, respectively. All fatty acids present in each oil-substrate, namely, palmitic, stearic, oleic, linoleic and linolenic acids, were consumed during the experiments, with no apparent preference (Figure 2.1). Among all the tested strains, *P. resinovorans* and *C. necator* DSM 428 had the highest storage yields (0.29±0.05 and 0.90±0.25 g g^{-1}, respectively) when cultivated in OODD (Table 2.4). These values are slightly higher than those reported for *P. resinovorans* cultivated in HPO (0.18 g g^{-1}) (Ashby and Solaiman, 2008) and *C. necator* DSM 428 cultivated in spent coffee grounds oil (0.88 g g^{-1}) (Obruca et al., 2014b).

On the other hand, the maximum volumetric productivity (r_p) values were also observed for *C. necator* DSM 428 (2.8±0.3 g L^{-1} day^{-1}) and *P. resinovorans* (1.1±0.1 g L^{-1} day^{-1}) cultivated in OODD.

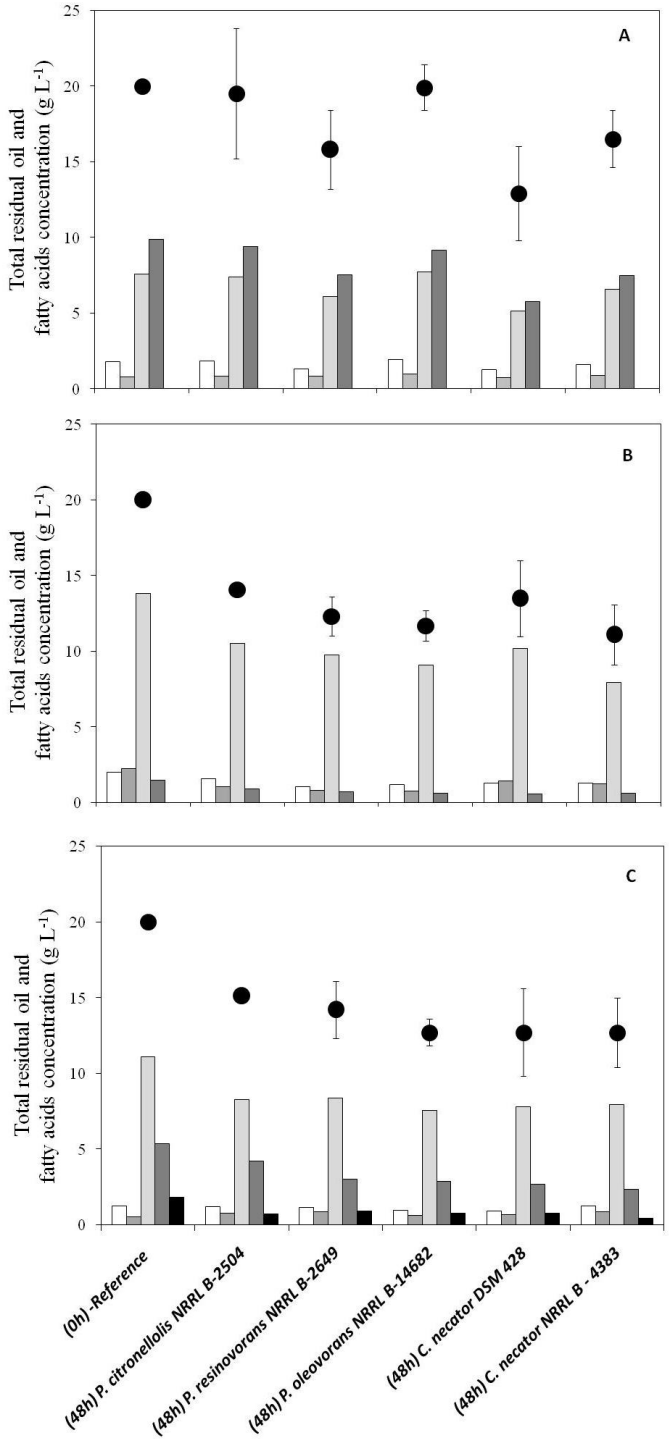

Figure 2.1: Residual oil quantification (●) and fatty acids composition (□, palmitic; ■, stearic; ■, oleic; ■, linoleic; ■, linolenic acids)in broth samples after 48h of cultivation in (A) UCO, (B) OOD and (C) FAB, for *P. citronellolis* NRRL B-2504, *P. oleovorans* NRRL B-14682, *P. resinovorans* NRRL B-2649, *C. necator* NRRL B-4383 and *C. necator* DSM 428.

Though FAB had a high free fatty acids content (35 wt.%) and it was efficiently used by some of the tested strains (*P. oleovorans* and *C. necator* DSM 428), it is a less interesting substrate to be used for PHA production because the cultures are not able to use the methyl esters fraction (as shown in the preliminary tests performed with FAME). The high content on methyl esters (65 wt.%) (Table 2.1) might have inhibited cell growth and polymer production. On the other hand, the available free fatty acids content might be in limiting levels to support both production and growth metabolism.

2.4.3. PHA characterization

The PHA synthesized by each bacterium from the tested oil-containing substrates was extracted and characterized in terms of their composition, molecular mass distribution (Table 2.5) and thermal properties (Table 2.6).

2.4.3.1. *Scl*-PHA

The *scl*-PHA producing strains, *Pseudomonas oleovorans* NRRL B-14682, *C. necator* DSM 428 and NRRL B-4383 produced poly-3-hydroxybutyrate, P(3HB), regardless of the substrate used for their cultivation (Table 2.5). *C. necator* has a Type I synthase, thus it is only able to synthesize 3HB and 3-hydroxyvalerate (3HV) monomers. Recently, Rathinasabapathy et al. (2014) and López-Cuellar et al. (2011) reported on the production of a *mcl*-PHA copolymer by *C. necator*, when canola oil was used as sole carbon source. However, in the present study, the fatty acids present in UCO, OODD and FAB (Table 2.2) were used neither as 3HV precursors nor for *mcl*-PHA monomer production.

The $\bar{M}_w$ of the P(3HB) produced by *P. oleovorans* and *C. necator* strains cultivated in UCO, OODD and FAB ranged from 1.0×10^5 to 2.9×10^5 g mol^{-1}, while the PDI values were 1.5-1.8. Though slightly lower, these values are close to those reported by Ashby and Solaiman, (2008) ($3.9x10^5$ and 2.0) for P(3HB) produced by *P. oleovorans* from hydrolyzed pollock oil.

The P(3HB) polymers produced by both *C. necator* strains exhibited T_g values ranging from -5.0±0.2 to 3.8±0.1 ºC and T_m ranging from 164.3±5.1 to 168.6±2.0 ºC (Table 2.6).

Table 2.5: Molar composition of the PHA produced by *P. citronellolis* NRRL B-2504, *P. oleovorans* NRRL B-14682, *P. resinovorans* NRRL B-2649, *C. necator* NRRL B-4383 and *C. necator* DSM 428, from different fatty acids-containing substrates, UCO, OODD and FAB.

	Microorganism	Substrate	3-hydroxyyalkanoates, methyl esters[a] (mmol%)						$\bar{M}_n$ (g mol^{-1}) x 10^5	$\bar{M}_w$ (g mol^{-1}) x 10^5	PDI	Reference
			3HB	3HHx	3HO	3HD	3HDd	3HTd				
mcl-PHA producing strains	***P. citronellolis* NRRL B-2504**	**OODD**	0	14±2.0	43±1.4	32±2.3	12±2.0	<1	0.2	0.3	1.5	This study
		FAB	0	10±0.1	36±0.1	40±0.2	14±0.2	<1	-	-	-	This study
		FFA	<1	10	48	28	8	2	0.4-0.7	0.9-1.6	2.2-2.6	Cromwick, Foglia and Lenz 1996
	***P. resinovorans* NRRL B-2649**	**UCO**	0	11±3.8	43±1.1	33±2.5	12±5.1	<1	0.3	0.4	1.3	This study
		OODD	0	19±1.1	44±0.3	28±1.6	9±2.5	<1	0.2	0.3	1.5	This study
		FFA	<1	9	37	32	12	2	0.7-0.8	1.3-1.8	1.8-2.3	Cromwick, Foglia and Lenz, 1996
		AF	<1	7-9	26-31	34-41	11-15	3-4	0.8	1.4	1.7	Ashby and Foglia, 1998
		VO	<1-1	8-9	29-37	30-35	5-14	2-3	0.7-1.0	1.1-1.8	1.6-1.8	Ashby and Foglia, 1998
scl-PHA producing strains	***P. oleovorans* NRRL B-14682**	**OODD**	100	0	0	0	0	0	1.4	2.2	1.6	This study
		FAB	100	0	0	0	0	0	2.0	2.9	1.5	This study
		HPO	100	0	0	0	0	0	1.9	3.9	2.0	Ashby and Solaiman, 2008
	***C. necator* DSM 428**	**UCO**	100	0	0	0	0	0	1.1	1.7	1.5	This study
		OODD	100	0	0	0	0	0	1.0	1.6	1.6	This study
		FAB	100	0	0	0	0	0	0.8	1.6	2.0	This study
		UCO	100	0	0	0	0	0	1.6	2.6	1.6	Martino et al., 2014
	***C. necator* NRRL B - 4383**	**UCO**	100	0	0	0	0	0	0.9	1.8	2.0	This study
		OODD	100	0	0	0	0	0	0.6	1.7	2.8	This study
		FAB	100	0	0	0	0	0	0.4	1.0	2.5	This study

[a] 3HB, 3-hydroxybutyrate; 3HHx, 3-hydroxyhexanoate; 3HO, 3-hydroxyocatnoate; 3HD, 3-hydroxydecanoate, 3HDd, 3-hydroxydodecanoate and 3HTd, 3-hydroxytetradecanoate.
(AF- Animal Fats; VO-Vegetable oils).

Table 2.6: Thermal properties of the polyhydroxyalkanoates produced from by *P. citronellolis* NRRL B-2504, *P. oleovorans* NRRL B-14682, *P. resinovorans* NRRL B-2649, *C. necator* NRRL B-4383 and *C. necator* DSM 428 in UCO, DEO and FAB as sole substrates.

	Microorganism	Substrate	T_g (ºC)	T_c (ºC)	ΔH_c (J g^{-1})	T_m (ºC)	ΔH_m (J g^{-1})	X_c (%)	Reference
***mcl*-PHA producing strains**	***P. citronellolis* NRRL B-2504**	**OODD**	-14.2±1.0	n.d.	n.d.	25.2±1.0	1.9±0.4	1±0.3	This study
		UCO	-28.9±0.1	n.d.	n.d.	43.3±0.1	9.9±0.9	7±0.6	This study
	***P. resinovorans* NRRL B-2649**	**OODD**	-15.8±0.8	n.d.	n.d.	35.6±1.2	8.3±0.3	6±0.2	This study
		AF	-46 to -43	n.a.	n.a.	39 - 44	9.5-11.4	6-8	Ashby and Foglia, 1998
		VO	-46 to -38	n.a.	n.a.	41 - 48	10.0-12.3	7-8	Ashby and Foglia, 1998
	***P. oleovorans* NRRL B-14682**	**OODD**	-5.0±0.01	27.5±0.1	25.1±2.3	156.5±4.1	52.5±0.3	36±1	This study
		FAB	-1.9±0.1	32.0±0.0	28.4±0.4	161.7±2.6	56.5±1.8	39±1	This study
		UCO	-5.0±0.2	39.2±0.0	28.8±0.4	168.6±2.0	78.1±2.0	53±1	This study
***scl*-PHA producing strains**	***C. necator* DSM 428**	**OODD**	-1.3±0.01	40.5±0.0	30.8±0.3	164.3±5.1	68.2±4.7	47±3	This study
		FAB	1.1±0.01	45.6±0.0	51.0±6.3	166.2±3.1	70.5±0.4	48±1	This study
		CO	n.a.	n.a.	n.a.	170.0	84.7	58	López-Cuellar et al., 2011
		UCO	2.5±0.01	42.0±0.1	17.6±0.3	167.2±2.1	58.0±1.3	40±1	This study
	***C. necator* NRRL B - 4383**	**OODD**	0.4±0.01	47.1±0.2	33.3±1.4	164.9±3.0	66.1±1.4	45±1	This study
		FAB	3.8±0.1	54.0±0.01	37.7±1.8	165.8±1.9	67.7±5.0	46±3	This study

n.d.- not detected
n.a. – data not available
(CO-Canola oil)

These values are in good accordance with those reported by Laycock et al. (2013), namely, T_g between -4 and 18 ºC, and T_m between 162-181 ºC.

The P(3HB) polymer produced by *P. oleovorans* cultivated in OODD and FAB, exhibited lower T_m (156.5±4.1 and 161.7±2.6 ºC) and T_g (-5.0±0.0 and -1.9±0.1 ºC) than the values reported in literature for this type of polymer. The lower T_g is in accordance with the lower values of $\bar{M}_w$ also determined for these homopolymers. The P(3HB) crystallinity ranged from 36±1 to 53±1 %, which are slightly lower than the values reported in literature (50-70 %) for this type of polymers (Laycock et al., 2013).

2.4.3.2. *mcl*-PHA

P. resinovorans and *P. citronellolis* produced *mcl*-PHA with slightly different monomer composition depending on the substrate used (Table 2.5). All *mcl*-PHA were composed by four main monomers, ranging in length from C_6 to C_{12}, suggesting that the degradation pathway of the different oil-containing substrates and the PHA synthesis pathway might be similar in both strains.

When cultivated on OODD and FAB, *P. citronellolis* produced copolymers mainly composed by 3-hydroxyoctanoate (3HO) (36±0.1-43±1.4 mmol%) and 3-hydroxydecanoate (3HD) monomers (32±2.3- 40±0.2 mmol%), with lower amounts of 3-hydroxyhexanoate (3HHx) (10±0.1-14±2.0 mmol%) and 3-hydroxydodecanoate (12±2.0-14±0.2) and trace amounts (<1 mmol%) of 3-hydroxytetradecanoate (3HTd). Cromwick, Foglia and Lenz (1996) reported the production of a copolymer with a similar composition, 3HO (48 mmol%) and 3HD (28 mmol%), from tallow FFA (animal fat). Muhr et al. (2013) also reported the production of *mcl*-PHA by *P. citronellolis* from tallow-based biodiesel. The polymer had similar 3HO and 3HD contents (40.0-46.5 and 35.8-39.8 mol%, respectively), and lower contents of 3HHD (6.9-9.0 mol%) and 3HHx (5.1 -6.5 mol%).

P. resinovorans also produced a polymer mainly composed of 3HO (43±1.1- 44±0.3 mmol%) and HD (28±1.6 - 33±2.5) with smaller amounts of 3HHx (11±3.8 - 19±1.1 mmol%) and 3HDd (9±2.5 - 12±5.1 mmol%) when cultivated in UCO and OODD. Similar PHA composition, namely, in terms of 3HO (26-37 mmol%), 3HD (32-41 mmol%), 3HHx (8-9 mmol%) and 3HTd (< 4 mmol%) have been reported for a polymer synthesized by *P. resinovorans* from different oil-containing substrates (e.g. FFA, animal fat and vegetable oil (Ashby and Foglia, 1998; Cromwik, Foglia and Lenz, 1996). In the latter studies the polymers also exhibited small amounts (<10%) on unsaturated PHA side-chains, such as 3-hydroxydecenoate ($C_{12:1}$), 3-hydroxytetradecenoate ($C_{14:1}$), determined by mass spectroscopy. However, in this study the unsaturation degree of the side chain monomers was not evaluated.

Pseudomonas strains are known to produce copolymers enriched in 3HO and 3HD monomers, when cultivated on substrates containing an even number of carbon atoms (Rai et al., 2011a), such as the fatty acids of the oil-substrates tested in the present study. Moreover, the presence of high oleic acid content in UCO (38±0.6 wt.%), OODD (70±1.0 wt.%) and FAB (55±0.3 wt.%) (Table 2.2) might have also contributed to *mcl*-PHA enriched in 3HO and 3HD monomers, according to that reported by Ashby and Foglia (1998).

The $\bar{M}_w$ and PDI values of the produced *mcl*-PHA polymers ranged between 0.3-0.4 x 10^5 g mol^{-1} and 1.1-1.7, respectively (Table 2.5). These values are lower than those reported for the same strains (0.9-1.8 x 10^5 g mol^{-1} and 1.6-2.6) (Ashby and Foglia, 1998; Cromwik, Foglia and Lenz, 1996) which may be due to the different cultivation conditions used, namely, the composition of the oil-containing substrates, the concentration of the carbon source and the stage of growth when the cells were harvested (Laycock et al., 2013).

The *mcl*-PHA produced by *P. resinovorans* and *P. citronellolis* were found to be highly amorphous (X_c < 7 %), as expected attending to their monomer composition. The diverse nature of the four co-monomers with high number of carbons and different bulky substituents make difficult the building-up of an organized polymeric structure, being the reason of such low crystallinity degrees. These fluid copolymers exhibit low T_g (-28.9±0.1 to -14.2±1.0ºC) and low T_m (25.2±1.0 to 43.3±0.1ºC). Low T_g and T_m values are commonly found for PHA produced from oil-containing substrates (-46 to -38 ºC) and higher T_m (39 to 48 ºC) (Ashby and Foglia, 1998). The different oil composition, namely, the ratio of saturated and unsaturated FFA chains may influence the final composition of the copolymer, consequently the physical-chemical and thermal properties. Furthermore, monomer' ratio in *mcl*-PHA (e.g. 3HO/3HD) may also have impact on these properties. For example, polymers with higher 3HO content and lower content on 3HD and/or 3HDd (e.g. *mcl*-PHA produced from OODD and UCO) are more fluid at room temperature, while polymers with high amounts of the latter monomers (e.g. *mcl*-PHA from FAB) exhibited a tacky character, which is in accordance to that reported by Ashby and Solaiman (2008).

2.5. Conclusions

Different inexpensive fatty acids-containing wastes were shown to be suitable substrates for cultivation of several bacterial strains for PHA production. OODD, which had previously not been tested, gave the best results in terms of cell growth and PHA synthesis, for all tested strains. The use of this substrate allowed for the production of either *scl*- or *mcl*-PHA polymers, depending on the strain used: *C. necator* was the best *scl*-PHA producer, while *P. resinovorans* yielded good *mcl*-PHA production. Hence, polymers with distinct properties, suitable for different applications, can be obtained from the same substrate (OODD) by cultivation of either bacteria.

3. CHAPTER 3

Production of *scl*-PHAs by *Cupriavidus necator* DSM 428

The results presented in this chapter (sub-chapter B) were published in one peer reviewed short communication:

Cruz, M.V., Paiva, A., Lisboa, P., Freitas F., Alves, V.D., Simões, P., Barreiros S., Reisa, M.A.M. Production of polyhydroxyalkanoates from spent coffee grounds oil obtained by supercritical fluid extraction technology. (2014) Bioresource Technology, 157, 360–363.

(A) Production of *scl*-PHAs by *Cupriavidus necator* DSM 428 when cultivated in used cooking oil (UCO)

3.1. Summary

C. necator DSM 428 was cultivated in bioreactor for PHA production with used cooking oil (UCO) as the sole carbon source. Different feeding strategies were tested, namely, batch, exponential feeding and DO-stat mode. Exponential feeding and DO-stat are common techniques, though rarely explored when oil-containing substrates are used as carbon source for PHA production. In the batch experiment, 15.5±1.5 g L^{-1} of cell dry mass was obtained, with a polymer content of 53±5.4 wt.%, giving an overall volumetric productivity of 5.8±0.62 g L^{-1} day^{-1}. The storage yield was found to be 0.77±0.01 g g^{-1}. With the exponential feeding strategy, the culture accumulated a higher polymer content, 84±4.5 wt% with high storage yield 0.65±0.03 g g^{-1}. However, the highest PHA volumetric productivity, 12.6±0.78 g L^{-1} day^{-1}, was obtained when the DO-stat mode was implemented. The PHA obtained in the three different experiments, was characterized in terms of their composition, physical-chemical, thermal and mechanical properties. All polymers were composed of 3-hydroxybutyrate monomers, P(3HB), exhibiting high molecular mass ranging from 0.6 to 2.6 x 10^5 g mol^{-1} with low polydispersity indexes of 1.2-1.6. Melting and glass transition temperatures were similar for the three different experiments, 172-174 and 3-4 ºC, respectively. P(3HB) exhibited a crystallinity ranging from 44 to 65%. The DO-stat mode was found to be the most suitable strategy among the tested ones for cultivation of *C. necator* with UCO, obtaining a polymer with the typical properties reported for P(3HB).

3.2. Introduction

The cultivation conditions required for PHA production are important factors for the optimization and improvement of this bioprocess, and for further implementation at large scale. Batch and fed-batch cultivation are widely used in the fermentation processes. Batch fermentation is the simplest and primary strategy for any bioprocess. This fermentation has been the most extensively used to investigate the influence of various process operating conditions, use of different microorganisms for production of different types of PHAs and bioconversion of 'novel' carbon sources, namely, agro-industrial wastes including cane molasses (Tripathi et al., 2013), pulp industry waste (Sathiyanarayanan et al., 2013), jatropha oil (Ng et al., 2010) and crude glycerol (García et al., 2013).

The strategy selected depends on the mechanism of PHA synthesis, by the different bacterial strains. Some bacteria requires nutrient limitation (e.g. nitrogen, oxygen, phosphate) and excess of carbon source for efficient production of PHA. This group includes, for example, *C. necator*, *Protomonas estorquens* and *Protomonas oleovorans*. On the other hand, other group of bacteria does not require nutrient limitation for PHA production and synthesis may occur during exponential growth phase (e.g. *Alcaligenes latus*, *Azotobacter vinelandii*) (Chee et al., 2010).

Fed-batch mode is a very suitable cultivation method to adopt, mainly with the microorganism belonging to the first group. In this case, the carbon source is supplemented at the beginning of the run and after a key nutrient depletion, fresh substrate is fed by: pulse feeding; continuous feeding with defined or exponential feed rate; control of nutrient feed through dissolved oxygen (DO) concentration (DO-stat mode) and regulation of pH (pH-stat mode). In a wide range of cases fed-batch can be considered the most efficient way of achieving high cell density cultures with high volumetric productivities, thus reducing production costs (Kaur and Roy, 2015). The process set-up requires the selection of suitable substrate and feeding strategy to control properly the concentration of the carbon source in the cultivation broth. Ideally, feeding strategies should be based on direct and online measurement of substrate in order to have a quick response, supplementing the culture according to its needs, avoiding under or overfeeding, which can be based for example on knowledge of microorganism's predicted growth rate and active biomass production. Commonly, batch experiments must be performed previously, in order to have information about culture's kinetic parameters.

Exponential feeding strategy can be designed to obtain a growth rate close to its maximum (μ_{max}) in the growth phase, while a linear or decaying linear feed rate is often used in a non-growth associated production phase (Sun et al., 2007). Some researchers had adopted that strategy to produce PHA with *Cupriavidus necator* DSM 545 (Mozumder et al., 2014) and *Pseudomonas putida* KT2440 (Sun et al., 2006) using glucose as sole carbon source.

Feeding, as in pH-stat and DO-stat modes may also be based on physiologic state of the cell (Lee et al., 1999), namely depending on acid production or oxygen utilization (Sun et al., 2006). However, as far as the author knows, there are no reports in the study of DO-stat mode for feeding UCO to PHA accumulating cultures. It is frequent to have pulse/intermittent feeding of oil-containing substrates, such as soybean oil (da Cruz Pradella et al., 2012), waste frying oil (Follonier et al., 2014) and waste rapeseed oil (Obruca et al., 2010).

The composition of oil based substrates and selected bacterial strain have impact on the process performance and polymer quality. Among the tested *scl*-PHA producers, *C. necator* DSM 428 was found to be a very robust bacterium, capable to utilize all the screened feedstocks for both cell growth and PHA accumulation, as reported in Chapter 2 (Tables 2.3 and 2.4). The best feedstocks for *C. necator* cultivation were found to be used cooking oil (UCO) and olive oil deodorizer distillate (OODD). UCO was selected for further studies for *scl*-PHA bioreactor production, because it is a readily available and inexpensive carbon source within those tested. Moreover, UCO has lower variability in terms of chemical composition than OODD, which is highly dependent on process refining conditions. The UCO used in bioreactor cultivations was the same used in experiments reported in Chapter 2.

Taking this into account, the main goal of this chapter was to assess the kinetic parameters of *scl*-PHA production from UCO in bioreactors operated under batch and fed-batch modes. Two different feeding strategies were tested, namely, exponential feeding and DO-stat mode, aiming at selecting the more suitable one, traducing the best microorganism performance in terms overall PHA production.

3.3. Material and Methods

3.3.1. PHA production

3.3.1.1. Microorganism and media

C. necator DSM 428 was reactivated from stock cultures kept at -80 ºC and cultivated as described in Chapter 2, section 2.3.2.1. Afterwards, the culture was transferred to 100 mL mineral medium (composition described in chapter 2, section 2.3.2.1) supplemented with 20 g L^{-1} UCO as sole carbon source. Inocula for the bioreactor experiments were incubated in an orbital shaker at 30 ºC and 200 rpm for 48 hours.

3.3.1.2. Bioreactor cultivation

Bioreactor cultivations were performed in 2 L bioreactors (total working volume of the bioreactor) (BioStat B-Plus, Sartorius, Germany), with an initial working volume of 1.5 L. The inoculum was 10% (v/v) of the initial reactor working volume. The bioreactor was a double wall (jacketed) culture vessel with round bottom, baffles and lifting handles equipped with two 6-paddle impeller.

C. neactor was cultivated in mineral medium (described in Chapter 2, section 2.3.2.1) initially supplemented with 20 g L^{-1} UCO. The cultivation conditions applied for each bioreactor experiment are described in Table 3.1.

Table 3.1: *C. necator* bioreactor experiments using UCO as sole carbon source under different operation modes.

Experiment	Operation Mode	$[UCO]_{initial}$ (g L^{-1})	$[NH_4^+]_{initial}$ (g L^{-1})	Feeding strategy	pH control
A	**Batch**	20	1	-	NaOH
B	**Fed-batch**	20	1	Exponential	NaOH
C	**Fed-batch**	20	1	DO-stat	NH_4OH; NaOH

In all experiments (A, B and C), the temperature was maintained at 30±1 ºC and the pH was controlled at 6.8±0.2 by the automatic addition of titration solution (2 M NaOH and/or 25% v/v NH_4OH). The air flow rate was kept constant (1 vvm- volume of air per volume of cultivation broth per minute) and the dissolved oxygen concentration (DO) was maintained at 30% air saturation by the automatic adjustment of the stirring rate (400 – 800 rpm). In experiments B and C the reactors were operated under nitrogen limitation in the fed-batch phase for enhanced PHA production.

Experiment A was operated in batch mode for 32 hours. The pH was controlled with 2 M NaOH. In experiment B, the bioreactor was operated with an initial batch phase of 20 hours, followed

by a fed-batch phase until 50 hours of the run. During the fed-batch phase, the culture was fed with UCO according to an exponential profile, as described by equation (11):

$$F_s(t) = q_s \times X \times e^{\mu(t-t_f)} \quad \text{Equation (11)}$$

where F_s(t) is the feeding rate (g UCO h^{-1} L^{-1}); q_s (gS gX^{-1} h^{-1}) is the biomass specific substrate uptake rate, X (g L^{-1}) is the active biomass concentration at the end of the exponential phase, μ (h^{-1}) is the specific growth rate, t (h) is the initial time of feeding and t_f (h) the end of batch time, respectively. The X and q_s were calculated based on previous batch experiments. Afterwards, the feeding was stopped and the cultivation was prolonged until 96 hours for consumption of the UCO fed to the bioreactor.

In experiment C, the pH was also initially controlled with 25% (v/v) ammonium hydroxide solution and then changed to 2 M NaOH at the end of exponential phase (22h) to impose nitrogen limiting conditions. The cultivation run was performed in batch phase for 18 hours followed by a fed-batch phase until 40 hours. During the fed-batch phase, the stirring rate was kept constant (500 rpm) and the DO was controlled at 30% air saturation by the automatic feeding with UCO.

Samples (15±5 mL) were periodically withdrawn from the bioreactor for CDM and PHA and residual UCO quantification.

3.3.1.3. Calculations

The maximum specific growth rate (μ_{max}, h^{-1}) was determined from the linear regression slope of the exponential phase of Ln $X_{(t)}$ versus time, where $X_{(t)}$ (g L^{-1}) is the active biomass, which was calculated following equation (4) (section 2.3.2.5, Chapter 2).

The biomass specific substrate uptake rate (q_s, gS gX^{-1} h^{-1}) was calculated by the slope of substrate consumption ($S_{(t)}$-$S_{(0)}$, g L^{-1}) versus the production of active biomass ($X_{(t)}$-$X_{(0)}$, g L^{-1}) from the beginning of the run (t=0) until time t, following equation (12):

$$\left[S_{(t)} - S_{(0)}\right] = \frac{q_s}{\mu}\left[X_{(t)} - X_{(0)}\right] \quad \text{Equation (12)}$$

The kinetic parameters (q_s, X and μ) used for the profile feeding of experiment B were calculated based in results obtained from the batch experiment A.

The biomass specific product formation (q_p, gPHA gX^{-1} h^{-1}) was determined similarly to q_s; by the slope of PHA production ($P_{(t)}$-$P_{(0)}$, g L^{-1}) versus the production of active biomass ($X_{(t)}$-$X_{(0)}$, g L^{-1}) from the beginning of the run (t=0) until time t (units?), following equation (13):

$$\left[P_{(t)} - P_{(0)}\right] = \frac{q_p}{\mu}\left[X_{(t)} - X_{(0)}\right] \qquad \text{Equation (13)}$$

3.3.1.4. Analytical techniques

The CDM, PHA and residual oil concentration over the cultivation run were quantified as described in Chapter 2, section 2.3.2.4, slightly modified. Briefly, 4-5 mL broth samples were mixed with *n*-hexane (1:1, v/v) and centrifuged (15 777 × *g*, 10 min). Afterwards, the biomass pellet was collected, washed with deionized water and lyophilized for the gravimetric CDM quantification, while 2-3 mL of the upper hexane layer containing the residual UCO were transferred to pre-weighed tubes and placed in a fume hood at room temperature for 24 h, for solvent evaporation and oil quantification. The PHA content in the bacterial cells was determined as described in section 2.3.2.4 of Chapter 2, with slight modifications. Briefly, the methanolysis of dried cells samples (2-3 mg) was performed with 1 mL 20% (v/v) sulphuric acid in methanol (Sigma-Aldrich, HPLC grade) and 1 mL heptadecane in chloroform (1 g L^{-1}) (Sigma-Aldrich, HPLC grade). The reaction took place at 100 ºC during 3.5 hours. In this case, heptadecane was used as internal standard. The resulting methyl esters were analysed as described in section 2.3.2.4 of Chapter 2.

3.3.2. PHA extraction and purification

At the end of the cultivation runs, the broth was collected, washed with n-hexane (1:1, v/v) to remove residual oil and centrifuged (7012 × *g*, 20 min) to collect the biomass. The biomass was washed twice with deionised water (200 mL).

PHA was recovered from dried biomass (~10 g) by Soxhlet (250 mL) extraction with chloroform, at 70 ºC, for 24 hours. Afterwards, the solution was filtered with 0.45 µm pore size filters (GxF, GHP membrane, PALL) to remove cell debris, and precipitated in cold ethanol (1:10, v/v) under strong stirring. The polymer was collected by centrifugation (7012 × *g*, 20 min), dried at room temperature and stored at 4 ºC.

3.3.3. Scanning electron microscopy

Cells from cultivation broth samples were observed by scanning electron microscopy (SEM). At the end of cultivation run, 1 mL sample broth was centrifuged (9800 × g, 2 min). The supernatant was discarded and the cell pellet was suspended in 1 mL phosphate buffered saline (PBS) solution and centrifuged again. The supernatant was discarded and 330 µL of PBS solution and 1 mL of 4% (v/v) formaldehyde solution were added to the cell pellet. The mixture was incubated for 2 h at 4 ºC to fix the cells. Afterwards, the cells were centrifuged (9800 × g, 2 min) and washed with PBS solution.

The supernatant was removed and 500 µL PBS and 500 µL ethanol 96% were added to the cells, in order to fix the cells. Scanning electron microscopy (SEM) observations were carried out using a Carl Zeiss AURIGA CrossBeam Focused Ion Beam SEM (FIB-SEM) workstation coupled with energy dispersive X-ray spectroscopy (EDS). The sample were previously coated with gold with an Ir conductive film for avoiding charge effects.

3.3.4. PHA characterization

3.3.4.1. PHA composition

Polymer composition and purity were evaluated by GC analysis, using the modified Lageveen et al. (1988) method described in section 2.3.2.4.

3.3.4.2. Molecular mass

Weight average ($\bar{M}_w$) and number average ($\bar{M}_n$) molecular mass were determined as described in section 2.3.3.1 of Chapter 2.

3.3.4.3. Thermal properties

The thermal properties of the polymers were determined by differential scanning calorimetry (DSC) as described in section 2.3.3.2 of Chapter 2.

3.4. Results and Discussion

3.4.1. PHA production in bioreactor

In this chapter, the cultivation of *C. necator* DSM 428 in bioreactor using UCO as the sole carbon source was studied by testing different cultivation strategies. Several bioreactor experiments were performed in order to determine the kinetic parameters related to cell growth and PHA production under different cultivation modes: two batch experiments that ran in parallel under the same cultivation conditions (experiment A); and two fed-batch experiments set at different feeding strategies exponential feeding (experiment B) and DO-stat mode (experiment C) (Table 3.1).

3.4.1.1. Batch cultivation

The two batch cultivations (experiment A) were performed for 35 hours using an initial UCO concentration of 20 g L^{-1}. Kinetic parameters, such as active biomass, PHA production and residual oil concentration were represented as the mean values obtained for both assays (Figure 3.1).

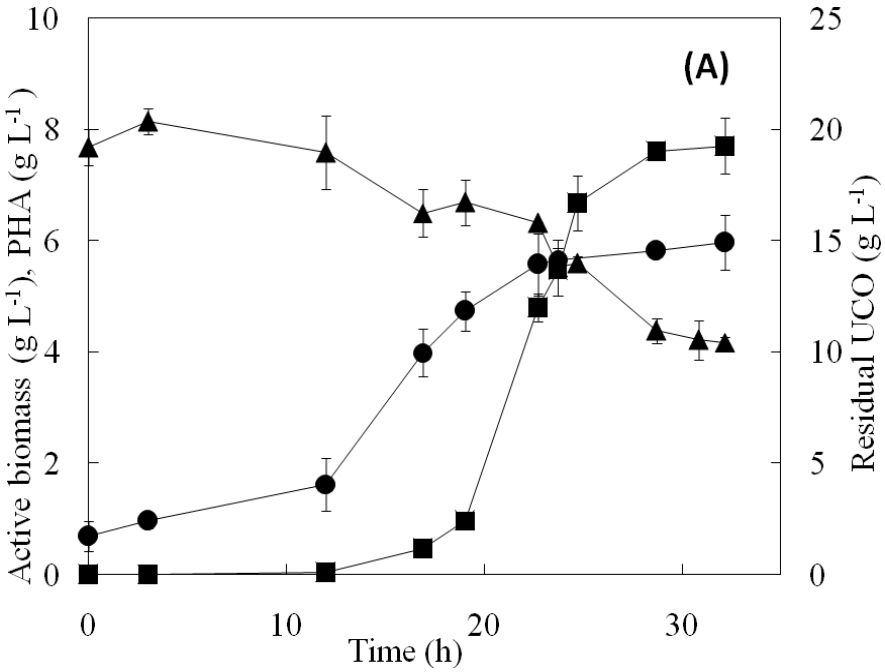

Figure 3.1: Quantification of residual UCO (▲), PHA (■) and active biomass (●) production from *C. necator* cultivated in batch mode with UCO as sole carbon source.

The culture grew with a maximum specific growth rate of 0.13±0.02 h^{-1} reaching an active biomass of concentration of 6.0±0.5 g L^{-1} at 23 hours of cultivation. PHA production started at around 10 hours, showing polymer production was not growth associated. At the end of the exponential growth phase (22 hours), 4.8±0.25 g PHA L^{-1} were achieved (Figure 3.1). Afterwards, the culture stopped growing, which was probably related to the depletion of the nitrogen source in the cultivation broth. Nevertheless, PHA continued to be accumulated up to 7.7±0.64 g L^{-1} (Figure 3.1). The final polymer content in the biomass was 53.0±5.4 wt.% and the PHA volumetric productivity was 5.8±0.62 g L day^{-1} (Table 3.2). The overall consumption of oil was 10.2±0.72 g L^{-1} and the storage and growth yields were 0.77±0.01 g g^{-1} and 0.54±0.01 g g^{-1}, respectively. The experimental procedure adopted for oil determintation might have a lack of accuracy, due to the difficulty in handling byphasic samples, i.e., hexane, oil and cultivation broth. Thus, the storage and growth yield determination might be afected due to the experimental error.

The biomass specific substrate uptake rate (q_s) and product formation (q_p) were 0.161±0.031 g UCO gX^{-1} h^{-1} and 0.235±0.031 g PHA gX^{-1} h^{-1}).

The values obtained in this study, for the PHA batch production, in terms of CDM (15.5±1.5 g L^{-1}) and PHA (7.7±0.64 g L^{-1}) were within those reported in literature, when emulsified palm oil, EPO (10 g CDM L^{-1} and 7.9 g PHA L^{-1}) (Budde et al., 2011a), soybean oil (SOY) (15 g CDM L^{-1} and 12.5 g PHA L^{-1}) (Park and Kim, 2011b) and waste rapeseed oil (WRO) (25 g CDM L^{-1} and 20 g PHA L^{-1}) (Obruca et al., 2014a) were used as carbon sources (Table 3.2). The overall volumetric productivity obtained in experiment A (5.8±0.62 g L^{-1} day^{-1}) was higher than that reported when EPO

(2.6 g L^{-1} day^{-1}) (Budde et al., 2011) and SOY (3.4 g L^{-1} day^{-1}) (Park and Kim, 2011) were used, but lower than that obtained with WRO (17 g L^{-1} day^{-1}) (Obruca et al., 2014a). However, in the later the storage yield was lower (0.67 g g^{-1}) than that obtained with UCO (0.77±0.01 g g^{-1}), EPO (0.61-0.84 g g^{-1}) and SOY (0.82 g g^{-1}), showing UCO is a suitable carbon source to be used in bioreactor production of PHA. Generally, when compared to carbohydrates, triglycerides (which are the main structures of vegetable oils) are considered better carbon sources in terms of PHA conversion yield, due to their metabolism pathway. The oxidation of fatty acids to acetyl-CoA uses a more conservative carbon pathway that that involved in oxidation of carbohydrates (da Cruz Pradella et al., 2012).

Several studies have been carried out describing PHA batch production by *C. necator* with several different substrates, including the oil-containing substrates (Budde et al., 2011; Park and Kim, 2011, Obruca et al., 2014; Morais et al., 2014). In fact, this cultivation strategy is very popular due to the flexibility and low operation costs (Gonzaléz-Contreras et al., 2015). However, batch cultures have the disadvantage of usually resulting in low yields and productivities (Peña et al., 2014). For this reason, fed-batch strategies have to be more explored to optimize PHA production.

3.4.1.2. Fed-batch cultivation with exponential feeding

C. necator was cultivated under fed-batch mode using an exponential feeding strategy. The initial UCO concentration was 20 g L^{-1}, similarly to experiment A.

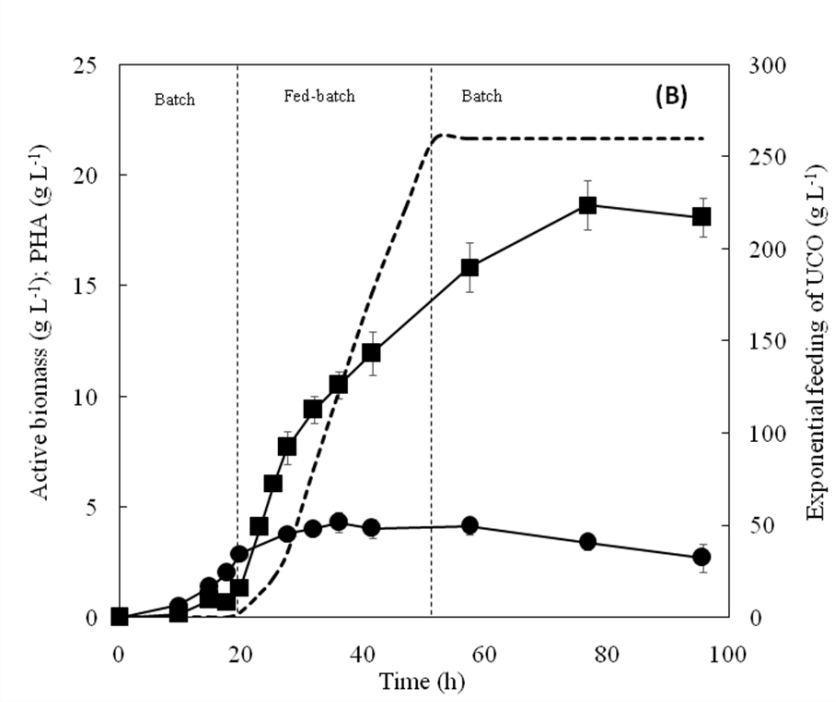

Figure 3.2: Quantification of PHA (■) and active biomass (●) production by *C. necator* when cultivated in fed-batch mode, by exponential feeding (⋯) of UCO over cultivation time.

During the initial batch phase (20 hours) the culture achieved and active biomass of 2.9±0.12 g L^{-1} and a polymer concentration of 1.4±0.31 g L^{-1} (Figure 3.2). During this time period the biomass polymer content reached 20±6.5 wt.%, which is similar to the value observed in experiment A , at the same cultivation time (17±1.5 wt.%). Afterwards, the culture was fed with UCO based on the exponential profile described on section 3.3.1.3 (Equation 11) until 50 h of the run (Figure 3.2). The exponential feeding strategy was designed to maintain maximal cell growth rate (0.14±0.02 h^{-1}), within the exponential growth phase. Thus, the substrate was supplied according the UCO consumption. In this case, the feeding rate was based on biomass specific substrate uptake rate of 0.161±0.031 g UCO gX^{-1} h^{-1} obtained in experiment A.

The oil feeding was stopped at 50 hours since it was observed an intense yellowish color in the bioreactor which was indicative of an accumulation of unconsumed UCO. Nevertheless, the experiment was prolonged up to 96 hours to allow the culture to use the accumulated UCO. This UCO accumulation in the bioreactor might have been caused by the over estimation of the profile feeding. In fact, the exponential feeding profile was also designed considering an active biomass concentration of 8.0 g L^{-1} at the beginning of fed-batch phase. However, by that time the real active biomass was only at 3.0 g L^{-1}, meaning the feeding rate was probably over estimated for this cultivation run.

The culture achieved final CDM and PHA concentrations of 21.3±0.93 and 17.9±0.88 g L^{-1}, respectively. This polymer production corresponds to a volumetric productivity of 4.5±0.22 g L^{-1} day^{-1}. At the end of the run, the biomass attained a polymer content of 84±4.5 wt.% (Table 3.2), which is very similar to the PHA accumulation (85-96 wt.%) reported in literature for *C. necator* using other oil-containing substrates (Kahar et al., 2004). Due to the small sample volume withdrawn over the cultivation run, it was not possible to accurately quantify the residual oil present in the broth in every sample, especially during the fed-batch phase, in which UCO accumulation could be observed. Hence, at the end of the run, using a large volume of cultivation broth, the overall consumption of oil, 28.0±1.30 g L^{-1} was determined. The growth and storage yields were 0.11±0.01 and 0.65±0.03 g g^{-1}, respectively. However, over the storage phase (23-96 h), the storage yield (0.74±0.09 g g^{-1}) was similar to that obtained in experiment A (0.77±0.01 g g^{-1}). Also, the storage yields obtained in experiment B (0.65 to 0.74 g g^{-1}) were within the range of values reported in literature for pulse feeding (0.61 to 0.85 g g^{-1}) (da Cruz Pradella et al., 2012; Kahar et al., 2004; Ng et al., 2010; Park and Kim, 2011). With the tested exponential feeding strategy it was possible to increase both CDM (from 15.5±1.5 to 21.3±0.93 g L^{-1}) and PHA accumulation (from 53±5.4 to 84±4.5 wt.%) comparing to the batch experiment A. However, the final PHA volumetric productivity was slightly lower (4.5±0.22 g L^{-1} day^{-1}) than that obtained in experiment A (5.8±0.62 g L day^{-1}). Since, UCO accumulated in the bioreactor and PHA volumetric productivity was not improved compared to experiment A, the feeding rate defined for this bioprocess might not be appropriate. Actually, there is not much research regarding the feeding strategies of oil-containing substrates with *C. necator* cultures and, for this reason, this strategy was tested. Further studies have to be performed with better leveled exponential

feeding rate. Exponential feeding has been demonstrated to be an efficient automated strategy that has been applied to other fed-batch cultures, such as, for example, *Pseudomonas putida* grown on glucose as carbon source (Sun et al., 2006) and *C. necator* using fructose and canola oil (Rathinasabapathy et al., 2014).

Recently, Mozumber and co-workers (2014) tested a similar exponential strategy for cultivation of *C. necator* DSM 545 using glucose as carbon source. Their study confirmed that exponential feeding of glucose was inefficient to maintain the substrate concentration at the optimal level for the culture since it resulted in a long term cultivation run with over or underfeeding. The authors think this might be due to deviations in the parameter values from the initially estimated values resulting in growth repression or cell starvation. Nevertheless, it might be a good strategy to be used in combination with other feeding techniques, such as a strategy based on alkali-addition monitoring, called 'combined substrate feeding', as Mozumber et al. (2014) suggested.

3.4.1.3. Fed-batch cultivation under a DO-stat mode

In experiment C, *C. necator* was cultivated in UCO for 39 hours (Figure 3.3). After a short lag phase, the culture had a maximum specific growth rate of 0.21±0.01 h^{-1} which was higher than that observed for experiments A and B, which might be related to pH control with ammonium hydroxide that promoted a faster cell growth.

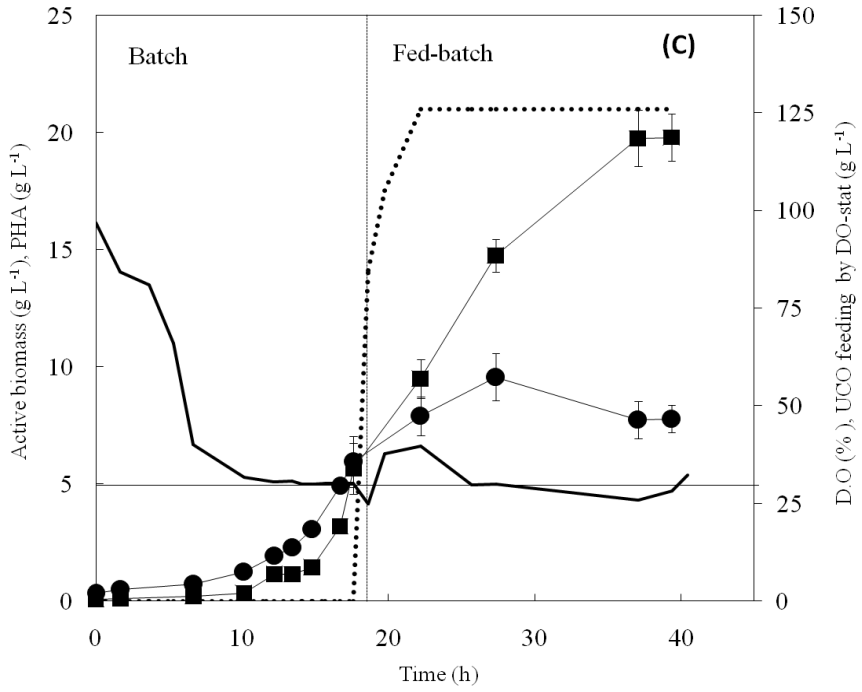

Figure 3.3: Quantification of PHA (■) and active biomass (●) production by *C. necator* cultivated under DO-stat mode (experiment C), i.e. UCO is automatically fed (….) as a function of DO concentration (—) that was kept at 30% air saturation.

During the initial batch phase (17 hours), 5.9±1.09 g L^{-1} of active biomass and 3.2±0.01 g L^{-1} of PHA were produced which were higher than those obtained for the same period of time in experiments A (4.5 g L^{-1} and 0.96 g L^{-1}, respectively) and B (2.9 g L^{-1} and 1.4 g L^{-1}). Since pH was controlled with ammonium hydroxide, the nitrogen was available in higher quantity. Thus, probably stimulated more growth in this time interval.

Afterwards, a DO-stat mode was implemented by feeding the culture with UCO as a function of the DO concentration that was set at 30% of air saturation (Figure 3.3). With this strategy, a maximum CDM of 27.2±0.46 g L^{-1} with a polymer content of 77±5.7 wt.% were achieved at 40 hours of cultivation (Table 3.2). Using this DO-stat mode of cultivation led to an overall PHA production almost triplicated (12.6±0.78 g L^{-1} day^{-1}) compared to that obtained in experiment B with the exponential feeding strategy (4.5±0.22 g L^{-1} day^{-1}) (Table 3.2).

Also, CDM and PHA production observed in experiment C (27.2±0.46 and 19.8±1.8 g L^{-1}, respectively) were improved when compared to experiment B (21.3±0.93 and 17.9±0.88 g L^{-1}, respectively) showing the automatic feeding implemented in experiment C might be a good feeding strategy to improve PHA production by *C. necator* using UCO. Actually, DO-stat feeding strategy does not depend on previous knowledge on culture's performance, being easier to implement in a bioprocess than for example the exponential feeding. The PHA content (77±5.7 wt.%) and storage yield (0.52±0.07 g g^{-1}) were found to be lower than the values obtained for experiment B (84±4.5 wt.% and 0.65±0.03 g g^{-1}, respectively). Probably, in this experiment, more carbon was deviated for cell growth and maintenance, than in previous experiments, as shown by the higher growth yield (0.21±0.02 g g^{-1}). In fact, by controlling the pH with ammonium hydroxide enhanced cell growth and, thus, more UCO was needed to fulfill the cell metabolism. The overall consumption of UCO in experiment C was 38.0±2.0 g L^{-1}, which was higher than that observed for experiment B (28.0±1.30 g L^{-1}).

In fact, the experiments reported in literature were designed in multiple stages of excess of carbon and nutrient limitation, over the cultivation run, promoting both high cell density and high cell PHA content. In this study, the fed-batch runs were focused on the PHA production, using different automated feeding strategies. Thus, no optimization of the nitrogen sources to promote high cell density cultivation was performed. Taking this into account, it was expectable to have lower values of CDM than those reported in literature.

Nevertheless, the PHA cell content obtained for experiment C (77±5.7 wt.%) was within the range obtained for pulse feeding with SOY (50 to 81 wt.%) (Kahar et al., 2004; Park and Kim, 2011 and da Cruz Pradella et al., 2012). The volumetric productivity obtained with DO-stat mode (12.6±0.78 g L^{-1} day^{-1}) was within the large range of values reported for fed-batch cultivations with SOY pulse feeding (6.3 to 60 g L^{-1} day^{-1}) (Kahar et al., 2004; Park and Kim, 2011). In fact, one of the big advantages of the automatic feeding strategy is to have the feeding as a function of a direct, fast and online response of the culture (i.e. dissolved oxygen concentration). There are some reports on the

successful production of PHA using DO-stat feeding strategy using *Cupriavidus* species. For example, using the DO-stat mode, *C. necator* was able to produce 7.7-13.2 g PHA L^{-1} with fructose and γ-butyrolactone as carbon sources (Kim, Lee and Kim, 2005). On the other hand, using the DO-stat mode, it was possible to regulate the 4-hydroxybutyrate (4HB) monomer in the copolymer composition from 0–67 mol% by sequential feeding of γ-butyrolactone and supplementing oleic acid to *Cupriavidus* sp. USMAA 1020 (Faezah et al., 2011). Furthermore, a combination of pH-stat with DO-stat strategies was used with *C. necator* H16 reaching >2 g PHA L^{-1} day^{-1} with a mixture of sodium salts of acetic, propionic and butyric acids (Huschner et al., 2015).

In fact, as far as the author know, there are no reports on the use of a DO-stat strategy to supplement oil-containing substrates, such as UCO, for the fed-batch cultivation of *C. necator* DSM 428 strain, which was shown in this study to be the best strategy among the tested ones.

Table 3.2: Kinetic parameters obtained for cultivation of *C. necator* DSM 428 in UCO in batch and fed-batch modes, with different feeding strategies, and comparison to values reported in literature using other oil-containing substrates.

Operation Mode	**Batch bioreactor (A)**	**Fed-batch bioreactor (B)**	**Fed-batch bioreactor (C)**	**Batch bioreactor**	**Batch bioreactor**	**Batch Bioreactor[a]**	**Batch bioreactor**	**Batch bioreactor**	**Fed-batch bioreactor**	**Fed-batch bioreactor**	**Fed-batch Bioreactor[a]**	**Fed-batch Bioreactor[b]**	**Fed-batch bioreactor**
Feeding strategy	-	Exponential Profile	DO-stat	-	-	-	-	-	Pulse[c]	Pulse	Pulse	Pulse	Pulse
Initial Volume (L)	1.5	1.5	1.5	20	0.4	2.5	1.35	4	20	5	2.5	10	7
Substrate	UCO	UCO	UCO	ROR	EPO	SOY	WRO	FAT	ROR	SOY	SOY	SOY	Jatropha
$[S]_{initial}$ (g L^{-1})	20	20	20	20	20	20	30	20	20	20	20	10-40	20
μ_{max} (h^{-1})	0.13±0.02	0.14±0.02	0.21±0.01	n.a.	n.a.	n.a	n.a.	0.15	n.a.	n.a.	n.a.	0.31	n.a.
CDM (g L^{-1})	15.5±1.5	21.3±0.93	27.2±0.46	6.3	10	15	25.4±0.9	11.2±2.26	15.4	118-126	32	25-83	65.2
PHA_{max} (wt.%)	53±5.4	84±4.5	77±5.7	19.7	79	83	79.2±4.2	56±2.42	41.3	72-76	78	50-81	76
PHA (g L^{-1})	7.7±0.64	17.9±0.88	19.8±1.8	1.2	7.9	12.5	20.1±1.2	6.4±1.50	6.4	85-96	25	13-67	50
X (g L^{-1})	6.0±0.5	3.4±0.35	7.8±0.59	5.1	2	2.5	n.a.	n.a.	9	30-33	7	15-20	15.2
$Y_{P/S}$ (g g^{-1})	0.77±0.01	0.65±0.03	0.52±0.07	n.a.	0.61	0.82	0.67	0.50±0.15	n.a.	0.72-0.76	0.8	0.61-0.85	0.78
$Y_{X/S}$ (g g^{-1})	0.54±0.01	0.11±0.01	0.21±0.02	n.a.	0.13	n.a	n.a.	n.a.	n.a.	n.a.	n.a.	n.a.	n.a.
r_p (g L^{-1} day^{-1})	5.8±0.62	4.5±0.22	12.6±0.78	0.4	2.6	3.4	17	7.9±1.68	2.1	21-24	6.25	16-60	25
Reference	This study	This study	This study	Füchtenbusch, Wullbrandt and Wullbrandt , 2000	Budde et al., 2011a	Park and Kim, 2011	Obruca et al., 2014	Morais et al., 2014	Füchtenbusch, Wullbrandt and Wullbrandt , 2000	Kahar et al., 2004	Park and Kim, 2011	da Cruz Pradella et al., 2012	Ng et al., 2010

[a] Using *C. necator* DSM 530;
[b] Using *C. necator* DSM 545.
[c] The culture was fed three times during cultivating run based on the DO concentrration decrease.
(ROR- residual oil from rhamnose production; EPO - emulsified palm oil; SOY - soybean oil; WRO - waste rapeseed oil; FAT-margarine fat waste).

3.4.2. Visualization of cell morphology

C. necator cells collected at the end of experiment B were observed by scanning electron microscopy (SEM) coupled with focused ion beam (FIB) (Figure 3.4).

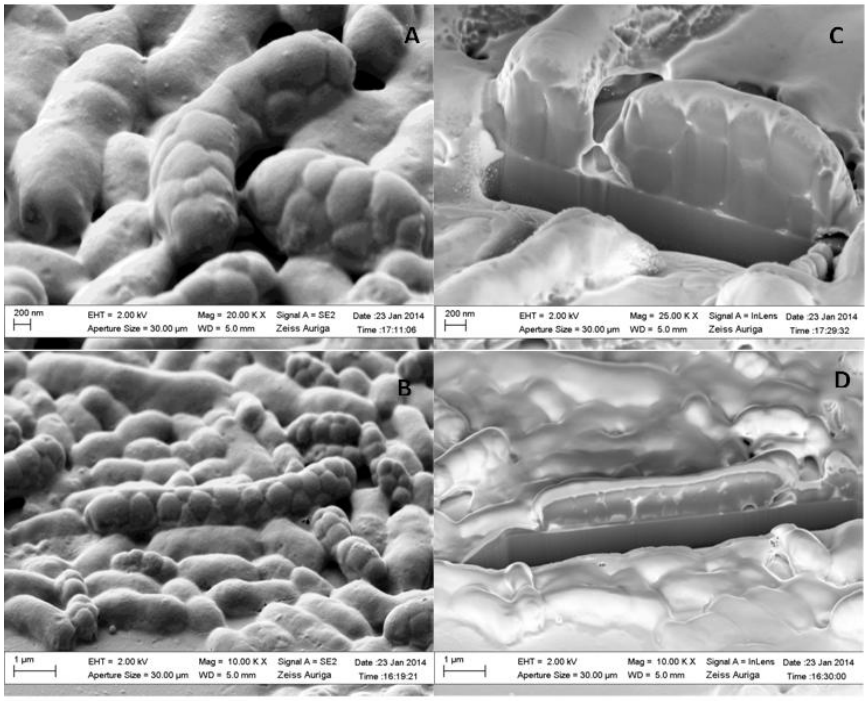

Figure 3.4: SEM images of the *C. necator* cells morphology at the end of experiment B: (A) isolated bacterial cells acquired at 2kV and 20K x magnification; (B) bacterial cells acquired at 2kV, 10K x magnification (C) SEM-FIB cross-section of image A at 2kV, 25K x magnification and (D) of image B at 2kV, 10K x magnification.

The observed cells were collected from experiment B, at the end of the run when the cells had the highest polymer content (84±4.5 wt.%). The main interest in this study was to observe the cells morphology and the intracellular granules.

Figure 3.4A and 3.4B exhibited the morphology of *C. necator* cells, at the final stage of the cultivation. Due to the maximum PHA accumulation obtained, several spherical eruptions were observed in the cells' surface. In the small cell of Figure 3.4A, approximately 7-8 individual spheres could be counted. Also, when the cells were cut with FIB and a cross-section was acquired, around 8 round-shaped granules could be distinguish. In the large cell of Figure 3.4B, approximately 16 spheres can be seen. However, in the cross-section image (Figure 3.4D) it is almost impossible to distinguish individual granules. This might be indicative of granules overlapping when the maximum polymer accumulation is achieved, thus forming clusters inside the cells. According to Laycock et al. (2013) an average of 10 granules of PHA can be produced

inside the bacterial cells comprising almost the entire its volume when maximum accumulation is achieved. These granules have a typical diameter of 0.2 to 0.7 mm and consist of 97.7 wt.% PHA, 1.8 wt.% protein and 0.5 wt.% lipids (Koller et al., 2010).

Commonly, observation of PHA granules is performed by transmission electron microscopy (TEM) equipment. Tian et al., (2005) studied the granule formation and degradation in *C. necator* wild strain. Also, Volova et al. (2013) studied the cells morphology and P(3HB) granule formation using TEM. The latter electron microscopy studies revealed a decreasing in cell size concomitant with enlargement of size and number of intracellular granules, and inhibition of cell division during intracellular polymer production (Volova et al., 2013).

Actually, as far as the author knows, SEM-FIB has not been used for cell morphology and granules observation. With FIB-SEM it was possible to obtain 3D images of the cells morphology, namely the spherical eruptions that cannot be observed by transmission electron microscopy. Thus, could be a suitable approach for further studies regarding cell morphology and granule formation, along the cultivation cycle.

3.4.3. PHA characterization

The polymer accumulated by *C. necator* cells during experiments A, B and C was extracted and characterized in terms of composition, molecular mass distribution and thermal properties (Table 3.3).

The polymer produced from UCO in all batch and fed-batch experiments was a 3-hydroxybutyrate homopolymer, poly(3-hydroxybutyrate), P(3HB), which is in accordance to the reported in literature for polymers produced by *C. necator* when cultivated in oil-containing substrates as sole carbon sources (Budde et al., 2011; da Cruz Pradella et al., 2012; Füchtenbusch, Wullbrandt and Steinbüchel, 2000; Kahar et al., 2004; Morais et al., 2014; Ng et al., 2010; Obruca et al., 2014a; Park and Kim, 2011). Actually, *C. necator* is also able to produce copolymers composed by different monomer units with the same and/or high number of carbons (e.g. C_4, C_5 and C_6), but only by medium supplementation with precursors of different monomer fractions. For example, propanol was used as precursor to obtain poly(3-hydroxybutyrate-*co*-3-hydroxyvalerate), P(3HB-3HV) (Obruca et al., 2010), and γ-butyrolactone was used to obtain poly(3-hydroxybutyrate-*co*-4-hydroxybutyrate) copolymers (Kahar et al., 2004).

Apparently, the operation mode affected the average ($\bar{M}_w$) and number ($\bar{M}_n$) molecular mass distribution of the produced P(3HB). Batch cultivation (experiment A) resulted in polymers with $\bar{M}_w$ and $\bar{M}_n$ values of 1.7 x 10^5 and 1.1 x 10^5 g mol^{-1}, respectively (Table 3.3).

Value of the same order of magnitude (2.6 and 1.7x 10^5 g mol^{-1}, respectively) were obtained for the P(3HB) polymer produced in experiment C, under DO-stat mode, while lower values (0.6 and 0.5x10^5 g mol^{-1}, respectively) were obtained in experiment B, under exponential feeding (Table 3.3).

In fact, the low average molecular mass P(3HB) obtained for the fed-batch B (0.6x10^5 g mol^{-1}) might be related to the prolonged cultivation time, until 96 hours. According, to Budde et al. (2011b), PHA is continuously turned over by *C. necator*, even under PHA storage conditions, and this turnover is accompanied by a decrease in average polymer molecular mass. Thus, apparently, it is important to harvest the biomass from the cultivation broth as soon as maximum PHA accumulation has been reached, as additional time will lead to a decrease in average polymer chain length (Budde et al., 2011b).

Table 3.3: Physical-chemical and thermal characterization of P(3HB) produced by *C. necator* from UCO and comparison to P(3HB) produced from other oil-containing substrates.

Properties	**Batch bioreactor (A)**	**Fed-batch bioreactor (B)**	**Fed-batch bioreactor (C)**	**Batch bioreactor**	**Batch bioreactor**	**Fed-batch bioreactor**
	UCO	UCO	UCO	WRO	FAT	SOY
$\bar{M}_w$ **(g mol^{-1}) x 10^5**	1.7	0.6	2.6	5.7	n.a.	12.5
$\bar{M}_n$ **(g mol^{-1}) x 10^5**	1.1	0.5	1.7	2.2	n.a.	3.3
PDI	1.6	1.2	1.6	2.7	n.a.	3.8
T_m **(ºC)**	172	174	174	n.a.	173	n.a.
T_g **(ºC)**	3	n.d.	4	n.a.	7.9	n.a.
ΔH_m **(J g^{-1})**	65	95	75	n.a.	82.6	n.a.
X_c **(%)**	44	65	52	n.a.	57	n.a.
References	This study	This study	This study	Obruca et al., 2014a	Morais et al., 2014	Park and Kim, 2011

n.d. - not detected

n.a. - not available

The $\bar{M}_w$ and $\bar{M}_n$ values obtained in this study were lower than those reported for P(3HB) produced from WRO (5.7 x 10^5 and 2.2 x 10^5 g mol^{-1}, respectively) (Obruca et al., 2014a) and SOY (12.5 x 10^5 and 3.3 x 10^5 g mol^{-1}, respectively) (Park and Kim, 2004), but of the same order of magnitude. However, very close to the lower value of the typically range of average molecular mass distribution (2-30 ×10^5 g mol^{-1}) of P(3HB) reported for different bacterial strains and carbon sources (Laycock et al., 2013). For example, P(3HB) with ultra-high molecular mass (2.7 x 10^6 g mol^{-1}) was produced by recombinant *E. Coli* JM109 from glucose (Kabe et al., 2012). The polydispersity index (PDI) of the polymers characterized in this study

were found to be lower (1.2-1.6) than those reported for P(3HB) obtained from WRO (2.7) (Obruca et al., 2014a) and SOY (3.8) (Park and Kim, 2004) (Table 2), meaning that the P(3HB) produced in this study was highly homogeneous.

Thermal properties were also assessed after polymer extraction and purification. Melting (172-174 ºC) and glass transition temperatures (3-4 ºC) of the P(3HB) were very similar, suggesting these thermal properties were independent on the feeding regime adopted for bioreactor experiment. Similar melting temperature (173 ºC) with higher glass transition temperature (7.9 ºC) was reported for P(3HB) produced from margarine fat waste (FAT) (Morais et al., 2014).

According to a recent review by Laycock et al. (2013), melting and glass transition temperatures of P(3HB) typically range between 162-181 and -4 and 18 ºC, respectively, depending of the bacterial strain, carbon source, polymer extraction and purification procedures, film forming techniques (e.g. solvent cast, melt pressed sheet) and aging time.

The crystallinity of P(3HB) varied from 44 to 65%. It was discussed before that molecular weight could be influenced by different cultivation strategies. However, since thermal properties seemed to be independent on cultivation mode, probably the crystallinity of the polymer might be more dependent on applied conditions during recovery step than in the biosynthesis. The variability in polymer's crystallinity might be associated to the different environmental conditions during recovery and purification (e.g. solvent evaporation rate), which were not controlled during this process. Thus, affecting the rate of molecule organization and aggregation, resulting in different P(3HB) crystallinity.

3.5. Conclusions

In this chapter, *C. necator* DSM 428 was cultivated with UCO in bioreactor under different operation modes and feeding strategies. The DO-stat feeding strategy was found to be the best strategy to improve the PHA production from UCO. With this strategy, the overall production of PHA was improved by 64% when compared to the exponential feeding strategy. However, the feeding rate set for exponential regime was not suitable for this bioprocess. Thus, new experiments have to be performed to better tune the feeding rate of UCO when exponential feeding regime is used. Further studies have to be performed to increase the cell growth, by testing, for example different nitrogen sources and carbon to nitrogen ratios. In the different experiments, *C. necator* produced the homopolymer P(3HB) that presented similar thermal properties, but different molecular mass distribution, depending on the feeding strategy adopted. The polymer with higher molecular mass was obtained with the DO-stat cultivation mode, showing again this can be a good operation which indicate this could be a good strategy for the production of P(3HB) by *C. necator* using UCO as substrate.

(B) Production of *scl*-PHAs from *Cupriavidus necator* DSM 428 cultivated in spent coffee grounds oil (SCG)

3.1. Summary

Spent coffee grounds (SCG) oil was obtained by supercritical carbon dioxide (sc-CO_2) extraction in a pilot plant apparatus. *Cupriavidus necator* DSM 428 was cultivated in 2 L bioreactor in batch and fed-batch modes (DO-stat) using extracted SCG oil as sole carbon source for production of polyhydroxyalkanoates (PHA). In batch cultivation the culture reached a cell dry weight of 16.7 g L^{-1} with a polymer content of 78.4% (w/w). The volumetric polymer productivity and storage yield were 4.7 g L^{-1} day^{-1} and 0.77 g g^{-1}, respectively. The polymer produced was a 3-hydroxybutyrate homopolymer with an average molecular mass of 2.34×10^5 g mol^{-1} and a polydispersity index of 1.2. The polymer exhibited brittle behaviour, with very low elongation at break (1.3 %), tensile strength at break of 16 MPa and Young's Modulus of 1.0 GPa. Results show that SCG can be a bioresource for polyhydroxyalkanoates production with interesting properties.

3.2. Introduction

After coffee processing and consumption, spent coffee grounds (SCG) are generated in large quantities: 6.0 Mton are estimated to be generated worldwide every year (Tokimoto et al., 2005). SCG are a lignocellulosic material and their chemical composition varies depending on the coffee beans source. They have a lipid content of up to 20 wt.% (Al-Hamamre et al., 2012; Andrade et al., 2012; Kondamudi et al., 2008).

Conventional oil extraction from SCG involves the use of hazardous organic solvents, such as *n*-hexane. Supercritical fluid extraction (SFE) provides an environmentally friendly alternative whereby extraction/separate recovery of oil and bioactive compounds from biomass can be done without their degradation (Brunner, 1994). Carbon dioxide is the most popular SFE solvent because it is non-flammable, readily available and has a low cost. Through manipulation of temperature and pressure, the density of $scCO_2$ can be adjusted to allow complete separation of oil and bioactive solutes contained in the matrix. Recently, the feasibility of SCG oil extraction by sc-CO_2 has been demonstrated (Couto et al., 2009).

Polyhydroxyalkanoates (PHAs) are biocompatible and biodegradable polyesters that exhibit physical-chemical, thermal and mechanical properties very similar to those of

conventional plastics (Akaraonye et al., 2010). Low cost oil-containing wastes/byproducts have been proposed as carbon sources for PHA production, since they exhibit high product to substrate yield (up to 0.8 g g^{-1}) (Akaraonye et al., 2010; Obruca et al., 2010). *C. necator* is a well known poly-3-hydroxybutyrate P(3HB) producer, able to reach high cellular content (up to 87%) using oleic substrates, namely jatropha oil (Ng et al., 2010), pure rapeseed and waste frying oils (Verlinden et al., 2011), and soybean oil (Park and Kim, 2011). To the best of the author knowledge, PHA production from SCG oil extracted with $scCO_2$ was not previously reported.

The main goal of Chapter 3B was to evaluate the fed-batch production of PHA from spent coffee grounds (SCG) oil. This oil was not tested during the screening study performed in Chapter 1 of this thesis, but it was chosen as substrate to test the versatility of the bioprocess. *C. necator* DSM 428 was cultivated on SCG oil as the sole carbon source under the same DO-stat mode shown to be the best strategy for cultivation of *C. necator* with UCO (Chapter 3A).

The SCG oil used in this study was extracted in a scaled-up supercritical carbon dioxide ($sc\text{-}CO_2$) apparatus. This work was performed in collaboration with Dr. Alexandre Paiva and his group (LAQV/REQUIMTE, FCT/UNL). The extraction of the SCG oil using $sc\text{-}CO_2$ was not the scope of the present work. Thus, the results obtained regarding the oil extraction will not be presented neither discussed in this thesis. However, the SCG oil composition is a key factor to better understand the culture performance, and in this sense, the SCG characterization was also discussed in Chapter 3B.

3.3. Material and Methods

3.3.1. Spent coffee grounds (SCG) characterization

SCG was supplied by NovaDelta – Comércio e Indústria de Cafés, S.A. (Campo Maior, Portugal), which is the largest Portuguese coffee company. The source of SCG was a network of collection points serviced by NovaDelta. SCG was dried in an oven with air circulation at 105 ºC, for 12 h, to remove moisture. The residual moisture content of dry SCG was measured by Karl Fischer titration, as described in section 2.3.1.2 Chapter 2.

3.3.1.1. Oil quantification by Soxhlet extraction

Soxhlet extraction was used as a reference method to determine the total oil content of dry SCG. Twenty grams of SCG and 200 mL of *n*-hexane were used per assay and the extraction was carried out for 6 hours at the solvent's boiling temperature (69 ºC). *n*-hexane was subsequently evaporated from the extracted oil by means of a rotary evaporator (Büchi Rotavapor).

3.3.1.2. Supercritical oil extraction from SCG

The supercritical extraction of SCG oil was conducted in a semi-continuous high pressure extraction pilot unit equipped with four extractors of 2 L each (internal diameter 6.4 cm; total length 59.6 cm), which can operate in parallel or in series in a counter-current, continuous mode. The extracted SCG oil was collected from the separators at 10 min intervals, weighed and stored in sterile and light protected flasks, at -20 ºC.

3.3.1.3. Free fatty acids quantification

The free fatty acids content of SCG oil was determined by titration, as described in section 2.3.1.1 of Chapter 2, with slight modifications. Briefly, 1 g of oil was added to 50 mL of 1:1 (v/v) ethanol:diethyl ether solvent mixture. A 0.1 M solution of potassium hydroxide in ethanol was added until the solution turned from yellow to pink. Phenolphthalein was used as pH indicator.

3.3.1.4. Acylglycerides content

The SCG oil was analyzed in terms of its content in mono-, di- and triglycerides, as described in section 2.3.1.1. of Chapter 2.

The fatty acid composition of the SCG oil was determined by direct transesterification of the lipids to the corresponding methyl esters as described in section 2.3.1.1. of Chapter 2, with slight modifications. Briefly, 10 mg of oil were transmethylated with 2 mL of a 95:5 (v/v) solution of methanol (chromatographic grade, 99.9% purity, Sigma Aldrich) and acetyl chloride. The solution was sealed in a Teflon-lined vial under nitrogen atmosphere and heated at 80 ºC for 1 h. The vial content was then cooled, diluted with 1 mL water, and extracted with 2 mL of *n*-hexane (chromatographic grade, 97% purity, Sigma Aldrich). The organic layer was dried over Na_2SO_4. The methyl esters were quantitatively analyzed by GC as the run method described in section 2.3.1.1. of the Chapter 2.

3.3.1.5. Unsaponifiable fraction analysis

The unsaponifiable oil fraction was determined using the AOCS Official Method Ca 6a-40 for vegetable oils. The direct saponification took place by adding 5 mL of a 25 M aqueous solution of potassium hydroxide to 5g of SCG oil dissolved in 30 mL of ethanol (95% purity, Panreac, Spain). The solution was gently boiled under reflux for 1h and the unsaponifiable matter was extracted with petroleum ether (MaiaLab, Portugal) and cleaned up with 10% (v/v)

ethanol/distilled water. The solvent was evaporated until dryness and the extract was weighed.

3.3.2. PHA production

3.3.2.1. Microorganism and media

Cupriavidus necator DSM 428 was reactivated from stock cultures as described in section 2.3.2.1 of Chapter 2. The inoculum for the bioreactor was prepared as described in section 3.3.1.1 of Chapter 3A. Briefly, one single colony from solid LB medium was inoculated in liquid LB medium and incubated in orbital shaker at 30 ºC and 200 rpm, for 24 hours. Afterwards, the culture was transferred to mineral medium (composition described in section 2.3.2.1 of Chapter 2) supplemented with 20 g L^{-1} of SCG oil as sole carbon source. Inocula for the bioreactor experiments were incubated at 30 ºC and 200 rpm for 48 hours.

3.3.2.2. Bioreactor cultivation

C. necator was cultivated in 2 L bioreactors (BioStat B-Plus, Sartorius, Germany), in batch and fed-batch modes. The batch production was performed in the same conditions as batch of experiment A described in section 3.3.1.2 of Chapter 3A. The fed-batch was operated in same conditions as experiment C (section 3.3.1.2 of Chapter 3A) with slight modifications. Briefly, the cultivation run occurred with an initial working volume of 1.5 L. The inoculum was 10% (v/v) of the initial reactor working volume. The temperature was maintained at 30±1 ºC and the pH was controlled at 6.8±0.2 by the automatic addition of 2 M NaOH. The reactor was initially operated in batch mode and then in fed-batch using ammonium limitation.

The air flow rate was kept constant (1 vvm- volume of air per volume of cultivation broth per minute) and the dissolved oxygen concentration (DO) was maintained at 30% air saturation by the automatic adjustment of the stirring rate (400 – 800 rpm) during the batch phase. During the fed-batch phase, the stirring rate was kept constant (500 rpm) and the DO was controlled at 30% air saturation by the automatic feeding with SCG oil (DO-stat mode).

Samples of 20 mL were periodically withdrawn from the bioreactor and used for the determination of the cell dry mass (CDM), residual oil concentration in the broth and PHA content in the biomass. The analyses were performed in duplicate.

3.3.2.3. Analytical Techniques

The CDM, PHA and residual oil concentration were determined as described in section 3.3.1.4 of Chapter 3A., with slight modifications. Briefly, 7 mL of the cultivation broth were mixed with *n*-hexane (1:3 v/v) and centrifuged (15 777 × *g*, 10 min). Three different fractions were obtained: a biomass pellet, an aqueous cell-free supernatant and an upper hexane layer

containing the residual oil.

The biomass pellet was washed twice with deionized water, and lyophilized to gravimetrically quantify the CDM. For quantification of the residual oil, 5 mL of the upper hexane layer containing the residual oil were transferred to pre-weighed tubes and placed in a fume hood at room temperature for 72 h, for solvent evaporation. The residual oil was gravimetrically quantified and its fatty acids composition was analyzed as described on section 3.3.1.4 of this chapter.

PHA content in the bacterial cells and its composition were determined as described in section 3.3.1.4 of Chapter 3A.

3.3.2.4. Calculations

The maximum specific growth rate (μ_{max}, h^{-1}), q_s (gS gX^{-1} h^{-1}) and q_p (gP gX^{-1} h^{-1}) were determined as described in section 2.1.3. of Chapter 3A. The active biomass ($X_{(t)}$, g L^{-1}), cell dry mass (CDM, g L^{-1}), PHA content (wt.%), growth ($Y_{X/S,}$ g g^{-1}) and storage ($Y_{P/S,}$ g g^{-1}) yields on SCG oil (S, g L^{-1}) and volumetric productivity (r_p, g L^{-1} day^{-1}) were calculated as described in section 2.3.2.5 of Chapter 2.

3.3.3. PHA extraction

The polymer was extracted from the lyophilized cells (previously washed as described in section 3.3.2.3), using chloroform as solvent (1 g of dry cells per 50 mL of $CHCl_3$), at 37 ºC, 250 rpm, over 24 hours. The solution was filtered (Filter-Lab, Ac cellulose, 0.2 µm/47 mm) under vacuum to remove cell debris, and the polymer was precipitated twice by adding the solution drop-by-drop into cold ethanol (1:10, v/v), under vigorous stirring, and dried at room temperature.

3.3.4. Polymer characterization

3.3.4.1. Physical-chemical properties

Polymer composition was determined by GC as described in section 2.1.3 of Chapter 3.A. The polymer's average molecular mass was determined using a Size Exclusion Chromatography (SEC), as described in section 2.3.3.1 of Chapter 2.

3.3.4.2. Thermal properties

Thermal analysis was performed by differential scanning calorimetry (DSC), as described in section 2.3.3.2 of Chapter 2.

3.3.4.3. Mechanical properties of polymer films

Homogeneous films were prepared by solvent casting in order to determine the polymer's mechanical properties. Purified PHA was dissolved in chloroform (20 g L^{-1}) and the solutions (10 mL) were transferred to glass Petri dishes (7 cm diameter), which were placed in a fume hood, at room temperature for 24 h, for slow solvent evaporation.

Tensile tests were carried out using a TA-Xt plus texture analyser (Stable Micro Systems, Surrey, England). Film strips (20×70 mm) were attached on tensile grips A/TG and stretched at 0.5 mm s^{-1} in tension mode. The tensile stress at break (τ, MPa) was calculated as the ratio of the maximum force to the initial films cross-sectional area, and the elongation at break (ε, %) was determined as the ratio of the extension of the sample upon rupture by the initial gage length. The Young's modulus (E, GPa) was calculated from the slope of the stress-strain curve in elastic region. These tests were performed in collaboration with Dr. Vitor Alves from CEER – Centro de Engenharia dos Biossistemas, Instituto Superior de Agronomia, Universidade de Lisboa.

3.4. Results and Discussion

3.4.1. SCG oil characterization

SCG was dried in order to have a water content below 1% to avoid emulsion formation during extraction of the oil. The Soxhlet extraction of SCG with *n*-hexane resulted in a maximum oil yield of 14.0% wt.% on a dry weight basis (g oil per 100 g of dry SCG), which is within the range of oil content reported in the literature for SCG. Using *n*-hexane as extraction solvent, Andrade et al. (2012) obtained an oil yield of 12.0 wt.% in 6 h extraction time, Al-

Hamamre et al. (2012) achieved 15.3 wt.% in 30 min and Abdullah and Koc (2013) 13% wt.% in 8h and Obruca et al. (2014b) 15.0 wt.% until solvent reflux was clear. The differences in these results may be associated with the coffee variety (coffee *arabica* and coffee *robusta*, for example, have various lipid contents), the conditions of preparation and the pretreatment of the raw materials.

The optimum conditions for the oil sc-CO_2 extraction from SCG were set at 50 ºC, 25 MPa, a solvent flow rate of 10 kg h^{-1} and a solvent to solid mass ratio of 35 kg of CO_2 per kg of dry SCG. At these conditions more than 90% of the total amount of SCG oil was extracted after ca. 1.5 h of extraction. At the conditions referred above, a continuous process for the supercritical extraction of SCG oil for the production of PHA was established. For this purpose, four extractors were used in series, three at a time. Once the SCG in the first extractor was exhausted, this extractor was removed from the circuit, the second extractor in the series became the first, the third became second, and the fourth extractor with fresh SCG became last in the series. This enabled the replacement of exhausted SCG with a fresh load, and ensured that at all times there were three extractors in operation. Comparing to n-hexane extraction method, with sc-CO_2 method less amount of oil was extracted. However, this continuous method is consider much less hazardous than solid-liquid extraction using toxic solvents such as n-hexane. Also, the fact of being continuous allow higher overall extraction. Feasibility of SCG oil extraction by supercritical CO_2 was demonstrated in a preliminary work (Couto et al., 2009) using a lab-scale high pressure extraction apparatus and a different SCG raw material. It was shown that sc-CO_2 extracted up to 85% of the total amount of SCG oil after 3 h of extraction at the best operating conditions of 50ºC and 25 MPa. With continuous process at pilot-scale better results were obtained.

The SCG oil extracted with hexane and sc-CO_2 had similar composition, being mostly composed of triglycerides (71.3%, wt.%), with low contents in mono- and diglycerides (0.7 and 5.8% wt.%, respectively), and free fatty acids (1.6%, wt.%) (Table 3.4). It was also detected the presence of other compounds, including tocopherols, sterols, esters of dipertenes, alcohols, sterols and fatty acids, accounting for up to 20 wt.% of the total composition of the oil.

Table 3.4: Composition of spent coffee grounds oil extracted by $scCO_2$.

Compounds	**wt.%**
Monoglycerides	0.7
Diglycerides	5.8
Triglycerides	71.3
Free Fatty Acids	1.6
Unsaponifiable (e.g. tocopherols, sterols)	5.5
Other compounds (e.g. esters of diterpene alcohols, sterols and fatty acids)[a]	15.1
Fatty acids composition[b]	**wt.%**
Palmitic acid ($C_{16:0}$)	39.7
Stearic acid ($C_{18:0}$)	8.9
Oleic acid ($C_{18:1}$)	12.9
Linoleic acid ($C_{18:2}$)	38.4

[a]Difference to 100%

[b]Fatty acids are designated by the number of carbon atoms; number of double bonds.

The fatty acid profile SCG oil extracted with sc-CO_2 is also shown in Table 3.4. Palmitic ($C_{16:0}$) and linoleic ($C_{18:2}$) acids were the major fatty acid components detected (39.7 and 38.4 wt.%, respectively), accounting for nearly 80% of all fatty acid-based compounds of SCG oil, which is in agreement with the results reported by Couto et al. (2009). Minor components were oleic (12.9%, wt.%) and stearic (8.9%, wt.%) oils. The results obtained for SCG oil, in terms of chemical composition, were very similar to those reported by Obruca et al. (2014), namely for palmitic (35.7 wt.%), linoleic (43.7 wt.%) and oleic (9.4 wt.%).

When compared the SCG oil to UCO (characterized in Results and Discussion of Chapter 2), similar content in diglycerides (6.7 wt.%), monoglycerides (0.4 wt.%) and free fatty acids (1.0 wt.%) was found. However, SCG oil had slightly lower triglycerides content (71 wt.%) comparing to UCO (83 wt.%). The fatty acids profile of SCG oil was different from the UCO. In the latter the main compounds were found to be oleic and linoleic acids, accounting for 88 wt.%. Notwithstanding, the SCG oil revealed a suitable composition and great potential to be used for C. *necator* cultivation and PHA production.

3.4.2. PHA production from SCG oil

3.4.2.1. Batch Cultivation

The SCG oil extracted by sc-CO_2 was used as the sole carbon source for cultivation of the bacterium *C. necator* DSM 428 to evaluate its potential for PHA production.

The production of PHA from SCG oil was performed in 2 L bioreactor in batch mode, with an initial SCG concentration of 20 g L^{-1}.

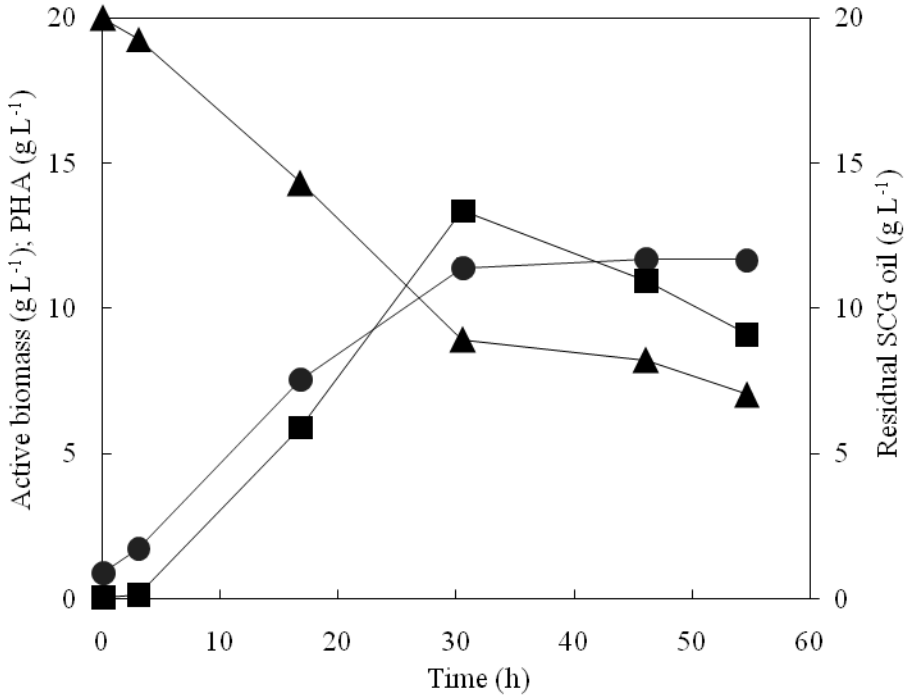

Figure 3.5: Active biomass (●), PHA (■) and residual SCG oil (▲) concentration during batch cultivation of *C. necator* DSM 428 with SCG oil as sole carbon source.

After inoculation, the maximum specific growth rate of 0.28 h^{-1}, with no lag-phase. Cell growth stopped at 30 hours, achieving 11 g L^{-1} active biomass concentration (Figure 3.5). At this time the CDM was 25 g L^{-1} with a polymer content of 54 wt.% (Table 3.5) corresponding to a maximum polymer concentration of 14 g L^{-1}. Afterwards, the polymer content reduced about 10 wt%, which might indicate the culture activated the depolymerase to consume their reserves (Gebauer and Jendrossek, 2006). In fact, from 30 hours until the end of the cultivation run the residual oil remained constant (7-8 g L^{-1}), indicating the culture consumed approximately 13 g L^{-1} SGC, stopping its consumption afterwards. Probably, the remaining carbon source corresponded to the oil fraction with less preference by the culture. Thus, the production of PHA was stopped and polymer started to be consumed for cell maintenance. The maximum volumetric productivity obtained in this experiment was 11.2 g L^{-1} day^{-1}.

The overall growth and storage yields were 0.85 and 0.70 g g^{-1}, respectively (Table 3.5). Biomass specific substrate uptake rate and product formation were 0.29 g UCO gX^{-1} h^{-1} and 0.30 g PHA gX^{-1} h^{-1}, respectively. Recently, Obruca et al. (2014b) also reported on the utilization of SCG oil by *C. necator* DSM 428 for PHA production. The biomass polymer content obtained in batch (43.9 wt.%) experiment was lower than that reported for batch (90 wt.%) of Obruca et al (2014). However, the values obtained in present experiments are within the values reported in the literature for *C. necator* cultivated on different oils (20-83%, w/w) (Chapter 3A- Table 3.2). The storage yield (0.70 g g^{-1}) on SCG oil, was slightly lower than that obtained by Obruca et al. (2014b) in batch (0.88 g g^{-1}) experiment. However, when calculated over the time interval between 0 and ~40h (before polymer's concentration start to decrease) the storage yield would be higher, 0.90 g g^{-1}. Those differences might be due the utilization of oils from different coffee sources, and consequently having different composition. Also, in Obruca et al. (2014b) the SCG oil was extracted with n-hexane, while in this study sc-CO_2 extraction was used. Differences in oil composition might impact culture performance, namely in terms of PHA production.

3.4.2.2. Fed-batch Cultivation

C. necator was also cultivated in fed-batch mode using the DO-stat mode successfully tested for *C. necator* cultivation with UCO (Chapter 3A).

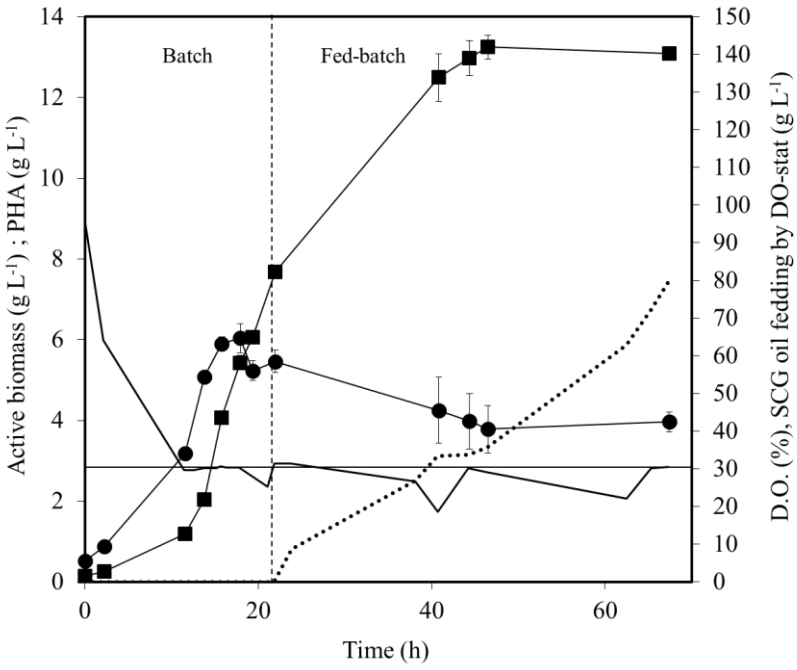

Figure 3.6: Active biomass (●) and PHA (■) concentration during cultivation of *C. necator* DSM 428 with SCG oil as sole carbon source. SGC oil is supplemented (⋯) by controlling the DO concentration (—) at 30% air saturation.

The cultivation was initiated with an oil concentration of 20 g L^{-1} and the reactor was operated in a batch mode for 22 h, followed by a fed batch phase (Figure 3.6), wherein SCG oil was supplied to the culture as a function of the DO concentration. Ammonium was only supplemented at the beginning of the run to promote cell growth. Afterwards, no more ammonium was given to the culture in order to impose nitrogen limitation and consequently PHA production.

No lag phase was observed (Figure 3.6) and the culture grew at a maximum specific growth rate of 0.15 h^{-1} (Table 3.5), achieving a maximum active biomass concentration of 5.5 g L^{-1} at the end of the batch phase (22 h). During the batch phase, the biomass accumulated up to 55 % (w/w) of PHA giving a polymer concentration of 6.0 g L^{-1}. In batch experiment (for the same period of time) the active biomass concentration was in higher concentration (~7.5 g L^{-1}) and polymer concentration was equal (~6.0 g L^{-1}).

The fatty acids profile of the SCG oil was also determined during the batch phase (Figure 3.7) to evaluate the preference of *C. necator* DSM 428 for each fatty acid available.

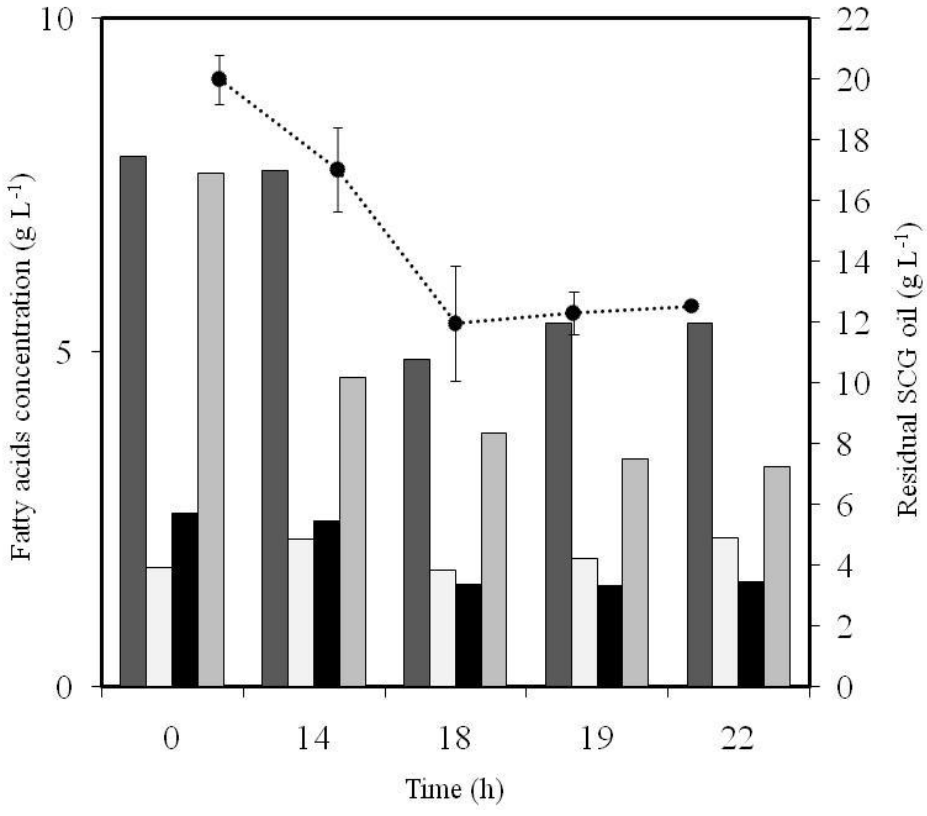

Figure 3.7: Consumption profile of the fatty acids of the SCG oil by *C. necator* DSM 428 during batch phase of the cultivation run. (▒) Palmitic acid; (■) Oleic acid; (□) Linoleic acid; (□) Stearic acid and (···●···) total oil concentration.

Palmitic ($C_{16:0}$), oleic ($C_{18:1}$) and linoleic acids ($C_{18:2}$) were consumed until 18h.

Afterwards, palmitic and oleic acids remained in the cultivation broth, while a slight consumption of linoleic acid was observed until 22h. Apparently, stearic acid ($C_{18:0}$) remained in the cultivation broth until the end of the batch phase, suggesting this culture has no preference for this fatty acid. *C. necator* cells have been reported as capable to grow well in palmitic, oleic and linoleic acids (Kahar et al., 2004; Ng et al., 2010). However, the preference of C. *necator* DSM 428 for each fatty acid during a cultivation run has not been widely discussed.

The presence of other compounds in the SCG oil, namely, sterols, tocopherols, esters, etc. (Table 3.4), had apparently no significant impact on cell growth and/or PHA production.

The fed-batch phase was initiated by automatically feeding the bioreactor with SCG oil at a flow rate that was a function of the DO (controlled at 30%). At the end of the cultivation run (67 h), a CDM of 16.7 g L^{-1} was achieved with a polymer content of 78.4 wt.%, corresponding to a PHA concentration of 13.1 g L^{-1} and a volumetric productivity of 4.7 g $L^{-1}day^{-1}$ (Table 3.5). Growth and storage yields on SCG oil of 0.66 and 0.77 g g^{-1}, respectively, were obtained.

Though, the overall productivity (4.7 g $L^{-1}day^{-1}$) was lower than that obtained when UCO was automatically fed by dissolved oxygen variation (12.6±0.78 g $L^{-1}day^{-1}$) (Chapter 3A, Table 3.2), the polymer accumulation (78.4 wt.%) and storage yields in SCG oil (0.77 g g^{-1}) was higher than that obtained for UCO (77±5.7 wt.% and 0.52 g g^{-1}, respectively). This might be indicate that SCG oil can be a suitable carbon source for PHA production, very comparable to vegetable oils.

Table 3.5: Kinetic parameters for the cultivation of *C. necator* using SCG oil.

Parameters	**SCG oil**		**SCG oil**	
Operation mode	Batch	Fed-batch	Batch	Fed-batch
Feeding strategy	-	DO-stat	-	Pulse
μ_{max} (h^{-1})	0.28	0.15±0.01	n.a.	n.a
CDM (g L^{-1})	20.8	16.7±0.36	29.4±1.4	55.4±1.3
X (g L^{-1})	11.7	6.0±0.36	n.a.	n.a.
PHA content (wt.%)	43.9	78.4±2.53	90.1±3.5	89.1±3.1
PHA (g L^{-1})	9.1	13.1±0.30	26.5±1.6	49.4±2.1
r_p (g L^{-1} day^{-1})	4.0	4.7±0.30	15.8	32
$Y_{X/S}$ (g X g^{-1} S)	0.85	0.66±0.03	0.98	0.92
$Y_{P/S}$ (g PHB g^{-1} S)	0.70	0.77±0.05	0.88	0.82
Reference	Present study		Obruca et al., 2014	

The feeding strategy (pulse feeding) adopted by Obruca et al. (2014) allowed for higher polymer contetent (89.1±3.1 wt.%) and CDM (55.4±1.3 g L^{-1}), and consequently a higher

polymer concentration was obtained at the end of the cultivation run (49.4±2.1 g L^{-1}) than when DO-stat was used (13.1±0.30 g L^{-1}). Unlike the present study, in fed-batch experiment ammonium was fed intermittently during the cultivation run and thus, the CDM has continued to increase during the fed-batch phase. Since the culture is able to grow and produce PHA simultaneously, the presence of ammonium during the fed batch is a commonly used strategy to improve the biomass concentration and, consequently, PHA concentration and productivity. Nevertheless, the goal of this work was to demonstrate the possibility of using SCG oil as a feedstock to produce PHA. Further, process optimization requires testing different strategies already described in the literature.

3.4.3. PHA characterization

3.4.3.1. Composition, molecular mass distribution and thermal properties

The GC analysis revealed that the PHA produced from SCG oil (in batch and fed-batch experiments) was a 3HB homopolymer, which is in accordance with previous experiments reported in literature for PHA synthesized by *C. necator* DSM 428 using carbohydrates or oil-containing substrates (Kahar et al., 2004; Ng et al., 2010). This seems to indicate that the chemical composition of the SCG oil minor components (Table 3.4), namely, in terms of unsaponifiable compounds, esters, alcohols etc., had no impact on the polymer's composition. This strain is commonly reported as P(3HB) producer. Notwithstanding, as discussed previously (Chapter 3A, Results and Discussion) it is possible to manipulate the polymer composition using different carbon sources, including oil-containing substrates. *C. necator* is capable to produce copolymers with different percentage of 3-hydroxyvalerate (3HV) when supplemented with precursors, such as organic volatile acids and/or alcohols (e.g. propionate, valerate, propanol, etc.) (Obruca et al., 2010). Recently, López-Cuellar et al. (2011) reported on PHA production containing four different monomers, ranging from 4 to 12 carbons, when canola oil was supplemented in a third stage of the fermentation process. In that case, the monomer structure of the PHA was strongly affected by the carbon sources used.

The chemical composition of the polymer also determines its physical-chemical, thermal and mechanical properties. Table 3.6 shows the properties of the polymer obtained from SCG oil in comparison to PHB obtained from neutral sugars (glucose and fructose), SCG oil and waste sesame oil.

Table 3.6: Physical-chemical and thermal properties of the PHB produced by *C. necator* from different substrates.

Properties	SCG oil	SCG oil	Waste sesame oil	Glucose/Fructose
$\bar{M}_w$ (g mol^{-1}) x 10^5	2.34	4.27-4.74	5.5	1.06
$\bar{M}_n$ (g mol^{-1}) x 10^5	1.91	1.70-2.14	5.0	3.5
PDI	1.2	2.2-2.5	1.1	3.2
T_c (ºC)	95.9[a]	n.a.	59.5[b]	n.a.
T_g (ºC)	8.4	n.a.	n.a.	4.9
T_m (ºC)	172.3	n.a.	172.0[b]	173.5
ΔH_m (J g^{-1})	85	n.a.	n.a.	80
X_c (%)	58	n.a.	n.a	56
References	Present study	Obruca et al., 2014b	Taniguchi, Kagotani and Kimura 2003	Fiorese et al., 2009

n.d. not detected

n.a. data not available

[a]heating and cooling cycles preformed at 10 ºC min^{-1}

[b]for the precise determination of T_c and T_m values, the samples were first melted at 190 °C and immediately quenched in liquid nitrogen before the measurement. Heating and cooling cycles preformed at 10 ºC min^{-1}.

The PHB exhibited a high molecular mass of 2.34 ×10^5 g mol^{-1} with a very low polydispersity index of 1.2, indicating that the polymer is highly homogeneous. The $\bar{M}_w$ value is close to that obtained for P(3HB) produced from SCG oil (4.27-4.74 x 10^5 g mol^{-1}) (Obruca et al., 2014) and waste sesame oil (5.5×10^5 g mol^{-1}) (Taniguchi, Kagotani and Kimura, 2003) and is lower than P3(HB) obtained from glucose/fructose mixture 1.06×10^6 (Fiorese et al., 2009) (Table 3.6). The latter exhibited higher polydispersity (3.2) than the P(3HB) produced from SCG oil. Molecular mass and polydispersity of P(3HB) obtained from UCO through fed-batch mode using DO-stat strategy (Chapter 3A) was very comparable (2.6 x10^5 g mol^{-1} and 1.6, respectively) to that obtained from SCG oil, showing the different fatty acid composition between UCO and SCG oil apparently had no impact on polymer's molecular mass.

Thermal properties were also assessed for P(3HB) produced from SCG. The analysis revealed a polymer with a melting point (T_m) of 172.3 ºC and a melting enthalpy (ΔH_m) of 85 J g^{-1}. T_m of P3(HB) from SCG oil is comparable to those obtained when using glucose/fructose (173.5 ºC) and waste sesame oil (172 ºC) (Table 3.6).

The glass transition temperature (T_g) was found to be 8.4 ºC and after the first melting of the sample of P(3HB), the polymer exhibited a crystallization temperature (T_c) of 95.9ºC, at a cooling rate of 10ºC min^{-1}. The polymer's crystallinity (X_c) was 58%, showing that the P(3HB) produced from SCG is a crystalline material. The crystallinity of the polymer depends on many factors, including its chemical structure, intermolecular interactions and processing conditions. However, the X_c of P(3HB) is, commonly, between 55-80% (Laycock et al., 2013).

P(3HB) obtained with UCO in fed-batch cultivation using DO-stat feeding stratagy (Chapter 3A) exhibited very similar melting temperature (174ºC) but slightly lower glass transition temperature (4ºC) than that from SCG oil. Also similar crystallinity (52%) was observed for P(3HB) obtained from fed-batch experiment using DO-stat, which might indicate that differences between UCO and SCG oil composition had no significant impact on thermal properties.

3.4.3.2. Mechanical properties

The mechanical properties of the PHA polymers can range from brittle to flexible and to elastic, depending on their side chain length structures. Normally, the polymers with short chain length monomers, such as P(3HB), exhibit high crystallinity, as shown in the previous section, being very brittle materials (Laycock et al., 2013). The P(3HB) polymer produced in this work was also analysed in terms of its mechanical properties. The films prepared with polymer produced from SCG oil revealed a tensile strength at break of 16 MPa along with a very low elongation at break of 1.3 %, and a Young's Modulus of 1.0 GPa, exhibiting a stiff and brittle behaviour.

Barham et al. (1984) reported on the mechanical properties of a melt pressed film of P(3HB) obtained from glucose. They found a polymer with a tensile strength ranging from 8 to 20 MPa, Young's Modulus ranging from 1.5 to 1.8 GPa and an elongation at break of 0.8 %. These results are similar to those obtained for P (3HB) produced from SCG oil. The variance may be due to different sample processing (e.g. extraction and film formation procedures), as well as aging time of the sample before analysis.

The physical-chemical properties of the polymer are very important parameters in determining its final application. Polymers with similar characteristics to those obtained in this work are often proposed for food packaging and paper coating (Bourbonnais and Marchessault, 2010; Bucci et al., 2005). On the other hand, using monomers of 3HB as building blocks for co-blending has been recently proposed, thus enhancing the final polymer applications to more noble areas (e.g. biomedical and pharmaceutical industries).

The process presented in this study, enabled to produce a polymer from a residue (SCG oil), possessing that polymer a good potential to be applied on packaging solutions for food products, namely the coffee itself, from which the residue has been generated at the first place.

3.5. Conclusions

It was demonstrated that SCG oil is suitable substrate for PHA production by *C. necator* DSM 428. With preliminary batch experiment, high polymer content (54 wt.%) was obtained. However, with DO-stat feeding strategy it was possible to improve polymer content up to 78 wt.%, resulting in a product yield of 0.77 Kg of PHA per Kg of SCG oil (97 Kg per ton of SCG processed), confirming that is a suitable feeding strategy to be used in this bioprocess.

P(3HB) exhibited very good properties when compared to similar polymers. Apparently, the differences in composition between vegetable oils, such as UCO and SCG oil, had no impact on polymer's molecular mass and thermal properties. Also, P(3HB) mechanical properties were similar to those of the polymer produced from other carbon sources, meaning the SCG oil is a low cost carbon source with minimal impact on polymer's properties.

Future work will be done to increase the productivity of the process and assess the molecular conformation of the polymer, in order to better understand its properties.

4. CHAPTER 4

Production of *mcl*-PHA from olive oil deodorizer distillate (OODD) and demonstration of the polymer's adhesive properties

The results presented in this chapter are under revision of a peer reviewed paper:

Cruz M.V., Araújo D., Alves V.D., Freitas F., Reis M.A.M. Characterization of medium chain length polyhydroxyalkanoate produced from olive oil deodorizer distillate. 2015 Int J Biol Macromol, 82, 243-248.

4.1. Summary

Olive oil deodorizer distillate (OODD) was used for the first time as the sole substrate for polyhydroxyalkanoates (PHA) in bioreactor production by the bacterium *Pseudomonas resinovorans*. A PHA content in the biomass of 36±0.8wt% was reached within 19 hours of cultivation. A final polymer concentration of 4.7±0.3 g L^{-1} was reached, corresponding to a volumetric productivity of 5.9±0.2 g L^{-1} day^{-1}. The PHA was composed of 3-hydroxyoctanoate (48.3±7.3 mol%), 3-hydroxydecanoate (31.6±2.6 mol%), 3-hydroxyhexanoate (12.1±1.1 mol%) and 3-hydroxydodecanoate (8.0±0.7 mol%) and it had a glue-like consistency that did not solidify at room temperature. The polymer was highly amorphous, as shown by its low crystallinity of 6±0.2%, with low melting and glass transition temperatures of 36±1.2 and -16±0.8 ºC, respectively. The polymer exhibited a shear thinning behavior and a mechanical spectrum with a predominant viscous contribution. Its shear bond strength for wood (67±9.4 kPa) and glass (65±7.3 kPa) suggests it may be used for the development of biobased glues.

4.2. Introduction

As discussed in Chapter 2, deodorizer distillates are among the major byproducts generated by the vegetable oil refining industry (Dumont and Narine, 2007, Gunawan and Ju, 2009). They are usually mixed with other byproducts in the neutralization step of the refining process, resulting in a low market value material that has negative impacts if discharged into the environment (Dumont and Narine, 2007). The production of vegetable oil deodorizer distillates is expected to increase as a result of the intensification of edible oils consumption by the growing human population (Dumont and Narine, 2007). Hence, it is important to search for alternative routes for the valorization of this byproduct to avoid its negative environmental impact and the costs associated with its disposal or treatment.

Vegetable oil deodorizer distillates are complex mixtures mainly composed of free fatty acids (FFA) (>50 wt%) that include palmitic, oleic and linoleic acids. Other compounds are also present in significant amounts, such as squalene, tocopherols and sterol esters (Dumont and Narine, 2007, Gunawan and Ju, 2009). The high FFA content (> 50%) of deodorizer distillates renders them a great potential for use as substrate for microbial cultivation and production of value-added bioproducts, thus adding value to the overall refining process. This approach has already been attempted for the production of biosurfactants by the bacterium *Pseudomonas aeruginosa* MR01 (Partovi, et al., 2013). Other FFA-rich substrates have also been described as suitable substrates for the production of polyhydroxyalkanoates (PHA) (Eggink, Waard and

Huijberts, 1995; Lo et al., 2005; Srivastava and Tripathi, 2013), but the use of vegetable oil deodorizer distillates has not been explored so far.

mcl-PHA are synthesized by a wide range of Gram-negative bacteria, mainly of the Genus *Pseudomonas* (Rai et al., 2011a, Kim et al., 2007) as discussed in Chapter 2 of this thesis. Depending on their composition, *mcl*-PHA can range from rubber-like to glue-like polymers, as they become enriched in longer chain monomers (Eggink, Waard and Huijberts, 1995; Lo et al., 2005; Srivastava and Tripathi, 2013). The polymers' monomer composition is dependent on the producing strain, as well as on medium composition, carbon source and cultivation conditions.

Due to their tacky behaviour at room temperature, *mcl*-PHA might be considered as alternative materials for the development of new biobased adhesives to replace the commercial petrochemical-derived adhesives and glues. Solvent-based adhesives and/or glues, such as polyvinyl acetate (PVA), epoxies, polyurethane, etc., are extensively used in many areas of application due to their good adhesion capacity to different materials, low price and fast curing times. However, most of them are non-biodegradable and hazardous products, whose production and use poses environmental and public health concerns (Kim and Netravali, 2013). Thus, alternative biobased materials, such as soy protein (Liu and Li, 2007), soy flour-based (Huang and Li, 2008), sea cucumber protein (Baranowska et al., 2011) and frog protein (Graham et al., 2005), are currently being investigated as potential substitutes of the conventional ones or as building blocks on glue manufacturing. *mcl*-PHA have, so far, not been tested for such area of application.

In Chapter 2, the ability of *P. resinovorans* to grow on olive oil deodorizer distillate (OODD) was demonstrated in batch shake flask assays. In this study, OODD was used for the first time as the sole substrate for the fed-batch bioreactor cultivation of *P. resinovorans* for the production of *mcl*-PHA aiming at exploring the potential properties of this polymer. The produced polymer was extracted from the biomass, purified and characterized in terms of its composition, molecular mass distribution and thermal properties, as well as its rheological properties and shear bond strength on wood and glass materials.

4.3. Material and Methods

4.3.1. Biopolymer production

Biopolymer production was carried out by cultivation of *Pseudomonas resinovorans* NRRL B-2649 in a 10 L bioreactor (total working volume) (BioStat B-Plus, Sartorius, Germany), with a initial working volume of 8.0 L. A 10% (v/v) inoculum was used. The mineral medium (composition described in Chapter 2, section 2.3.2.1) was supplemented with OODD (20 g L^{-1}) as the sole substrate. The temperature was maintained at 30±1 ºC and the pH-value was controlled at 6.8±0.2 by the automatic addition of 2M NaOH. The air flow rate was kept constant (1vvm- volume of air per volume of cultivation broth per minute) and the dissolved oxygen level (DO) was maintained at 30% air saturation by the automatic adjustment of the stirring rate (400 – 800 rpm). An OODD pulse of 15 g L^{-1} was supplied to the culture after 4 hours of cultivation. Samples (15±5 mL) were periodically withdrawn from the bioreactor for biomass, PHA and OODD quantification.

4.3.2. Analytical techniques

Cell dry mass (CDM) and OODD concentration in the broth were determined as described in section 3.3.1.4 of Chapter 3A. PHA content and composition were determined by gas chromatography (GC), according to the method described in section 2.3.2.4 of Chapter 2.

4.3.3. Biopolymer extraction

PHA was recovered from dried biomass (~10 g) by Soxhlet (250 mL) extraction with chloroform, at 70ºC, for 24 hours and purified as described in section 3.3.2 of Chapter 3.

4.3.4. Biopolymer characterization

4.3.4.1. Composition

Polymer composition and purity were evaluated by GC analysis, using the modified Lageveen et al. (1988) method described in section 2.2.4 of Chapter 2.

4.3.4.2. Molecular mass

Weight average ($\bar{M}_w$) and number average ($\bar{M}_n$) molecular mass were determined as described in section 2.3.3.1 of Chapter 2.

4.3.4.3. Thermal properties

The thermal properties of the polymers were determined by differential scanning calorimetry (DSC) as described in section 2.3.3.2 of Chapter 2.

4.3.4.4. Apparent viscosity and viscoelastic properties

The apparent viscosity and the viscoelastic properties of the *mcl*-PHA were accessed using a controlled stress rheometer (HAAKE MARSIII, Thermo Scientific) equipped with a plate-plate serrated geometry (diameter 20mm), with a gap of 1mm, at a temperature of 20 ºC. Flow curves were determined using a steady state flow ramp in the range of shear rate from 10^{-3} to 10 s^{-1}. Frequency sweeps were conducted for frequency ranging from 10^{-2} to 10^{2} *Hz*, with a constant shear stress within the linear viscoelastic region.

4.3.4.5. Shear bond stress tests

The polymer's adhesive capacity was assessed using wood (AKI store, Portugal) and glass (Deltalab S.L.) strips (2.6×7.6×0.22 cm and 2.6×7.6×0.11 cm, respectively). Prior to the tests, the wood strips were placed in a desiccator with silica gel, at room temperature, for 24 hours, for moisture removal. The shear bond strength of the biopolymer in wood-wood and glass-glass joints was determined, according to Kim and Netravali (2013), with some modifications. Briefly, the *mcl*-PHA (~70 mg) was spread homogenously at the end of the strips in a superficial area of 5.0±0.2 cm^2. The specimens were overlapped and hand-pressured for 10 seconds. The thickness of the *mcl*-PHA layer was determined with a digimatic micrometer (Mitutoyo Corporation). Two commercial binder clips, with an applied tension of 24.1±4.8 kPa, were placed in the joint area of the strips in order to improve the gluing process during the curing time. Two short pieces of the same material were attached to the other ends to avoid undergoing torsion in the grip during the shear test. For comparison, the same shear bond strength tests were performed using commercial glue (UHU Power Universal Flex + Clean, 50-100% acetone, 10 to <25% ethyl acetate) in wood and glass.

Shear strength measurements were carried out using a TA-XT plus texture analyser (Stable Micro Systems, Surrey, England). The specimens were attached on tensile grips A/TG and an axial force was applied at a crosshead speed of 0.5 mm s^{-1} until the joints of wood-wood and glass-glass were totally separated. The maximum load at break (F, kN) was recorded and the shear bond stress (τ_1, kPa) was calculated as described by equation 14:

$$\tau_1 = \frac{F}{A} \qquad \text{Equation (14)}$$

where A (m^2) is the superficial area covered by the adhesive.

Three sets of 5 samples were prepared for each material, to evaluate the impact of using different curing conditions: the first set was conditioned at 20±1ºC for a total of 16hours, while the other two sets were first kept at either 50±1ºC or-18±1 ºC, respectively, for 2 hours, followed by 14 hours at 20±1ºC.

4.4. Results and Discussion

4.4.1. *mcl*-PHA production

Previous work (Chapter 2) showed that the bacterium *Pseudomonas resinovorans* is able to grow on FFA-rich substrates, such as OODD, and accumulate PHA, in shake flask experiments. In this work, OODD was used in bioreactor cultivation of *P. resinovorans* under controlled conditions. As reported in Chapter 2 (Results and Discussion) the OODD used as substrate had a FFA of 64.0±0.02 wt%, being oleic acid the main fatty acid component (69.9±1.0 wt%), with lower amounts of palmitic (10.3±0.1 wt%), stearic (10.1±1.6 wt%), linoleic (8.0±0.8 wt%) and linolenic (0.9±0.1 wt%) acids.

There was no observable lag phase (Figure 4.1) and just after inoculation the culture entered an exponential growth phase, with a specific cell growth rate of 0.19±0.02 h^{-1} Table 4.1.

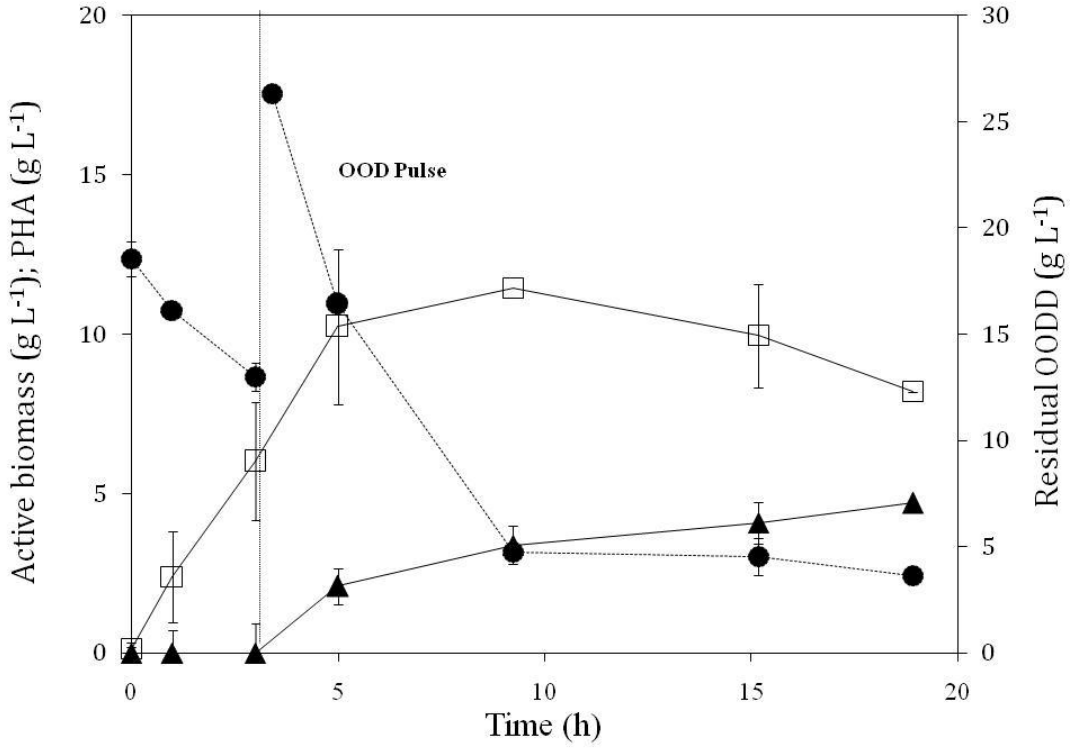

Figure 4.1: Fed-batch production of mcl-PHA from *P. resinovorans* NRRL B-2649 using OODD as sole carbon source (□, active biomass;▲, PHA concentration; ●, OODD concentration).

During the first 4 hours of cultivation no polymer production was observed, meaning the OODD consumption (7.0±0.7 g L^{-1}) was probably being deviated for biomass production (6.0±1.3 g L^{-1}) and maintenance. Afterwards, an OODD pulse of 15 mL was given to the culture in order to stimulate PHA production, by supplying an excess of carbon source. A maximum active biomass of 11.5±0.23 g L^{-1} were reached (Table 4.1) at 9 hours of cultivation.

Table 4.1: Kinetic parameters of *mcl*-PHA production by *P. resinovorans* cultivated in different oil-containing substrates.

Parameters	**OODD**	**Olive oil**	**Hydrolysed pollock oil**	**Hydrolysed pomace +Used cooking oil**	**Tallow-FFA**
Cultivation mode	Fed-batch bioreactor	Batch shake flask	Batch bioreactor	Batch bioreactor	Batch shake flask
Volume (L)	10	0.5	0.5	3.7	1.0
μ_{max} (h^{-1})	0.19±0.02	n.a.	n.a.	n.a.	n.a.
CDM (g L^{-1})	12.7±0.64	3.4±0.2	4.7	6.1-10.2	1.3±0.1
X_{final} (g L^{-1})	8.2±0.1	n.a	n.a	n.a.	n.a
X_{max} (g L^{-1})	11.5±0.23	n.a.	2.2	4.7-9.0	n.a.
PHA content (wt%)	36.0±0.3	43.1±2.2	53.2	12.4-23.3	14.6±0.5
PHA (g L^{-1})	4.7±0.3	1.5±0.2	2.5	1.2-1.4	0.2±0.02
r_p (g L^{-1} day^{-1})	5.9±0.2	0.8±0.1	0.8	0.7-1.2	0.1±0.01
$Y_{X/S}$ (g g^{-1})	0.28±0.1	n.a.	n.a.	n.a.	n.a.
$Y_{P/S}$ (g g^{-1})	0.21±0.2	n.a.	0.18	n.a.	n.a.
Reference	This study	Ashby and Foglia, 1998	Ashby and Solaiman, 2008	Follonier et al., 2014	Cromwick, Foglia and Lenz,1996

A polymer content in the biomass of 36±0.8 wt% was reached at the end of the 19 hours cultivation, corresponding to an overall PHA production of 4.7±0.3 g L^{-1} and a volumetric productivity of 5.9±0.2 g L^{-1} day^{-1} (Table 4.1). The overall consumption of OODD was 29 g L^{-1}.The growth and storage yields were found to be 0.28±0.1 and 0.22±0.2 g g^{-1}, calculated over the growth and storage phases, respectively. Higher polymer content in the biomass were reported for *P. resinovorans* cultivated on other oil-containing substrates, such as olive oil (43.1±2.2 wt%) (Ashby and Foglia, 1998) and hydrolysed pollock oil (53.2 wt%) (Ashby and Solaiman, 2008). However, OODD resulted in a considerably higher overall volumetric productivity, 5.9±0.2 g L^{-1} day^{-1}, than those substrates, 0.8 g L^{-1} day^{-1}. Given these results, although the bioprocess is still not optimized, OODD is apparently a promising substrate for cultivation of *P. resinovorans* and *mcl*-PHA production.

4.4.2. PHA characterization

4.4.2.1. Composition

The PHA produced by *P. resinovorans* from OODD was found to be a co-polymer mainly composed by 3-hydroxyocatonate (3HO) (48±7.3 mol%) and 3-hydroxydecanoate (3HD) (31±2.6 mol%), with lower amounts of 3-hydroxyhexanoate (3HHx) (12±1.1 mol%) and 3-hydroxydodecanoate (3HDd) (8±0.7 mol%). Trace amounts of 3-hydroxytetradecanoate (3HTd) (<1 mol%) were also detected. An identical polymer composition was obtained in previous work (Chapter 2) by cultivation of *P. resinovorans* on OODD in batch shake flaks, namely in terms of 3HHx (19±1.1 mol%), 3HO (44±0.3 mol%) and 3HD (28±1.6 mol%).

Substrates with high oleic acid content, such as OODD (69.9±1.0 wt%),were reported as good carbon sources for the synthesis of 3HO- and 3HD-enriched co-polymers (Ashby and Foglia, 1998). Except for the higher 3HO content (29-37 mol%), the composition of the OODD-derived mcl-PHA was similar to that reported for the biopolymers produced by *P. resinovorans* from vegetable oil (Ashby and Foglia, 1998) that was composed of 3HO (29-37 mol%), 3HD (30-35 mol%), 3HHx (8-9 mol%), 3HDd (5-14 mol%) and 3HTd (2-3 mol%).

The polymer's purity was found to be 95.0±1.8% (mean of quadruplicate analysis), which was similar to that reported for other *mcl*-PHA polymers (95.5%) obtained by conventional solvent extraction with chloroform (Kathiraser et al., 2007). A lipid fraction was detected in the polymer's GC analysis, indicating that the purification procedure by ethanol precipitation did not completely remove the fatty acids remnants from the cultivation broth. Although in this study the biomass was washed with hexane for oil removal, some OODD fatty acids might still remained adsorbed to the cells, and the subsequent chloroform extraction and ethanol precipitation were apparently not enough for their complete removal. For applications in which highly pure materials are required, such as biomedical uses, the polymer should be submitted to more intensive purification procedures, such as, for example, performing additional solubilisation/precipitation steps in chloroform/ethanol or the use of other non-solvents for polymer precipitation.

4.4.2.2. Molecular mass distribution

The produced *mcl*-PHA exhibited an average molecular mass ($\bar{M}_w$) of 0.3×10^5 g mol^{-1}, with a polydispersity index (PDI) of 1.5. The polymer's $\bar{M}_w$ was lower than the values reported for *mcl*-PHA produced by the same bacterial strain cultivated in other oil-containing substrates, such as free fatty acids, tallow and vegetable oil ($1.1\text{-}1.8\times10^5$) (Cromwick, Foglia and Lenz, 1996; Ashby and Foglia, 1998). On the other hand, it had a lower PDI than those reported by Ashby and Foglia, (1998) and Cromwick, Foglia and Lenz (1996) (1.8-2.3), which indicates it is

a more homogeneous polymer. These differences in molecular mass distribution of oil-derived *mcl*-PHA are probably related to the cultivation conditions used during the production processes, namely, the composition and concentration of the carbon source, the stage of growth when the cells are harvested and the feeding strategies (Laycock et al., 2013).

4.4.2.3. Thermal properties

The *mcl*-PHA synthesized by *P. resinovorans* from OODD had melting (T_m) and glass transition (T_g) temperatures of 36.0±1.2 and -16.0±0.8 ºC, respectively. In addition, the polymer was essentially amorphous, exhibiting a very low crystallinity value of 6.0±0.2%. Comparing to values reported in literature, similar crystallinity (6-8%) and T_m (39-48 ºC) values were exhibited by the *mcl*-PHA produced from tallow free fatty acids and olive oil (Ashby and Foglia, 1998) that were mainly composed of 3HO and 3HD. However, the T_g obtained for OODD-derived *mcl*-PHA was higher than that reported for tallow-FFA and olive oil (-46 to -38 ºC), which may be related to the residual content of OODD components (e.g. fatty acids) in the extracted polymer, as discussed above. In fact, the T_g in lipid-polymer systems is highly variable, since the molecules derived from triglycerides structures can act as both cross-linkers and plasticizers. It is known that cross-linking phenomena bring the polymer backbone closer together, reducing the molecular mobility and consequently an increase in T_g might be observed (Laycock et al., 2013).

4.4.2.4. Apparent viscosity and viscoelastic properties

The apparent viscosity of the polymer was measured at 20ºC, for shear rates ranging from 10^{-3} to 10 s^{-1} (Figure 4.3A). A Newtonian plateau was observed, followed by shear-thinning for shear rate values above 0.01 s^{-1}. The experimental data was fitted to the simplified Carreau model:

$$\eta = \frac{\eta_0}{\left[1+(\lambda\dot{\gamma})^N\right]} \qquad \text{Equation (15)}$$

in which the viscosity of the second Newtonian plateau (at infinite shear rate) was neglected, that is considered to be valid in this work since it was never approached. η_0 is the viscosity of the first Newtonian plateau, $\dot{\gamma}$ is the shear rate, λ is a time constant and N is a dimensionless parameter which may be related to the exponent of the power law (n) by $N = (1-n)/2$. The Carreau parameters obtained that best describe the flow curve are: η_0= 4207±25, λ= 43±2 and N= 0.22±0.01.

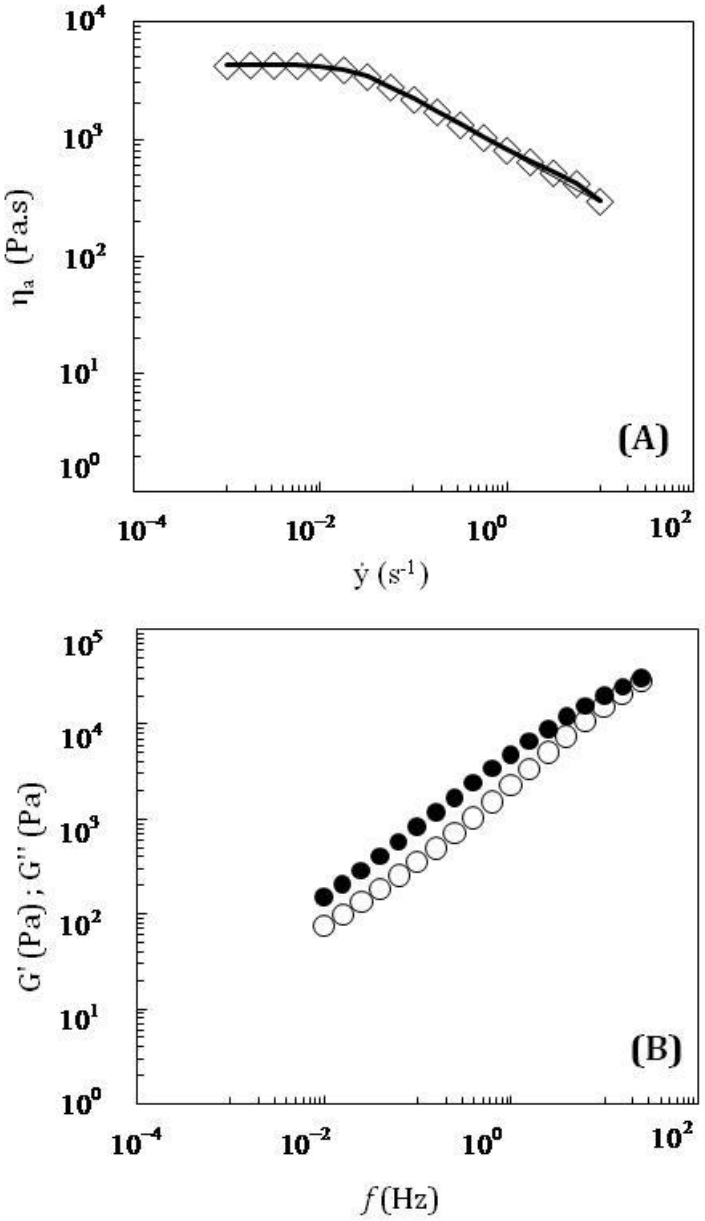

Figure 4.2: Apparent viscosity and viscoelastic properties of *mcl*-PHA produced by *P. resinovorans* cultivated in OODD: (A) Flow curve; (◇) experimental data (–) Simplified Carreau model; and (B) Mechanical spectrum.storage [*G*'(●)] and loss moduli [*G*'' (○)].

The mechanical spectrum obtained at 20ºC for the OODD-based *mcl*-PHA (Figure 4.3B) shows a high dependence of storage (*G*') and loss moduli (*G*'') with the frequency. In addition, for almost all frequency range, *G*'' values were higher than those of *G*', except at higher frequencies, where a cross-over is perceived at a frequency of about 40 Hz. This liquid-like behaviour is generally observed for polymeric systems with entangled polymer chains, and was also presented for other bonding materials, such as thermoplastic polyurethane (Torró-Palau et

al., 2001) 3-hydroxyoctanoate-*co*-3-hydroxyhexanoate (Chardron et al., 2010) and poly(3-hydroxyoctanoate) (Nerkar, et al., 2015). However, the referred rheological studies were carried out at temperatures above the polymers' melting temperatures. In this work, the rheological properties of the OODD-based *mcl*-PHA were measured at a temperature below the melting temperature (T_m = 36ºC). Even so, the OODD-based *mcl*-PHA exhibited a shear thinning behaviour and a mechanical spectrum with a predominant viscous contribution.

4.4.2.5. Shear bond stress

The obtained polymer had a very sticky behavior at room temperature, suggesting the possibility of its use as adhesive (Figure 4.4).

Figure 4.3: *mcl*-PHA produced by *P. resinovorans* with OODD, after extraction and purification procedures.

Hence, the adhesive properties of the OODD-derived mcl-PHA produced by *P. resinovorans* were evaluated for two types of materials, namely, wood (organic) and glass (inorganic). As far as the author knows, this was the first time a *mcl*-PHA has been tested as adhesive to bond wood or glass specimens.

Shear bond strength tests were performed using three different curing procedures, namely, pre-conditioning at -18, 20 or 50ºC, for 2 hours, followed by 14 hours at 20 ºC. As can be observed (Figure 4.5), the polymer's bond strength capability slightly depended on the curing procedure and on the selected material.

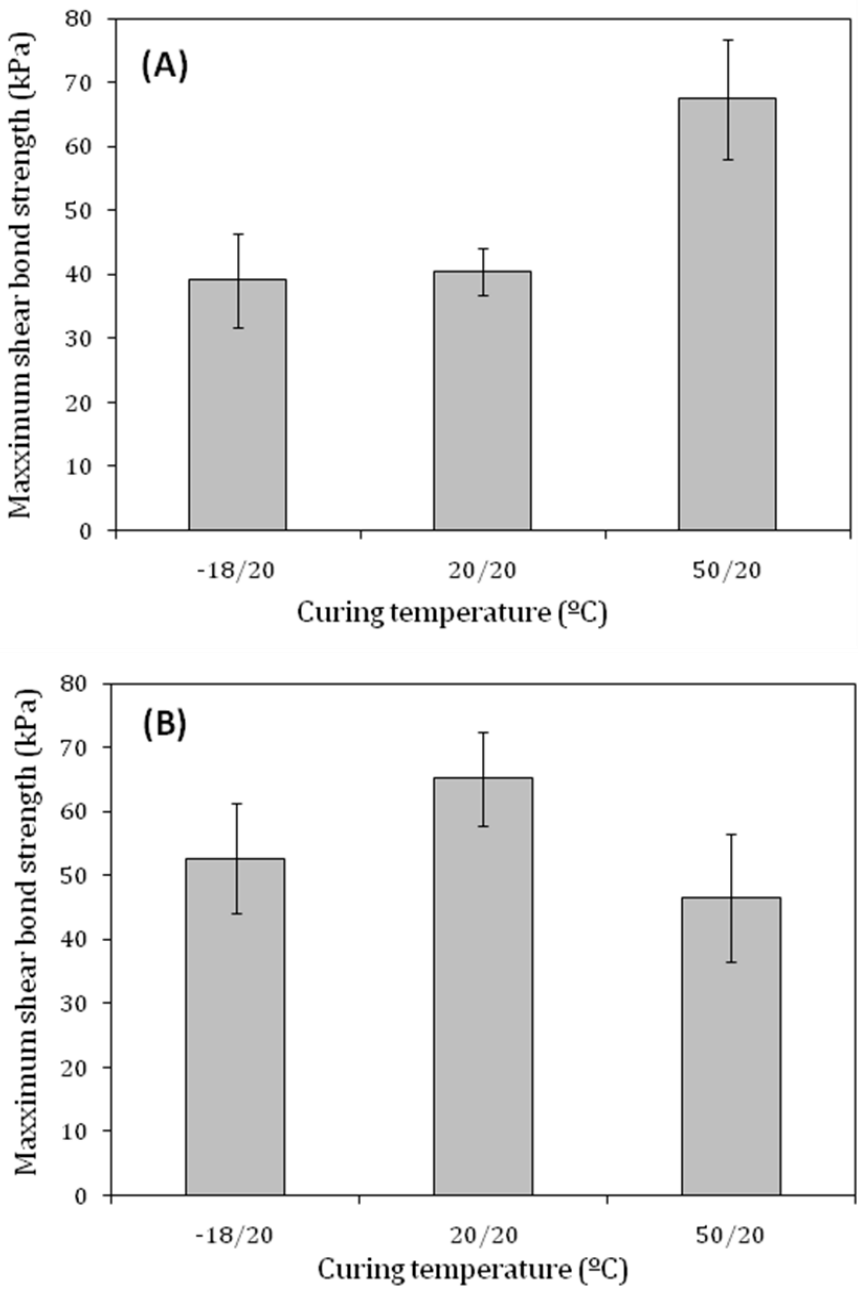

Figure 4.4: Shear bond stress of *mcl*-PHA recorded after different curing temperatures in wood (A) and glass (B) materials.

The wood samples conditioned at -18 and 20ºC exhibited similar maximum shear bond strength values of 39±7.2 and 41±3.6kPa, respectively. Apparently, reducing the curing temperature below the polymer's T_g (-16 ºC) did not affect the adhesiveness properties of the *mcl*-PHA for wood. However, curing at higher temperature, 50 ºC, resulted in higher shear bond strength (67±9.4kPa) (Figure 4.5A). In fact, the conditioning temperature was above the polymer's T_m (36ºC), which has probably resulted in a higher penetration of the melted polymer into the wood matrix. This might have improved polymer interaction with the wood components

(Kim and Netravali, 2013), ultimately resulting in the higher bond strength observed for these samples.

Higher bond strength values were found for the glass specimens glued with the OODD-derived *mcl*-PHA, for all curing procedures (Figure 4.5B).The highest bond strength of *mcl*-PHA was found to be 65±7.3kPa for the samples conditioned at 20 ºC. Slightly lower values, 53±8.5and 47±10.0kPa, were found for samples conditioned at -18 and 50ºC, respectively. In fact, conditioning the sample at 50 ºC, which is above the polymer's T_m, caused some polymer to flow out of the bonded area, thus decreasing the amount of adhesive in the joint. On the other hand, conditioning at -18 ºC, i.e. below the T_g, rendered the polymer molecules less mobility, which might have reduced the polymer/glass surface interactions, affecting the *mcl*-PHA bond strength on glass.

Some authors have reported on shear bond strength of natural glues in wood specimens. Soy protein concentrate (Kim and Netravali, 2013) and protein-based frog glues (Graham et al., 2005) were found to have good adhesive properties in wood, exhibiting shear bond strength values of 1200 and 1700kPa, respectively. Although these values are higher than the ones obtained for the OODD-derived *mcl*-PHA (<70 kPa), this polymer has the advantage of being hydrophobic. Protein-based glues are hydrophilic, which renders them more susceptible to humidity, limiting their applicability.

For comparison, commercial glue was also tested in wood and glass specimens, under identical conditions. The shear bond strength values obtained for wood and glass materials were 542±90.4 and 127±23.6 kPa, respectively. As expected, these results were higher than those obtained when *mcl*-PHA was used as adhesive (<70 kPa). However, it is important to notice that the OODD-derived *mcl*-PHA was used without any formulation, as it was recovered from the biomass. The commercial glue, on the other hand, is a product formulated with other several components (e.g. crosslinkers, catalysts, organic solvents, etc.) (Landrock, 2008). Surprisingly, the maximum shear bond strength value obtained for commercial glue in glass material was only two times higher than that obtained for crude *mcl*-PHA in glass. This may suggest that the *mcl*-PHA might be a good precursor for development of natural-based glues, with the advantage of being biodegradable and less hazardous. Furthermore, the adhesive properties of the polymer can still be improved by formulating the *mcl*-PHA into novel biobased glues.

4.5. Conclusions

A *mcl*-PHA was produced in bioreactor experiment by *Pseudomonas resinovorans* using deodorizer distillate, a fatty acids rich byproduct from the olive oil refining industry, as sole substrate.

The biopolymer had a glue-like behavior at room temperature and was tested to glue wood and glass specimens. Although low, the shear bond strength results suggest that the OODD-derived *mcl*-PHA might find use used in the development of novel biodegradable and biocompatible glues. The opportunity to use a cheap feedstock to produce a potential high value product was shown with these results.

5. CHAPTER 5

Online monitoring of PHA produced from used cooking oil (UCO) with near-infrared spectroscopy (NIRS)

The results presented in this chapter were published in one peer reviewed original research paper:

Cruz, M.V., Sarraguça, M.C., Freitas, F., Lopes, J.A., Reis, M.A.M. Online monitoring of P(3HB) produced from used cooking oil with near-infrared spectroscopy. 2015. Journal of Biotechnology, 194, 1-9

5.1. Summary

Online monitoring process for the production of polyhydroxyalkanoates (PHA), using cooking oil (UCO) as the sole carbon source and *Cupriavidus necator*, was developed. A batch reactor was operated and poly-(3-hydroxybutyrate) homopolymer was obtained. The biomass reached a maximum concentration of 11.6±1.7 g L^{-1} with a polymer content of 63±10.7 wt.%. The yield of product on substrate was 0.77±0.04 g g^{-1}. Near infrared (NIR) spectroscopy was used for online monitoring of the fermentation, using a transflectance probe. Partial least squares regression was applied to relate NIR spectra with biomass, UCO and PHA concentrations in the broth. The NIR predictions were compared with values obtained by offline reference methods. Prediction errors to these parameters were 1.18 g L^{-1}, 2.37 g L^{-1} and 1.58 g L^{-1} for biomass, UCO and PHA, respectively, which indicates the suitability of the NIR spectroscopy method for online monitoring and as a method to assist bioreactor control.

5.2. Introduction

PHA production using water immiscible carbon sources, such as fatty acids-containing substrates, is a very challenging process, due to the physical-chemical nature of the cultivation broth. Due to the presence of residual oil, i.e. the non-consumed oil, the offline quantification of the multi-components (e.g. active biomass, PHA, water and oil) involves the use of hazardous organic solvents with further multi-step analysis, which are time consuming, difficult process monitoring and control, and delay the effective process improvements and decision making. To overcome this limitation, online monitoring techniques in terms of cell growth, substrate consumption and product formation must be developed (Arnold et al., 2002a).

Near infrared (NIR) spectroscopy is a non-destructive analytical technique, which has been gaining interest in the biotechnology industry due to its advantages over other analytical techniques, such as minimal sample preparation and/or pretreatments, high speed of spectrum acquisition (within a second or less), the simultaneous detection and/or quantification of multi-components and the possibility of coupling fiber optic probes for *in-situ* measurements (Arnold et al., 2002b; Lourenço et al., 2012). NIR spectroscopy measurements are usually performed in three modes: transmittance (e.g. for low cell density fermentation broths, transparent liquids and suspensions), reflectance (e.g. for high cell density fermentation broths, opaque liquids and/or solids and powders)and transflectance, which combines the transmission and reflection modes (e.g. allows the measurements of transparent and turbid liquids and semi-solid samples) (Lourenço et al., 2012). The spectrum taken during a fermentation run comprises information from all broth NIR active constituents yielding. The NIR spectra complexity generally requires multivariate statistical analysis, such as principal component analysis (PCA) and partial least squares (PLS) for spectral interpretation and modelling (Martens and Naes, 1996). NIR

spectroscopy has been applied in bioprocess modelling with multiple objectives (Hall et al., 1996; Suehara and Yano, 2004; Tosi et al., 2003). Some representative applications of NIR in bioprocesses monitoring are: the estimation of biomass, glucose, lactic and acetic acids, in *Staphylococcus xylosus* ES13 fermentation (Tosi et al., 2003); the estimation of biomass, glucose and acetate, in choleratoxin production by *Vibrio cholerae* in a fed-batch cultivation (Navrátil et al., 2005); and the estimation of glycerol, methanol and biomass in the production of a monoclonal antibody by *Pichia pasto*ris (Goldfeld et al., 2014). Despite of the many implementations of NIR spectroscopy for bioprocesses monitoring reported over the past two decades, only a minor percentage of them indeed applied the technique *in-situ* with a real-time monitoring application in mind, as a recent review by Lourenço et al. refers (Lourenço et al., 2012).

The goal of the present work is to show the potential of NIR spectroscopy for monitoring the production of PHA and biomass, and the consumption of used cooking oil (UCO), by *Cupriavidus necator* DSM 428. Partial least squares (PLS) regression was applied to relate the NIR spectra with biomass, UCO and polymer contents. To the best of our knowledge, this is the first time NIR spectroscopy is used to simultaneously monitor the production of PHAs and biomass, using oil-containing substrates as the sole carbon source. Samples collected from four different bioreactors were used to calibrate and validate PLS calibrations. In order to assess the quality of the produced polymer at the end of cultivation run, the polymer was characterized in terms of its monomer composition, average molecular mass and polydispersity index.

5.3. Material and Methods

5.3.1. Polymer production

5.3.1.1. Bioreactor cultivation

Cupriavidus necator DSM 428 was cultivated in a mineral medium with the composition described in section 2.3.2.1 of Chapter 2, supplemented with 20 g L^{-1} of UCO. The cultivation was performed in quadruplicate experiments in 2 L bioreactors (BioStat B-Plus, Sartorius, Germany), with a 10% (v/v) inoculum as described in section 3.3.1.1 and 3.3.1.2 of Chapter 3A. The bioreactors were operated under the same conditions of experiment A reported in section 3.3.1.2 of Chapter 3A.

Samples (15 mL) were periodically withdrawn from the bioreactor for biomass, PHA and residual UCO quantification. The volumetric consumption rate (g L^{-1} h^{-1}) of the fatty acids of UCO was given by the slope of the trend line adjusted to the residual concentration of each

fatty acid (g L^{-1}) versus the same period of time t (h). Growth ($Y_{X/S,}$ g g^{-1}) and storage ($Y_{P/S,}$ g g^{-1}) yields on UCO were calculated for the same period of time, in the accumulation phase as described in section 2.3.2.5 of Chapter 2.

5.3.1.2. Analytical techniques

Cell dry mass (CDM), residual UCO concentration in the broth and PHA content and composition were determined as described in section 2.3.2.4 of Chapter 2. Also, PHA content and composition were determined by gas chromatography (GC), according to the method described in section of 2.3.2.4 of Chapter 2.

Since the UCO utilized in this work was from different lot of UCO used in experiments reported in Chapter 2, analysis of the oil composition was also performed. The mono-, di- and triglycerides content and fatty acid composition of UCO were determined according to the methods described in section 2.3.1.1 of Chapter 2. Free fatty acids were determined by titration according to AOCS official method Ca 5a-40 (section 2.3.1.1, Chapter 2). All analyses were performed in duplicate.

5.3.2. PHA extraction and characterization

Aiming at removing the residual UCO content in the biomass, at the end of the cultivation run, the broth was collected and washed with hexane (1:1, v/v) and centrifuged at (7012 × *g*, 20 min). The supernatant containing hexane and residual UCO was discharged and the resulting biomass pellet was washed twice with deionized water and lyophilized for 48h.

The polymer was extracted from the lyophilized cells and purified as described in section 3.3.2 of Chapter 3A.

The purified polymer's average molecular mass ($\bar{M}_w$) and polydispersity index were determined as described in section 2.3.3.1 of Chapter 2.

5.3.3. Near infrared spectroscopy

5.3.3.1. Software and equipment

Diffuse reflectance NIR spectra were recorded on a Fourier transform near infrared analyzer (FTLA 2000, ABB, Québec, Canada). The spectrophotometer is equipped with an indium-gallium-arsenide (InGaAs) detector and powder sampling accessory (ACC101, ABB, Québec, Canada), with a 2 cm diameter window, enabling diffuse reflectance measurements on

a 0.28 cm^2 illumination area. The spectrum was acquired with a resolution of 8 cm^{-1} as an average of 32 spectra in the wavenumber range between 10000 and 4000 cm^{-1}. The instrument is controlled via the Grams LT software (version 7, ABB, Québec, Canada). A background was made before every set of measurements using PTFE (SKG8613G, ABB, Québec, Canada). The samples were measured in triplicate and the average spectrum considered.

Transflectance NIR spectra were recorded on a Fourier transform near infrared analyzer (Antaris I, Thermo Nicolet, Madison WI, USA) equipped with a transflectance probe (Flex, Solvias, Basel, Switzerland), with a mechanical pathlength of 1mm (total optical pathlength of 2 mm). The analyzer is equipped with an indium-gallium-arsenide (InGaAs) detector enabling measurements in a wavenumber range between 10000 and 4000 cm^{-1}. Each spectrum was recorded with an 8 cm^{-1} resolution as an average of 16 scans. The equipment is controlled via the Result software package (ThermoNicolet, Madison WI, USA). Before analyzing the samples, a background spectrum was acquired with a dried empty probe. Afterwards, samples spectra were acquired sequentially at room temperature by cleaning the probe with deionized water between each measurement.

All NIR spectra was processed with Savitzky-Golay smoothing (Savitzky and Golay, 1964) using a 31 points filter width using a 2nd order polynomial.

5.3.3.2. Preliminary analysis

Lyophilized biomass obtained as described in 3.3.2. of Chapter 3A was added to 10 mL of deionized water and vigorously shaken. This suspension was then diluted in water to obtain concentrations ranging from 1.0 to 200 g L^{-1}. These biomass suspensions were analyzed by NIR spectroscopy in diffuse reflectance and transflectance modes (as described on section 5.3.3.1 of this chapter) with the goal of evaluating the most appropriate measuring mode.

The ability of NIR spectroscopy to simultaneously detect and distinguish biomass, polymer and UCO in the cultivation broth was evaluated. To this end, eight aqueous samples containing fixed amounts of biomass (1.0 and 10 g L^{-1}), polymer (<10 and >70% wt.% and oil (0 and 10 g L^{-1}) were prepared as described in Table 5.1:

Table 5.1: Biomass, UCO and P(3HB) concentration of samples retrieved from one fermentation experiment.

Samples	Biomass (g L^{-1})	UCO (g L^{-1})	P(3HB) (wt.%)
S1	1.0	10	<10
S2	10	10	<10
S3	1.0	10	>70
S4	10	10	>70
S5	1.0	0.0	<10
S6	10	0.0	<10
S7	1.0	0.0	>70
S8	10	0.0	>70

These samples were measured in the transflectance mode with an optical path length of 2 mm.

Finally, raw samples of dry biomass, purified polymer (extracted from dry cells) and UCO were measured by NIR spectroscopy in order to unveil their pure spectral profiles. This information will allow a better interpretation of PLS models structure for these analytes. Biomass and polymer were measured in reflectance mode while UCO was measured in transmittance mode (optical path length of 6 mm).

5.3.3.3. Bioreactor monitoring

Eighty-two broth samples from four bioreactor experiments were collected over cultivation time as described in section 5.3.1.1. These samples were analyzed by NIR spectroscopy in transflectance mode (as described in section 5.3.3.1) immediately after collection. Samples from three batches (70 samples) were selected to develop and optimize PLS models for biomass, PHA and UCO. From these, 49 samples (70%) were used to estimate and optimize the PLS models and 21 samples (30%) for models testing. Samples from the remaining batch (12 samples) were used as a totally independent test set (i.e. samples collected from a batch not used in the calibration). Therefore the test set was composed of 33 samples.

5.3.3.4. Data Analysis

Chemometric modeling was performed with Matlab version 8.3 (MathWorks, Natick, MA, USA) and the PLS Toolbox version 7.5 (Eigenvector Research Inc., Wenatchee, WA, USA).Principal component analysis (PCA) (Jolliffe, 2002) was applied here to analyze the spectral differences between biomass, PHA and UCO. Partial least squares (PLS) (Geladi and Kowalski, 1986) analysis was used to calibrate NIR spectra against biomass, UCO and PHA concentrations determined as described on section 5.3.1.2 of this chapter. Before application of

PCA and PLS the spectral data and the target variables (biomass, PHA and UCO concentrations) in the case of PLS were subjected to mean-centring (Martens and Naes, 1996). To optimize the number of latent variables (LVs) in the PLS models for biomass, PHA and UCO, the leave-one-out cross-validation procedure was used using the set of 49 samples collected from three bioreactor batches. The optimal number of LVs (LV_{opt}) was set to k when the equation (16) was verified (Martens and Naes, 1996).

$$\frac{RMSECV_k - RMSEC_{k+1}}{RMSECV_1 - RMSECV_{10}} < 0.05 \qquad \text{Equation (16)}$$

In equation 16, the root-mean-square error of cross-validation ($RMSECV_k$) is the value for k LVs. To model each parameter it is important to exclude spectral regions containing information unnecessary to model that parameter, to avoid interferences. Therefore, to improve the NIR wavenumber range to use in the PLS models, a method based on the sequential screening of all possible contiguous spectral windows was adopted. Briefly, an unitary window size of 40$cm^{-1}$was selected for this method. For each spectral window, the leave-one-out method was performed on the 49 calibration samples and the RMSECV for the optimal number of LVs was stored (see Equation 16). The optimal wavenumber window will be the one yielding the lowest RMSECV.

The external validation was made by projecting the spectra of the test samples onto the PLS model. The model error was estimated in terms of the root-mean square error of prediction (RMSEP).

5.4. Results and Discussion

5.4.1. Production of PHA from UCO

Cupriavidus necator DSM 428 was cultivated for 50 hours in UCO (20g L^{-1}) as the sole carbon source. Biomass, PHA production, residual UCO and fatty acids concentration were evaluated over cultivation time, in three batch experiments (Figure 5.1A and 5.1B). The culture exhibited a maximum specific growth rate of 0.12±0.02 h^{-1} until 22 hours of cultivation, with no detectable lag phase (Figure 5.1A). At the end of the cultivation run, a CDM of 11.6±1.7 g L^{-1} and a polymer concentration of 7.4±1.9 g L^{-1} were achieved, which corresponded to a polymer volumetric productivity (r_p) of 3.6±0.5 g L^{-1} day^{-1} (Table 5.2).

Table 5.2: Kinetic parameters obtained for PHA production by *C. necator* DSM 428 using UCO and other oil-containing substrates.

Parameters	**UCO** [a]	**UCO**	**UCO** [b]	**FCO**	**EPO**
Cultivation mode	Batch bioreactor	Batch bioreactor	Batch Shake flask	Batch Shake flask	Multiple batch bioreactor system
Volume (L)	2	10	0.05	0.05	0.04
μ_{max} (h^{-1})	0.12±0.02	0.14	n.a.	n.a.	n.a
CDM (g L^{-1})	11.6±1.7	10.4	13.2±0.2	13.8±0.6	10
X (g L^{-1})	4.2±0.6	6.6	n.a.	n.a.	2.00
P(3HB) content (wt.%)	63±10.7	37	72±1	66±0.3	79
P(3HB) (g L^{-1})	7.4±1.9	3.8	9.5±0.3	9.0±0.3	8
r_p (g L^{-1} day^{-1})	3.6±0.5	3.4	n.a.	n.a.	n.a
$Y_{X/S}$ (g g^{-1})	0.23±0.1	0.51	n.a.	n.a.	n.a.
$Y_{P/S}$ (g g^{-1})	0.77±0.04	0.29	n.a.	n.a.	0.84
Reference	Present study	Martino et al., 2014	Kamilah et al., 2013	Kamilah et al., 2013	Budde et al., 2011a

[a] values are presented as mean of three different batches ± standard deviation.
[b] palm oil-based
(FCO-fresh cooking oil; EPO - emulsified palm oil)

During the exponential growth phase (nitrogen availability), the biomass PHA content was 48±11.3 % (w/w), while at the end of the accumulation phase (nitrogen limitation) a content of 63±10.7 % (w/w) was reached.

Similar polymer concentration (7.7±0.64 g L^{-1}) and slightly higher CDM (15.5±1.5 g L^{-1}) were obtained in batch experiment performed in Chapter 3A. (Results and Discussion). Also the polymer content (53±5.4 %wt.) was very close to that obtained in this study, indicating the kinetic values obtained in the four experiments performed in this study are in accordance to those obtained in the first studies performed with UCO.

Values obtained in this study are higher than the ones previously reported for cultivation of *C. necator* on identical substrate. Martino et al. (2014) obtained maximum CDM and PHA concentrations of 10.4 and 3.8 g L^{-1}, respectively, and a polymer content of 37% wt.% (Table 5.2).

Nevertheless, the P(3HB) concentration and the polymer content obtained in the present study were close to the values (8.00-9.50 g L^{-1} and 66-79%(w/w), respectively) reported by Kamilah et al. (2013) and Budde et al. (2011a) for cultivation on palm oil-based or emulsified palm oil substrates. The observed differences may be related to the variability on the fatty acids units present in the oil-containing substrates. Moreover, each waste oil substrate can also have different food compounds (e.g. vitamins, liposoluble nutrients) absorbed during the frying procedure, which may impact the microorganisms' performance from batch to batch.

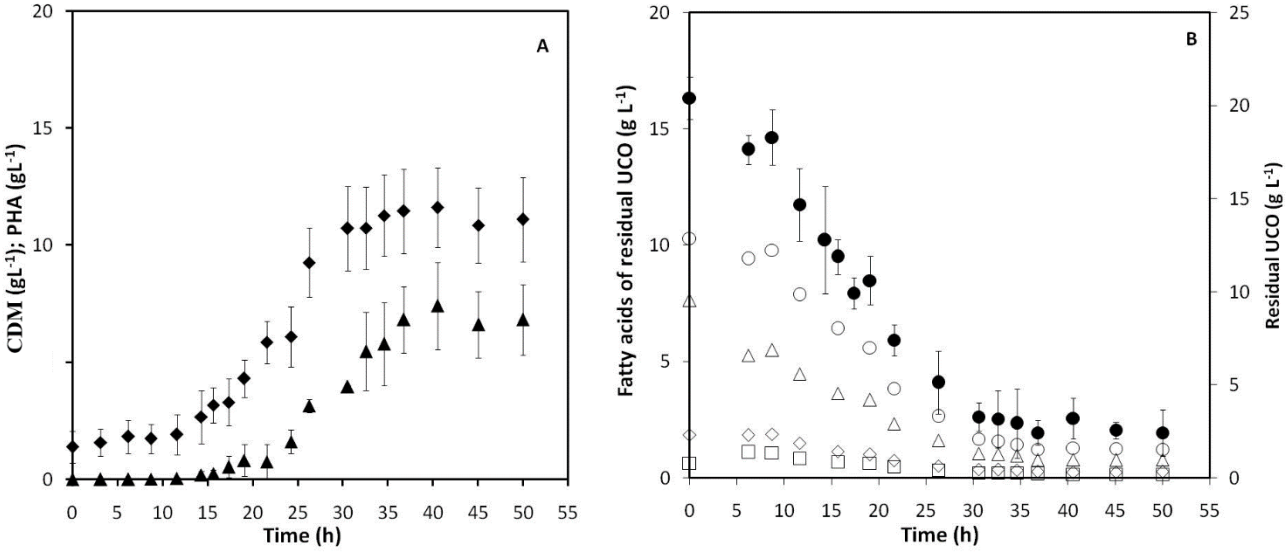

Figure 5.1: Production of PHA by *C. necator* DSM 428 using UCO as the sole carbon source. A. Cell dry mass (◆) and PHA (▲) concentration, over fermentation time; B. Residual UCO (●) and fatty acids composition: palmitic acid (C16:0 ,◇), stearic acid (C18:0 , □), oleic acid (C18:1, △), linoleic acid (C18:2, ○) and linolenic acid (C18:3 - ✱), over fermentation time. Values are presented as mean of three different batches ± standard deviation.

The UCO was composed mainly of triglycerides (94.5±12.5 %, wt.%), with minor contents of diglycerides (2.0±1.0 wt.%), monoglycerides (2.0±1.0 %, wt.%) and free fatty acids (1.05±0.35 %, wt.%). Similar composition was reported for UCO used in experiments of Chapters 2 and 3A, namely in terms of triglycerides (83.4±9.13 wt.%) and free fatty acids (1.0±0.35 wt.%). However, in the latter slightly lower content of mono (0.4±0.10 wt.%) and higher content of diglycerides (6.7±0.39 wt.%) were found. The major fatty acids detected were linoleic (50.28±0.23 %, w/w) and oleic (37.27±0.17 %, w/w) acids, followed by palmitic (9.01±0.04 %, w/w) and stearic (3.04±0.01 %, w/w) acids, with traces of linolenic acid (< 0.1±0.01 % w/w). Similar fatty acid profile has been reported for by Martino et al. (2014) and Abidin et al. (2013). However, the acylglycerides content were slightly different (65% tryglycerides, 21% diglycerides and 6% monoglycerides, wt.%) than the results reported in this study. Although the two types of UCO are from the same source (restaurant) and from the same manufacturer, the different lots of oil may be exposed to different frying times. The frying time can induce different mechanisms in the cleavage of fatty acids chains to the main glycerol structure. Thus, the final composition in terms of acylglycerides can be affected.

An overall consumption of 18.0±1.4 g L^{-1} of UCO was observed until 37 hours of cultivation, remaining thereafter a residual concentration of 2.4±1.23 g L^{-1} (Figure 5.1B). In

Figure 5.1B the concentration of each UCO fatty acid component along the cultivation run are also represented. Apparently, all fatty acids started to be consumed at the same time, but at different rates: linoleic (0.37 g^{-1} L^{-1} h^{-1}) and oleic (0.20 g^{-1} L^{-1} h^{-1}) acids were consumed faster than palmitic (0.07 g^{-1} L^{-1} h^{-1}) and stearic (0.03g^{-1} L^{-1} h^{-1}) acids, suggesting the culture's preference in terms of the available fatty acids. This is in agreement with Kahar et al. (2004) and Ng et al. (2010), which reported *C. necator* preference of linoleic, oleic and palmitic acids over other fatty acids (e.g. linolenic acid). Indeed, linoleic, oleic and palmitic acids accounted for more than 96 % (w/w) of the UCO fatty acids' composition. Due to its residual content in the UCO (<0.1±0.01 % w/w), linolenic acid was not monitored over the cultivation time. The use of plant oils containing less linolenic acid may improve the process performance, since its presence has been suggested to retard and/or inhibit *C. necator* cell growth (Rao et al., 2010). Thus, UCO rich in oleic, linoleic and palmitic acids, and poor in linolenic acid may be more adequate feedstocks for PHA production by this microorganism.

The polymer yield on substrate was 0.77±0.04 g g^{-1}, which was equal to that obtained in batch experiments reported in Chapter 3A (0.77±0.01 g g^{-1}) and higher than that obtained by Martino et al. (2014) (0.29 g g^{-1}) (Table 5.2). In the latter, the growth yield was higher (0.51 g g^{-1}) than in the present study (0.23±0.1 g g^{-1}). Although in Martino et al. (2014) similar cultivation conditions were used, the experiment was terminated at the end of the exponential growth phase (27 h of cultivation) when the nitrogen source was exhausted and cell growth was restricted. Hence, higher growth yields and lower storage yields were observed. In the present study, the cultivation run was prolonged until 50 h, which allowed the culture to enter the accumulation phase, under nitrogen limitation, thus favouring the storage yield over the growth yield.

The polymer was characterized in terms of its composition, average molecular mass and polydispersity index. As expected, *C. necator* synthesized a 3-hydroxybutyrate homopolymer, poly-3-hydroxybutyrate, P(3HB). The polymer average molecular mass of 1.7×10^5 g mol^{-1} and a polydispersity index (PDI) of 1.6 were obtained, which is the same value obtained for P(3HB) from batch experiments of Chapter 3A. Also, this is in accordance to the values reported in the literature. Typically, the average molecular mass of P(3HB) ranges between 2.0×10^5 to 3.0×10^6, with PDI that vary from 1.5 to 2.0 (Laycock et al., 2013).

5.4.2. NIR spectroscopy

5.4.2.1. Preliminary spectral analysis

Commonly, microbial cultivation broths are very complex matrices (e.g. due to the presence of suspended particles, feeding of complex carbon sources, etc.), making NIR spectroscopy analysis challenging (Arnold et al., 2002b). In the present case, a further

complexity, i.e. intracellular polymer, was introduced. For this reason, some preliminary tests were performed in order to optimize and select the appropriate spectral acquisition mode for the NIR measurements. Different biomass concentrations, ranging between 1 and 200 g L^{-1} (see section 5.3.3.2 of this chapter), were analyzed by NIR spectroscopy in diffuse reflectance (Figure 5.2a) and transflectance modes (Figure 5.2b).

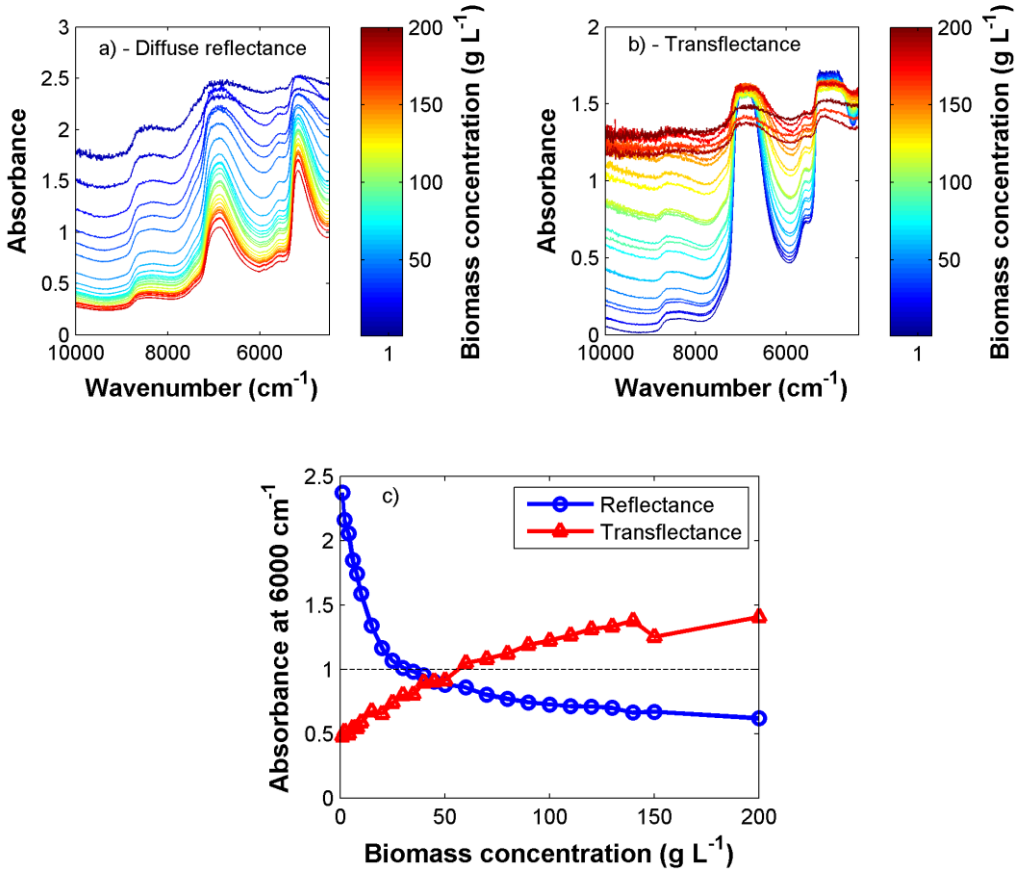

Figure 5.2.: a) Diffuse reflectance and b) transflectance NIR spectra of biomass aqueous solutions ranging from 1.0 to 200 g L^{-1} c) absorbance at 6000 cm^{-1} from the NIR spectra in presented in a) and b) as a function of biomass concentration.

As the concentration of biomass increased, more clear bands with less noise and lower absorbance could be observed in the diffuse reflectance spectrum (Figure 5.2a). In contrast, when the samples were analyzed in the transflectance mode, a lower signal-to-noise ratio and higher absorbances were observed with increasing biomass concentration. The biomass concentration resulting in a NIR spectrum with absorbances below 1 was defined as the threshold in which one measuring mode should be used in detriment of the other. The absorbance at 6000 cm^{-1} was chosen for this analysis since it is located in the highest absorbance spectral region of the spectrum, not considering the saturated regions.

By plotting the absorbance at 6000 cm^{-1} as a function of the biomass concentration (Figure 5.2c), it was concluded that the reflectance mode could be used for biomass concentrations above 30 g L^{-1}, while the transflectance mode could be used for biomass concentrations below 60 g L^{-1}.

In this study, the biomass concentration in the bioreactor broth ranged between 0.40 and 13.70 g L^{-1} (Table 5.2). Thus, all samples withdrawn from the bioreactor were measured in transflectance mode. The same strategy was followed by several authors (Roychoudhury et al., 2007;Tamburini et al., 2003; Tosi et al., 2003).

A PCA was performed on the samples described in section 5.3.3.2 (see Table 5.1), where contents of biomass, polymer and UCO were varied (Figure 5.3).

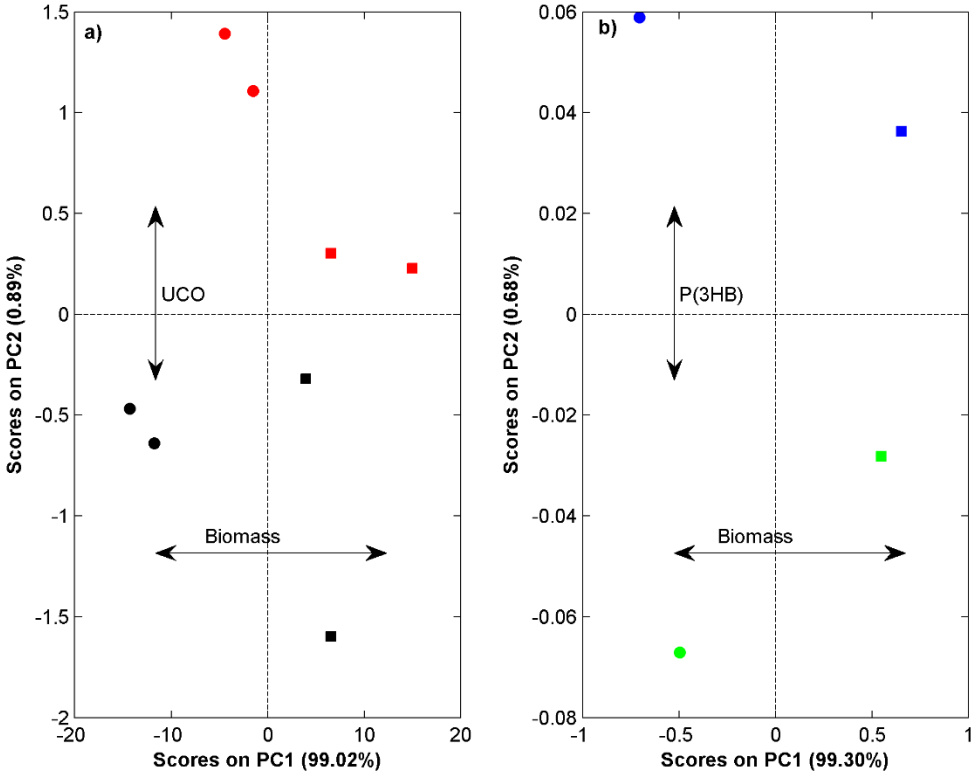

Figure 5.3: PCA score plots of NIR spectra of fermentation samples. a) Samples containing oil in a concentration of 10 g L^{-1} (red) and without oil (black). b) Samples without UCO containing and low content (<10% w/w) (blue) and a high content (> 70% w/w) of P(3HB) (green). The symbols in a circular shape correspond to a concentration of biomass of 1.0 g L^{-1} and the square symbols correspond to a biomass concentration of 10 g L^{-1}.

The NIR spectra was modelled with PCA considering the spectral windows covering the ranges 9808.2 – 7278.0 cm^{-1}, 5928.1-5311.0 cm^{-1} and 4771.0 – 4308.2 cm^{-1}. The separation observed in the first component is due to the biomass concentration and the separation observed

in the second component is due to the presence of UCO in the samples (left panel of Figure 5.3). When analysing only the samples without UCO (samples S5 to S8), in the 4771.0 - 4308.2 cm^{-1} range, it is possible to identify a separation based on the biomass content in the first component and a separation based on polymer content in the second component. As observed in the PCA scores, the biomass concentration is the major contribution to the spectra variability, mainly due to scattering effects (this will be discussed latter). The polymer is less visible in the spectra since it is a polyester and UCO is mainly composed of triglycerides (as discussed in section 5.4.1). Both have CH_2 and CH_3 groups, which lead to similar overlapped bands in the NIR spectrum.

5.4.2.2. Bioreactor monitoring

The NIR spectroscopy method is intended to be used as an analytical method able to provide real-time estimations of the major bioprocess variables to be coupled with the process control routines. Two methods can be envisaged for this task. Ideally, the transflectance probe can be immersed in the reactor broth (*in-situ* method). Alternatively, at-line analysis from bioreactor samples, hereby called online method, prevents some loss of signal sensibility (higher signal-to-noise ratio), gas phase effects (bubbles), probe fouling (if no automatic probe cleaning device is used) and effects caused by non-perfect mixing creating spatial gradients inside the reactor (Arnold et al., 2002a). Additionally, to estimate models for bioreactor variables, it is advisable that the same sample is measured by NIR spectroscopy and reference methods (section 5.3.1.2) and this can be accomplished with the online strategy involving a sampling procedure. Hence, a better calibration model is usually obtained in this situation and this is the reason this method was hereby preferred to the *in-situ* situation although both were possible. One of the major problems of NIR spectroscopy when being used in aqueous systems is high absorbance of the water OH groups.

As can be seen in Figure 5.4, the spectra are dominated by the bands around 7100 cm^{-1} and 5200 cm^{-1}, which correspond to the second and first overtone, respectively, of the fundamental vibration of the OH group in water.

Another important characteristic of the NIR spectra in fermentation batch wise runs is the baseline increase due to increasing biomass concentration. This phenomenon can be seen in Figure 5.4. Biomass, due to the induced light diffusion, influences NIR absorbance in two ways: a multiplicative effect mainly caused by the rise of the optical path length and an additive effect that leads to the decrease of the intensity of the incident radiation reaching the detector.

The result of these effects is that very little photons will finally manage to cross the medium inside the probe, explaining the low transmittance values and the high absorbance.

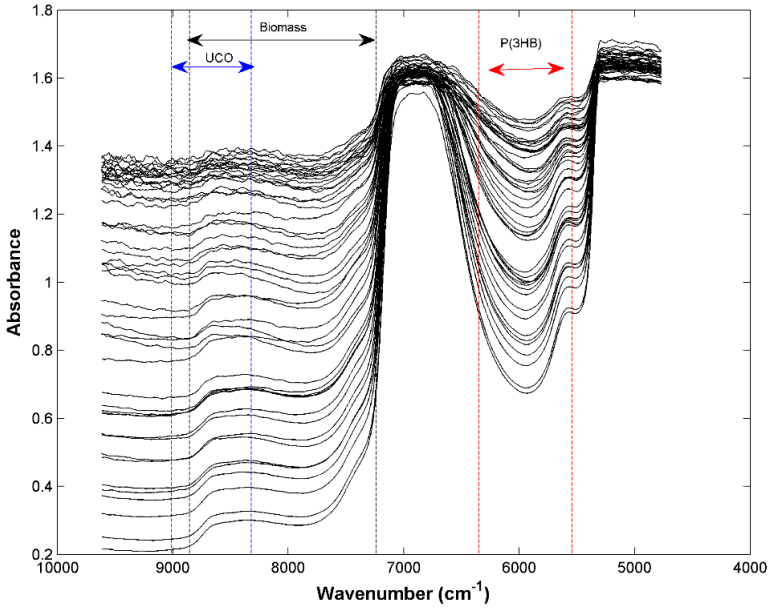

Figure 5.4: NIR spectra used for calibration with the indication of the spectral regions used in the optimized PLS models for the quantification of each parameter.

Both effects can be minimized by using mathematical pre-processing methods, such as the second derivative, to reduce the additive effects, and multiplicative scatter correction to reduce the multiplicative ones (Næs et al., 2002).In the particular case of this work, the Savitzky-Golay smoothing algorithm with a 31 points width filter was selected. This means that no minimization of the scattering effects due to biomass content was applied.

Models for biomass, PHA and UCO based on PLS regression were optimized according to the wavenumber region optimization described in section 5.3.3.4. of this chapter. For each parameter, a total of 78000 PLS cross-validation models were performed in order to test all spectral windows and possible LVs. Results can be presented under the format of contour plots where axes represent the initial and final wavenumber and colours represent the RMSECV for that particular window PLS model (Figure 5.5).

The best wavenumber regions were selected according to the minimum obtained RMSECV. Note that for all situations, combinations of different regions yielding low RMSECV values were attempted but no improved models were obtained. Therefore, the spectral regions chosen for the PLS models were 8555.5-7239.5 cm^{-1},9009.8-8319.4 cm^{-1} and 5542.4-6313.8 cm^{-1} for biomass, UCO and P(3HB) quantification, respectively. These selected regions were compared with pure spectra obtained for dried biomass, pure UCO and pure and dried P(3HB) (Figure 5.6). In the dried biomass spectrum, the region with relevant chemical information was found to be between 6000 $cm^{-1}$and 4000 cm^{-1}. Notwithstanding, by observing Figure 5.5, the selected spectral region for biomass prediction is 8555.5-7239.5 cm^{-1} which is different from

that given by the pure material spectrum. In fact, between 8555.5 cm^{-1} and 7239.5 cm^{-1} what is being modelled is the baseline increase (due to light scattering effects) produced by the increasing biomass concentration over the cultivation run. Thus, no relevant chemical information was withdrawn from that region.

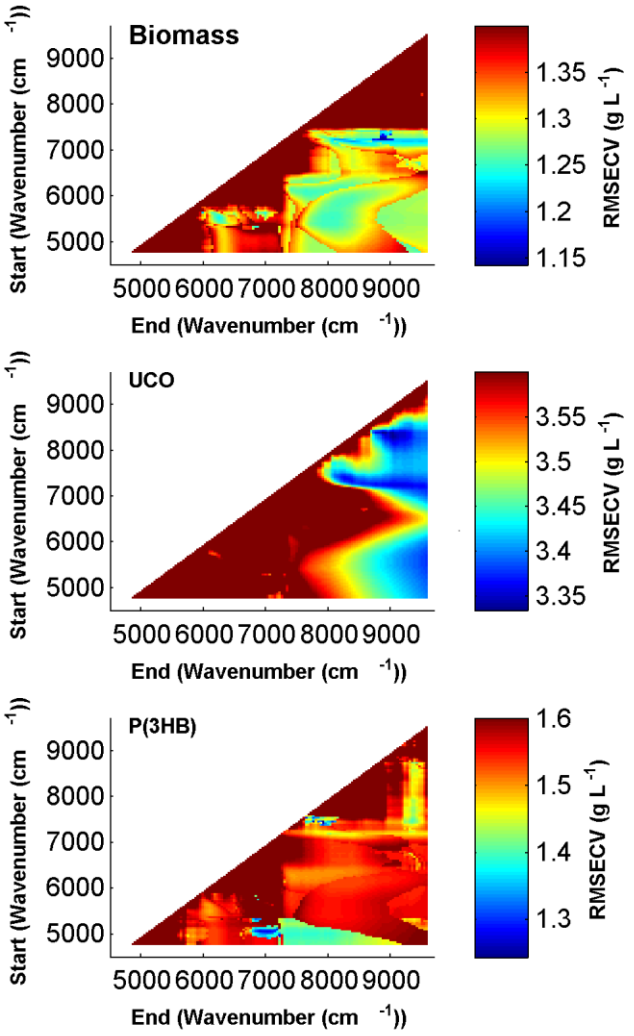

Figure 5.5: Spectral range optimization results colored according to the RMSECV value for biomass, UCO and P(3HB) quantification.

In the case of UCO concentration, the selected spectral region (9009.8-8319.4 cm^{-1}) corresponds to the second overtone of the CH vibration in CH_2 and CH_3 groups (Figure 5.6), which are strongly present in this substrate. NIR spectrum of pure P(3HB) (Figure 5.6) showed several bands between 5542.4-6313.8 cm^{-1}, corresponding to the first overtone region of the CH vibration of the CH, CH_2 and CH_3 groups that, in fact, are the groups present in the polymer.

After the PLS models optimization it was possible to project onto each model the test set spectra to verify how NIR based predictions matched with the values generated by the reference methods. This was performed considering the 21 samples collected from three batches

(the batches from where the calibration samples were collected) and the 12 samples from a forth batch (none sample of this batch was used in the calibration).

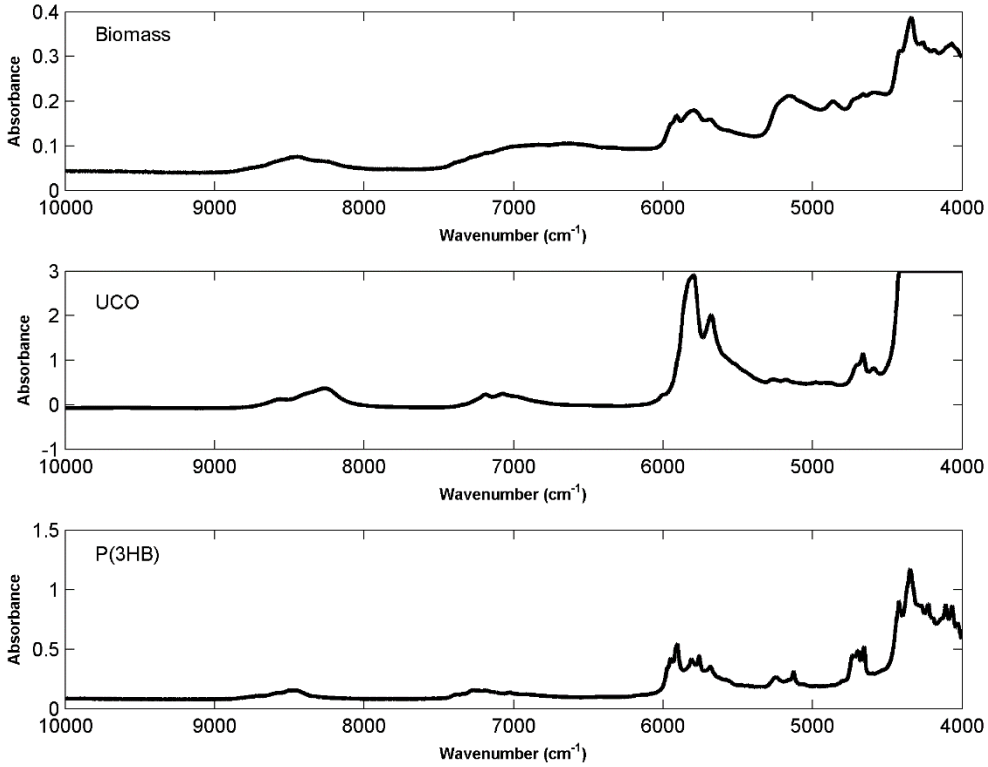

Figure 5.6: NIR spectra of dry biomass (diffuse reflectance), pure P(3HB) (diffuse reflectance) and UCO (transflectance).

Predictions for the calibration and test samples were compared with reference values for the three parameters (Figure 5.7).The vertical dash line in the test samples plots (right panel of Figure 5.7) denotes the point after which the samples arise from a batch run not used in the calibration. It is clear that the NIR spectroscopy predictions match very accurately the values obtained by the reference methods. A detailed description of models' results is given in Table 5.3.

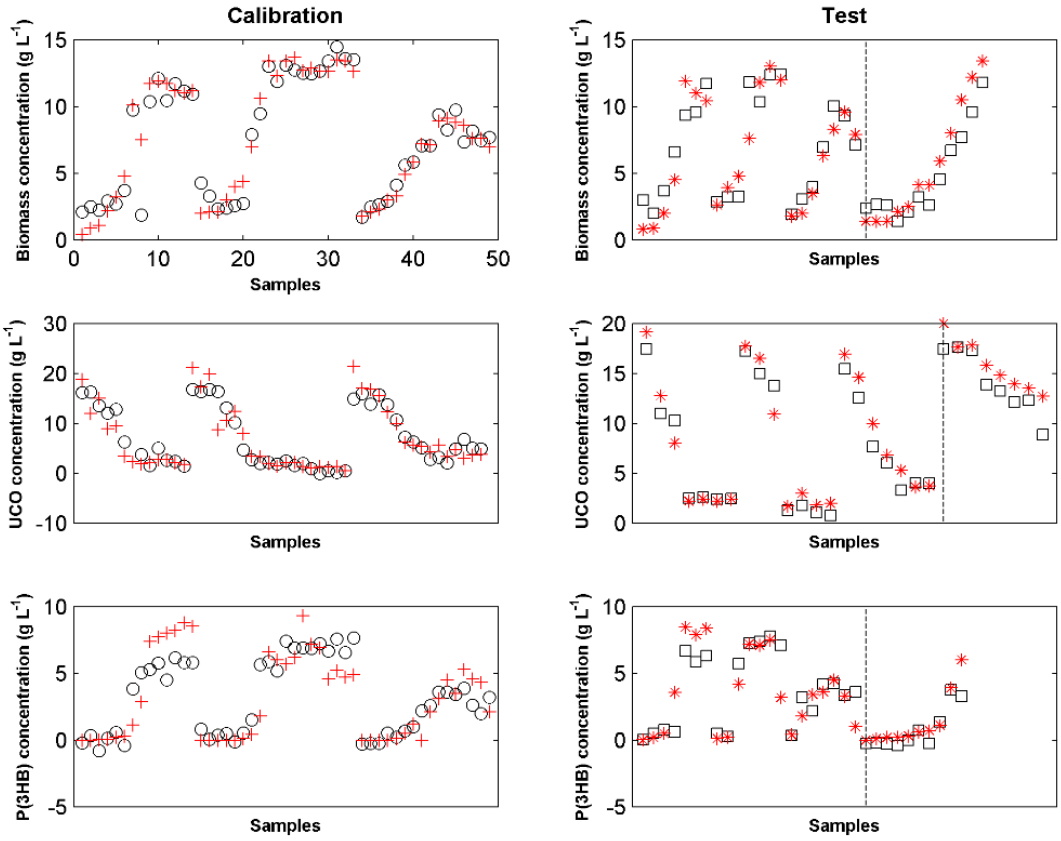

Figure 5.7: Reference method (black symbols) and NIR spectroscopy based PLS predictions (red symbols) for biomass, UCO and P(3HB) (left: calibration samples, right: validation samples).

In general, models yielded very similar errors considering calibration (cross-validation errors) and the validation sets which is an indication that they were correctly estimated. The increase of biomass concentration over cultivation runs could be accurately followed, both in the calibration and the test samples.

The error was 1.18 g L^{-1} (8.4%) for the calibration samples and 1.57 g L^{-1} (12%) for the test samples. The residual UCO concentration could also be followed, with errors of 2.37 g L^{-1} (11%) for the calibration samples and 1.61 g L^{-1} (8.8 %) for the test samples. The errors for the P(3HB) content were slightly higher, with a cross-validation error of 1.58 g L^{-1} (17%) and a test error of 1.37 g L^{-1} (16%). Because measurements are made in transflectance, which is an hybrid of transmission and diffuse reflectance, it is possible that the intracellular nature of the polymer, makes its detection by NIR spectroscopy more problematic than UCO which is an extracellular component of the cultivation broth.

Table 5.3: Calibration and validation of the NIR spectroscopy based PLS models for *C. neactor* DSM 428 biomass, UCO and P(3HB) concentrations and comparison with models from other fermentation processes reported in the literature.

Analytes	Biomass	UCO	P(3HB)	Biomass	Biomass
Model type		PLS		PLS	PLS
Wavenumber (cm^{-1})	8855.5-7239.5	9009.8 -8319.4	5542.4-6313.8	14285.7-5555.6	4878.1-4255.3
LV	5	2	3	n.a.	n.a.
			Calibration[3]		
Range ($g\ L^{-1}$)	0.4-13.7	0.5-21.4	0-9.3	0-16	0-17
Samples	49	47	49	110	110
RMSECV ($g\ L^{-1}$)	1.2	2.4	1.6	0.9	0.86
RE_{cv} (%)	8.8	11.4	16.9	5.6	5.1
$R_{cal}{}^2{}_{CV}$	0.93	0.86	0.74	0.95	0.98
			External Validation[c]		
Range ($g\ L^{-1}$)	0.8-13.0	1.7-19.1	0.01-8.4	0-16	n.a.
Samples	33	29	31	n.a.	42
RMSEP ($g\ L^{-1}$)	1.6	1.6	1.4	0.8	1.45
RE_{test} (%)	12.4	8.8	16.3	5.0	8.5
R^2_{test}	0.86	0.96	0.78	0.95	0.97
References	This Study	This Study	This Study	Tosi et al. (2003)[a]	Arnold et al. (2002)[b]

[a] Dispersive spectrometer coupled with an interactance fiber optic system; chemometric model - PLS, pre-processing - 2nd derivate. The results for calibration and external validation are given as standard error of calibration (SEC) and standard error of prediction (SEP), respectively.
[b] Imersion (trasmission) probe; chemometric model - PLS, pre-processing - 2nd derivate. The results for calibration and external validation are given as SEC and SEP, respectively.
[c] The calibration/external validation procedure is explained in section 5.3.3.4 (Data Analysis)

As far as authors are aware, the monitoring of PHA and biomass production, together with the consumption of an oil-containing carbon source (such as UCO), is being reported for the first time. Nevertheless, NIR spectroscopy has already been used for monitoring multi-analytes of fermentation broth in different bioprocesses. Arnold et al. (2002a) developed a PLS model for monitoring the biomass during *E.coli* fermentation, using 110 to calibrate the model (Table 5.3).

They achieved calibration and validation errors of 0.86 g L^{-1} (5.1 %) and 1.45 g L^{-1} (8.5%), respectively, which are in accordance with those obtained for the biomass of *C.necator*

in this study. Also, Tosi et al. (2003) reported on the quantification of multi-analytes during *Staphylococcus xylosus* ES13 fermentation. Biomass, glucose, lactic and acetic acids concentrations were calibrated by PLS regression of second derivate NIR spectra, with errors of 0.9 (5.6%), 3.0 (5.1%), 1.5 (6.5%) and 0.9 (4.7%), respectively (Table 5.3). However these results were obtained with different bioprocesses, based on the use of different microorganisms, carbon sources and products and thus a direct comparison is difficult. The intracellular nature of the product, P(3HB), and the immiscibility of the substrate, UCO, considerably makes their monitoring by NIR spectroscopy more difficult, but despite that, results prove to be very accurate and of very much importance in the context of process control. Generally, data collected from three to six fermentation runs are sufficient to provide suitable variation in multi-analyte level (Arnold et al., 2002b). Further improvements like increasing the number of cultivation broth samples by increasing the number of batches, may be performed in order to even lower the NIR based model errors for these parameters (Arnold et al., 2002b) but the hereby developed models have enough quality to assist with important information a bioreactor control strategy. A next-step would be to verify if the probe immersed in the medium would provide consistent spectra by avoiding the aforementioned possible problems and thereby estimating these parameters online from an in-situ probe.

5.5. Conclusions

P(3HB) is produced by *Cupriavidus necator* DSM 428 cultivated in UCO as the sole substrate. A storage yield of 0.77±0.04 g $g^{-1}$and a volumetric productivity of 3.6±0.5 g L^{-1} day^{-1} were obtained. NIR spectroscopy was successfully used, for the first time as online monitoring tool of PHA, biomass production and oil-containing substrate. Indeed, it was possible to calibrate and validate PLS models with R^2 of 0.96, 0.86 and 0.78 for UCO, biomass and P(3HB),respectively. This method was validated as an online method able to provide estimation of these three important process variables with no significant analytical operation costs.

6. CHAPTER 6

General conclusions and Future Work

6.1. General Conclusions

In this thesis, the production of polyhydroxyalkanoates (PHA) from different oil-containing substrates and bacterial strains was studied. Different low cost oil-containing wastes were shown to be suitable substrates for cultivation of several bacterial strains for PHA production, namely, used cooking oil (UCO), fatty acids-byproduct from biodiesel (FAB) and olive oil deodorizer distillate (OODD). Among the tested substrates, OODD, which had previously not been tested, gave the best results in terms of cell growth and PHA synthesis, for all tested strains. The use of OODD substrate allowed for the production of either *scl*- or *mcl*-PHA polymers, depending on the strain used: *C. necator* DSM 428 was the best *scl*-PHA producer, while *P. resinovorans* yielded good *mcl*-PHA production. Hence, polymers with distinct properties, suitable for different applications, can be obtained from the same substrate (OODD) by cultivation of either bacteria. UCO also demonstrated great potential to be used as sole carbon source for *C. necator* cultivation, not only because higher polymer content was achieved but also because it is a feedstock largely available. Taking this into account, UCO was selected to produce *scl*-PHA by *C. necator* DSM 428 and OODD was selected to produce *mcl*-PHA by *P. resinovorans*.

C. necator was cultivated in bioreactor under different operation modes and feeding strategies of UCO. The DO-stat feeding strategy was found to be the best strategy to improve the PHA production from UCO, among those tested. With this strategy, the overall production of PHA was improved by 64% when compared to the exponential feeding strategy. In the different experiments, *C. necator* produced the homopolymer P(3HB) that presented similar thermal properties, but different molecular mass distribution, depending on the feeding strategy adopted. The polymer with higher molecular mass was obtained with the DO-stat cultivation mode, showing this can be a good operation mode for the production of P(3HB) by *C. necator* using UCO as substrate.

SCG oil was selected as carbon source for external validation (from the initial screening) of PHA bioreactor production from different oil-containing substrates. It was demonstrated that SCG oil is a good substrate for PHA production by *C. necator* DSM 428. With preliminary batch experiment, high polymer content (54%) was obtained. However, with DO-stat feeding strategy it was possible to improve polymer content up to 78 % (w/w), resulting in a product yield of 0.77 Kg of PHA per Kg of SCG oil (97 Kg per ton of SCG processed), showing this can be a suitable feeding strategy to be used in this bioprocess.

P(3HB) exhibited very good properties when compared to similar polymers. Apparently, the differences of composition between vegetable oils, such as UCO and SCG oil, had no impact on polymer's molecular mass and thermal properties. Also, mechanical properties of P(3HB) were similar to those of P(3HB) produced from other sources, meaning the SCG oil is a

robust and low cost carbon source with minimal impact on polymer's properties.

Pseudomonas resinovorans produced a *mcl*-PHA in bioreactor experiment by using OODD as sole carbon source, a fatty acids rich byproduct from the olive oil refining industry. The biopolymer had a glue-like behavior at room temperature and was tested to glue wood and glass specimens. Although low, the shear bond strength results suggest that the OODD-derived *mcl*-PHA might be used in development of novel biodegradable and biocompatible glues.

Since the use of oil-containing substrates in water cultivation media constitute a complex biphasic matrix, monitoring tools can be very helpful in the determination of kinetic parameters. In this sense, near infrared spectroscopy (NIRS) was successfully used, for the first time as online monitoring tool of PHA, biomass production and oil-containing substrate. It was demonstrated that it is possible to calibrate and validate partial least square (PLS) models with R^2 of 0.96, 0.86 and 0.78 for UCO, biomass and P(3HB), respectively. This method was validated as an online method able to provide estimation of these three important process variables with no significant analytical operation costs.

The tested oil-containing substrates, such as UCO and OODD showed to be very good alternative carbon sources in PHA production by using either *C. necator* or *P. resinovorans*, to produce different type of PHA.

6.2. Future work

In this work, three different oil containing substrates were selected to be used as sole carbon source in *scl*- and *mcl*-PHA production, using different types of bacterial strains. However, further interesting work, related to this research area can be developed in the future, namely:

- Isolation of new bacterial strains from oil-containing substrates and evaluation of their capability to accumulate PHA;
- Test other oil-containing wastes (e.g. animal fats) as carbon sources for the different bacterial strains tested in this work;
- Evaluate the impact of different fatty acids ratio in the PHA production, bacterial growth and physical-chemical, thermal and mechanical properties of the polymer;
- Optimization of the mineral media, namely, the nitrogen source (e.g. urea, ammonium sulfate, etc) and carbon-to-nitrogen ratio in order to improve the cell growth for the selected strains;
- Optimization of the PHA productivity by testing different process parameters (e.g. pH, dissolved oxygen, temperature, aeration rate, etc) of the cultivation in UCO, OODD and FAB.
- Test other extraction and purification methods (e.g. the use of super critical carbon dioxide), in order to avoid the use of toxic organic solvents, such as chloroform;
- Improve the production, purification and extraction of *mcl*-PHA from *P. resinovorans* in order to have a polymer suitable to be used in biomedical areas;
- Deep characterization of the *mcl*-PHA obtained from *P. resinovorans* and OODD, in terms of thermal and mechanical properties, has to be done, in order to develop new possible applications;
- Calibrate the NIR models to fed-batch processes, and to other PHA production process, using different oil-containing substrates and bacterial strains.

Further, pilot scale process validation and a technical-economical analysis are required in order to evaluate the economic viability of the process.

References

Abdullah, M., Koc A.B., 2013. Oil removal from waste coffee grounds using two-phase solvent extraction enhanced with ultrasonication. Renewable Energy 50, 965-970.

Abidin, S.Z., Patel, D., Saha, B., 2013. Quantitative Analysis of Fatty Acids Composition in the Used Cooking Oil (UCO) by Gas Chromatography-Mass Spectrometry (Gc-Ms). Can. J. Chem. Eng. 91, 1896-1903.

Aeschelmann, F., Carus, M., 2015. Bio-based Building Blocks and Polymers in the World, Capacities, Production and Applications : Status Quo and Trends towards 2020, nova-Institut GmbH, 1-23.

Akaraonye, E., Keshavarz, T., Roy, I., 2010. Production of polyhydroxyalkanoates: The future green materials of choice. J. Chem. Technol. Biotechnol. 85, 732–743.

Akgün, N. A., 2011. Separation of squalene from olive oil deodorizer distillate using supercritical fluids. Eur. J. Lipid Sci. Technol. 113, 1558–1565.

Albuquerque M.G.E., Concas S, Bengtsson S, Reis M.A.M., 2010. Mixed culture polyhydroxyalkanoates production from sugar molasses: The use of a 2-stage CSTR system for culture selection. Bioresour Technol,101, 7112–22.

Al-Hamamre Z., Foerster S., Hartmann F., Kröger M., Kaltschmitt M., 2012. Oil extracted from spent coffee grounds as a renewable source for fatty acid methyl ester manufacturing. Fuel 96, 70-76.

Allen, A.D., Anderson, W.A., Ayorinde, F.O., Eribo, B.E., 2010. Biosynthesis and characterization of copolymer poly(3HB-co-3HV) from saponified *Jatropha curcas* oil by Pseudomonas oleovorans. J. Ind. Microbiol. Biotechnol. 37, 849-856.

Andrade K.S., Goncalvez R.T., Maraschin M., Ribeiro-do-Valle R.M., Martínez J., Ferreira S.R.S., 2012. Supercritical fluid extraction from spent coffee grounds and coffee husks: Antioxidant activity and effect of operational variables on extract composition. Talanta 88, 544-552.

Arnold, S.A., Gaensakoo, R., Harvey, L.M., McNeil, B., 2002a. Use of at-line and in-situ near-infrared spectroscopy to monitor biomass in an industrial fed-batch Escherichia coli process. Biotechnol. Bioeng. 80, 405-413.

Arnold, S.A., Harvey, L.M., McNeil, B., Hall, J.W., 2002b. Employing near-infrared spectroscopic methods of analysis for fermentation monitoring and control: Part 1, method development. Biopharm. Int. 15, 26-34.

Ashby, R.D., Foglia. T.A., 1998. Poly(hydroxyalkanoate) biosynthesis from triglyceride substrates. Appl. Microbiol. Biotechnol. 49, 431–437.

Ashby, R.D., Solaiman, D.K.Y., 2008. Poly(hydroxyalkanoate) biosynthesis from crude alaskan pollock (*theragra chalcogramma*) oil. J. Polym. Environ. 16, 221–229. doi:10.1007/s10924-008-0108-5

Ashby, R.D., Solaiman, D.K.Y., Foglia, T.A, 2002. The synthesis of short- and medium-chain-length poly(hydroxyalkanoate) mixtures from glucose- or alkanoic acid-grown P*seudomonas oleovorans.* J. Ind. Microbiol. Biotechnol. 28, 147–153.

Ashby, R.D., Solaiman, D.K.Y., Foglia, T.A., 2004. Bacterial poly(hydroxyalkanoate) polymer production from the biodiesel co-product stream. J. Polym. Environ. 12, 105–112.

Ashby, R.D., Solaiman, D.K.Y., Foglia, T.A., Liu, C.K., 2001. Glucose/lipid mixed substrates as a means of controlling the properties of medium chain length poly(hydroxyalkanoates). Biomacromolecules 2, 211-216.

Atlić, A., Koller, M., Scherzer, D., Kutschera, C., Grillo-Fernandes, E., Horvat, P., Chiellini, E., Braunegg, G., 2011. Continuous production of poly([R]-3-hydroxybutyrate) by *Cupriavidus necator* in a multistage bioreactor cascade. Appl. Microbiol. Biotechnol. 91, 295–304.

Azócar, L., Ciudad, G., Heipieper, H.J., Navia, R., 2010. Biotechnological processes for biodiesel production using alternative oils. Appl. Microbiol. Biotechnol. 88, 621–636.

Baranowska, M., Schlobmacher, U., McKenzie, J.D., Müller, W.E.G., Schröder, H.C., 2011. Isolation and characterization of adhesive secretion from cuvierian tubules of sea cucumber *Holothuria forskli (Echinodermata: Holothuroidea*). Evidence-based Complement. Altern. Med. 2011, 1-13.

Barham, P.J., Keller, A., Otun. E.L., Holmes. P.A., 1984. Crystallization and morphology of a bacterial thermoplastic: poly-3-hydroxybutyrate. J. Mater. Sci. 19, 2781–2794.

Bondioli, P., Mariani, C., Lanzani, A., Fedeli, E., Muller, A., 1993. Squalene recovery from olive oil deodorizer distillates. J. Am. Oil Chem. Soc. 70, 763–766.

Bourbonnais, R., Marchessault, R.H. 2010. Application of Polyhydroxyalkanoate Granules for Sizing of Paper. Biomacromolecules, 11, 989–993

Brunner, G., 1994. Gas Extraction, Springer, Berlin.

Budde, C.F., Riedel, S.L., Hubner, F., Risch, S., Popovic, M.K., Rha, C., Sinskey, A.J., 2011a. Growth and polyhydroxybutyrate production by *Ralstonia eutropha* in emulsified plant oil medium. Appl. Microbiol. Biotechnol. 89, 1611-1619.

Budde, C.F., Riedel, S.L., Willis, L.B., Rha, C., Sinskey, A.J., 2011b. Production of poly(3-hydroxybutyrate-co-3-hydroxyhexanoate) from plant oil by engineered *Ralstonia eutropha* strains. Appl. Environ. Microbiol. 77, 2847–2854.

Cavalheiro J.M.B.T, de Almeida M.C.M.D., Grandfils C, da Fonseca M.M.R., 2009. Poly(3-hydroxybutyrate) production by *Cupriavidus necator* using waste glycerol. Process Biochem;44:509–15.

Chanprateep S., 2010. Current trends in biodegradable polyhydroxyalkanoates. J.Biosci. Bioeng.110(6), 621–632.

Chanprateep, S., Abe, N., Shimizu, H., Yamane, T., Shioya, S., 2001. Multivariable control of alcohol concentrations in the production of polyhydroxyalkanoates (PHAs) by *Paracoccus denitrificans*. Biotechnol. Bioeng. 74, 116–124.

Chanprateep, S., Kikuya, K., Shimizu, H., Shioya, S., 2002. Model predictive controller for biodegradable polyhydroxyalkanoate production in fed-batch culture. J. Biotechnol. 95, 157–169.

Chardron, S., Bruzaud, S., Lignot, B., Elain, A., Sire, O., 2010. Characterization of bionanocomposites based on medium chain length polyhydroxyalkanoates synthesized by *Pseudomonas oleovorans*. Polymer Testing 29(8), 966-971.

Chee, J.-Y., Yoga, S.-S., Lau, N., Ling, S., Abed, R.M.M., Sudesh, K., 2010. Bacterially Produced Polyhydroxyalkanoate (PHA): Converting Renewable Resources into Bioplastics. Curr. Res. Technol. Educ. Top. Appl. Microbiol. Microb. Biotechnol. 1395–1404.

Chen, G.-Q., 2009. A microbial polyhydroxyalkanoates (PHA) based bio- and materials industry. Chem. Soc. Rev. 38, 2434–2446.

Chen, G.-Q., 2010. Industrial Production of PHA. Plast. from Bact. Nat. Funct. Appl. 14, 121–132.

Choi, J., Lee, S.Y., 1999. Factors affecting the economics of polyhydroxyalkanoate production by bacterial fermentation. Appl. Microbiol. Biotechnol. 51, 13–21.

Couto R. M., Fernandes J., Gomes da Silva M.D.R., Simões P. C., 2009. Supercritical fluid extraction of lipids from spent coffee grounds. J. Supercrit. Fluids 51, 159–166.

Cromwick, A.M., Foglia, T., Lenz, R.W., 1996. The microbial production of poly(hydroxyalkanoates) from tallow. Appl Microbiol Biotechnol 46. 464–469.

Da Cruz Pradella, J.G., Ienczak, J.L., Delgado, C.R., Taciro, M.K., 2012. Carbon source pulsed feeding to attain high yield and high productivity in poly(3-hydroxybutyrate) (PHB) production from soybean oil using *Cupriavidus necator*. Biotechnol. Lett. 34, 1003–1007.

Dumont, M.-J., Narine. S.S.,2007. Soapstock and deodorizer distillates from North American vegetable oils: Review on their characterization, extraction and utilization. Food Res. Int. 40, 957-974.

Eggink, G., Waard. D., Huijberts. P.,1995. Formation of novel poly(hydroxyalkanoates) from long chin fatty acids. Can. J.Microbiol, 41. 14-21.

Elbahloul, Y., Steinbüchel, A., 2009. Large-scale production of poly(3-hydroxyoctanoic acid) by Pseudomonas putida GPo1 and a simplified downstream process. Appl. Environ. Microbiol. 75, 643–651.

El-shami, S.M., El-mallah, M.H., El-hamidi, M., 2013. Study of the Bioactive Components of Deodorizer Distillates Produced from Edible Oil Processing to Be Used as Potential Sources of Natural Components 27, 763–769.

Endres, H.-J., Siebert-Raths, A., 2011. Engineering Biopolymers. Eng. Biopolym. 71–148.

Faezah, A. N., Rahayu, A., Vigneswari, S., Majid, M.I.A, Amirul, A.A., 2011. Regulating the molar fraction of 4-hydroxybutyrate in Poly(3-hydroxybutyrate-co-4-hydroxybutyrate) by biological fermentation and enzymatic degradation. World J. Microbiol. Biotechnol. 27, 2455–2459.

Fiorese M.L., Freitas F., Pais J., Ramos A.M., Reis M.A.M., Aragão G.M.F., 2009. Recovery of P(3HB) produced by *Ralstonia eutropha* by solvent extraction with propylene carbonate. Eng. Life Sci. 9(6), 454-461.

Follonier, S., Goyder. M.S., Silvestri. A.C., Crelier. S., Kalman. F., Riesen. R., Zinn. M., 2014. Fruit pomace and waste frying oil as sustainable resources for the bioproduction of medium-chain-length polyhydroxyalkanoates. Int. J. Biol. Macromol, 71. 42–52.

Freitas F., Alves V.D., Pais J., Costa N., Oliveira C., Mafra L., Hilliou L., Oliveira R., Reis M.A.M., 2009. Characterization of an extracellular polysaccharide produced by a Pseudomonas strain grown on glycerol. Biores. Technol. 100, 859-865.

Füchtenbusch, B., Wullbrandt, D., c, A., 2000. Production of polyhydroxyalkanoic acids by *Ralstonia eutropha* and *Pseudomonas oleovorans* from an oil remaining from biotechnological rhamnose production. Appl. Microbiol. Biotechnol. 53, 167–172.

Fukui, T., Abe, H., Doi, Y., 2002. Engineering of *Ralstonia eutropha* for production of poly(3-hydroxybutyrate-co-3-hydroxyhexanoate) from fructose and solid-state properties of the copolymer. Biomacromolecules 3, 618–624.

Fukui, T., Doi, Y., 1998. Efficient production of polyhydroxyalkanoates from plant oils by *Alcaligenes eutrophus* and its recombinant strain. Appl. Microbiol. Biotechnol. 49, 333–336.

García, I.L., López, J. a., Dorado, M.P., Kopsahelis, N., Alexandri, M., Papanikolaou, S., Villar, M. A., Koutinas, A.A., 2013. Evaluation of by-products from the biodiesel industry as fermentation feedstock for poly(3-hydroxybutyrate-co-3-hydroxyvalerate) production by *Cupriavidus necator*. Bioresour. Technol. 130, 16–22.

Gebauer, B., Jendrossek, D., 2006. Assay of Poly(3-Hydroxybutyrate) Depolymerase Activity and Product Determination App. Environ. Micorb., 72(9), 6094–6100.

Geladi, P., Kowalski, B.R., 1986. Partial least-squares regression - a tutorial. Anal. Chim. Acta 185, 1-17.

Goldfeld, M., Christensen, J., Pollard, D., Gibson, E.R., Olesberg, J.T., Koerperick, E.J., Lanz, K., Small, G.W., Arnold, M.A., Evans, C.E., 2014 Advanced near-infrared monitor for stable real-time measurement and control of Pichia pastoris bioprocesses. Biotechnol. Prog. 30, 749-759.

Gonzaléz-Contreras, M., Anaya-Reza, O., Sales-Cruz, M., Lopez-Arenas., T., 2015. Dynamics and operation analysis of the PHB (polyhydroxybutyrate) fermentation, Krist V. Germaey, Jakob K. Huusom and Rafiqul Gani (Eds.), 12th International Symposium on Process Systems Engineering and 25th European Symposium on Computer Aided Process Enginnering.

Graham, L.D., Glattauer, V., Huson, M.G., Maxwell, J.M., Knott, R.B., White, J.W., Vaughan, P.R., Peng, Y., Tyler, M.J., Werkmeister, J. a., Ramshaw, J. A., 2005. Characterization of a protein-based adhesive elastomer secreted by the Australian frog Notadenbennetti. Biomacromolecules6, 3300–3312.

Gunawan, S., Ju. Y.-H., 2009. Vegetable oil deodorizer distillate: Characterization, utilization and analysis. Sep. Purif. Rev. 38(3), 207-241.

Hall, J.W., McNeil, B., Rollins, M.J., Draper, I., Thompson, B.G., Macaloney, G., 1996. Near-infrared spectroscopic determination of acetate, ammonium, biomass, and glycerol in an industrial *Escherichia coli* fermentation. Appl. Spectrosc. 50, 102-108.

Hassan, M.A., Yee, L.N., Yee, P.L., Ariffin, H., Raha, A.R., Shirai, Y., Sudesh, K., 2013. Sustainable production of polyhydroxyalkanoates from renewable oil-palm biomass. Biomass and Bioenergy 50, 1–9.

Hazer, B., Torul. O., Borcakli. M., Lenz. R.W., Fuller. R.C., Goodwin. S.D., 1998. Bacterial production of polyesters from free fatty acids obtained from natural oils by *Pseudomonas oleovorans*. J. Environ. Pol. Deg. 6(2).109-113.

Heinrich, D., Madkour, M.H., Al-Ghamdi, M. a, Shabbaj, I.I., Steinbüchel, A., 2012. Large scale extraction of poly(3-hydroxybutyrate) from *Ralstonia eutropha* H16 using sodium hypochlorite. AMB Express 2, 59.

Hillairet, F., Borovska, H., 2011. Double counting: the impact. Biofuels international, 9:5

Huang, J., Li, K., 2008. A new soy flour-based adhesive for making interior type II plywood. JAOCS, J. Am. Oil Chem. Soc. 85, 63–70.

Huijberts, G.N.M., Eggink, G., 1996. Production of poly(3-hydroxyalkanoates) by *Pseudomonas putida* KT2442 in continuous cultures. Appl. Microbiol. Biotechnol. 46, 233–239.

Huschner, F., Grousseau, E., Brigham, C.J., Plassmeier, J., Popovic, M., Rha, C., Sinskey, A.J., 2015. Development of a feeding strategy for high cell and PHA density fed-batch fermentation of *Ralstonia eutropha* H16 from organic acids and their salts. Process Biochem. 50, 165–172.

Jain, R., Kosta, S., Tiwari, A., 2010. Polyhydroxyalkanoates : A way to sustainable development of bioplastics. Chronicles Young Sci. 1, 10–15.

Jain, R., Tiwari, A., 2014. Homology modelling of PHA synthases in *Cupriavidus necator*. International Journal of Universal Pharmacy and Bio Sciences 3(3):214-223

Jamshidian, M., Tehrany, E.A., Imran, M., Jacquot, M., Desobry, S., 2010. Poly-Lactic Acid: Production, applications, nanocomposites, and release studies. Compr. Rev. Food Sci. Food Saf. 9, 552–571.

Jolliffe, I.T., 2002. Principal Component Analysis, Second ed. Springer-Verlag, New York.

Kabe, T., Tsuge, T., Kasuya, K., Takemura, A., Hikima, T., Takata, M., Iwata, T., 2012. Physical and Structural Effects of Adding Ultrahigh-Molecular- Weight Poly[(R)-3-hydroxybutyrate] to Wild-Type Poly[(R)-3-hydroxybutyrate]. Macromolecules , 45, 1858−1865.

Kahar, P., Tsuge, T., Taguchi, K., Doi, Y., 2004 High yield production of polyhydroxyalkanoates from soybean oil by *Ralstonia eutropha* and its recombinant strain. Polym. Degrad. Stabil. 83, 79-86.

Kamilah, H., Tsuge, T., Yang, T.A., Sudesh, K., 2013 Waste cooking oil as substrate for biosynthesis of poly(3-hydroxybutyrate) and poly(3-hydroxybutyrate-co-3-hydroxyhexanoate): Turning waste into a value-added product. Malaysian Journal of Microbiology 9, 51-59.

Kathiraser, Y., Kheireddine M., Aroua, Ramachandran, K.B. and Tan I.K.P., 2007. Chemical characterization of medium-chain-length polyhydroxyalkanoates (PHAs) recovered by enzymatic treatment and ultrafiltration. ChemTechnol Biotechnol 82, 847–855.

Kaur, G., Roy, I., 2015. Strategies for Large-scale Production of Polyhydroxyalkanoates. Chem. Biochem. Eng. Q. 29, 157–172.

Keshavarz, T., Roy, I., 2010. Polyhydroxyalkanoates: bioplastics with a green agenda. Curr. Opin. Microbiol. 13, 321–326.

Kim, D.Y., Kim, H.W., Chung, M.G., Rhee, Y.H., 2007. Biosynthesis, modification, and biodegradation of bacterial medium-chain-length polyhydroxyalkanoates. J. Microbiol. 45, 87–97.

Kim, J.S., Lee, B.H., Kim, B.S., 2005. Production of poly(3-hydroxybutyrate-co-4-hydroxybutyrate) by *Ralstonia eutropha*. Biochem. Eng. J. 23, 169–174. doi:10.1016/j.bej.2005.01.016

Kim. J.T., Netravali, A.N., 2013. Performance of protein-based wood bioadhesives and development of small-scale test method for characterizing properties of adhesive-bonded wood specimens. J. Adhes. Sci. Technol. 27, 2083–2093.

Koller M, Braunegg G. 2015. Biomediated production of structurally diverse poly(hydroxyalkanoates) from surplus streams of the animal processing industry. Polimery 2015;60(5).

Koller M, Salerno A, Strohmeier K, Schober S, Mittelbach M, Illieva V, Chiellini E, Braunegg G. 2014. Novel precursors for production of 3-hydroxyvalerate-containing poly [(R)-hydroxyalkanoate]s. Biocatal Biotransf, 32(3):161-167.

Koller, M., Salerno, A., Dias, M., Reiterer, A., Braunegg, G., 2010. Modern biotechnological polymer synthesis: A review. Food Technol. Biotechnol. 48, 255–269.

Kondamudi N., Mohapatra S.K., Misra M., 2008. Spent Coffee Grounds as a Versatile Source of Green Energy. J. Agric. Food Chem. 56, 11757–11760.

Kunasundari, B., Sudesh, K., 2011. Isolation and recovery of microbial polyhydroxyalkanoates. Express Polym. Lett. 5, 620–634.

Lageveen, R.G., Huisman, G.W., Preusting, H., Ketelaar, P., Eggink, G., Witholt, B., 1988. Formation of Polyesters by *Pseudomonas oleovorans*: Effect of Substrates on Formation and Composition of Poly-(R)-3-Hydroxyalkanoates and Poly-(R)-3-Hydroxyalkenoates. Appl. Environ. Microbiol. 54, 2924–2932.

Landrock, A. Adhesives Technology Handbook. 2008, Ed. Sina Ebnesajjad, William Andrew, 4, 47-48.

Laycock, B., Halley, P., Pratt, S., Werker, A., Lant, P., 2013 The chemomechanical properties of microbial polyhydroxyalkanoates. Prog. Polym. Sci. 38, 536-583.

Le Meur, S., Zinn, M., Egli, T., Thöny-Meyer, L., Ren, Q., 2012. Production of medium-chain-length polyhydroxyalkanoates by sequential feeding of xylose and octanoic acid in engineered Pseudomonas putida KT2440. BMC Biotechnol. 12, 53.

Lee, J., Lee, S.Y., Park, S., Middelberg, A.P.J., 1999. Control of fed-batch fermentations. Biotechnol. Adv. 17, 29–48.

Lee, J.H., Hong, J., Lim, H.C., 1997. Experimental optimization of fed-batch culture for poly-beta-hydroxybutyric acid production. Biotechnol. Bioeng. 56, 697–705.

Lee, S.Y., Choi, J.I., 2001. Production of microbial polyester by fermentation of recombinant microorganisms. Adv. Biochem. Eng. Biotechnol. 71, 183–207.

Lee, W.H., Loo, C.Y., Nomura, C.T., Sudesh, K., 2008. Biosynthesis of polyhydroxyalkanoate copolymers from mixtures of plant oils and 3-hydroxyvalerate precursors. Bioresour. Technol. 99, 6844–6851.

Lemoigne, M., 1926. Produits de déshydration et de polymérisation de l'acide β-oxobutyrique. Bull. Soc. Chem. Biol. 8: 770–782.

Lepage G, Roy CC. 1986 Direct transesterification of all classes of lipids in a one-step reaction. J Lipid Research;27:114–20.

Liu, Q., Luo, G., Zhou, X.R., Chen, G.Q., 2011. Biosynthesis of poly(3-hydroxydecanoate) and 3-hydroxydodecanoate dominating polyhydroxyalkanoates by b-oxidation pathway inhibited Pseudomonas putida. Metab. Eng. 13, 11–17.

Liu, Y., Li, K., 2007. Development and characterization of adhesives from soy protein for bonding wood. Int. J. Adhes. Adhes. 27, 59–67.

Lo, K. W., Chua, H., Lawford, H., Lo, W. H., Yu, P. H. F., 2005. Effects of fatty acids on growth and poly-3-hydroxybutyrate production in bacteria. Appl. Biochem.Biotechnol.122(1-3),575-580.

López-Cuellar, M.R., Alba-Flores, J., Rodríguez, J.N.G., Pérez-Guevara, F., 2011. Production of polyhydroxyalkanoates (PHAs) with canola oil as carbon source. Int. J. Biol. Macromol. 48, 74–80.

Lourenço, N.D., Lopes, J.A., Almeida, C.F., Sarraguça, M.C., Pinheiro, H.M., 2012 Bioreactor monitoring with spectroscopy and chemometrics: a review. Anal. Bioanal. Chem. 404, 1211-1237.

Lu, J., Tappel, R.C., Nomura, C.T., 2009. Mini-Review: Biosynthesis of Poly(hydroxyalkanoates). Polym. Rev. 49, 226–248.

Lunt, J., 2014. Marketplace Opportunities for Integration of Biobased and Conventional Plastics.

Martens, H., Naes, T., 1996. Multivariate calibration. John Wiley and Sons Chichester.

Martino, L., Cruz, M.V., Scoma, A., Freitas, F., Bertin, L., Scandola, M., Reis, M.A.M., 2014 Recovery of amorphous polyhydroxybutyrate granules from *Cupriavidus necator* cells grown on used cooking oil. Int. J. Biol. Macromol., 71, 117-123.

Mohammadi, M., Hassan, M.A., Shirai, Y., Man, H.C., Ariffin, H., Yee, L.-N., Mumtaz, T., Chong, M.-L., Phang, L.-Y., 2012. sp. EB172 by Simple Digestion with Sodium Hydroxide. Sep. Sci. Technol. 47, 534–541.

Morais, C., Freitas.F., Cruz, M. V., Paiva, A., Dionísio, M., Reis, M.A.M., 2014. Conversion of fat-containing waste from the margarine manufacturing process into bacterial polyhydroxyalkanoates. Int. J. Biol. Macromol. 71, 68–73.

Mozumder, M.S.I., De Wever, H., Volcke, E.I.P., Garcia-Gonzalez, L., 2014. A robust fed-batch feeding strategy independent of the carbon source for optimal polyhydroxybutyrate production. Process Biochem. 49, 365–373.

Muhr, A., Rechberger, E.M., Salerno, A., Reiterer, A., Schiller, M., Kwiecień, M., Adamus, G., Kowalczuk, M., Strohmeier, K., Schober, S., Mittelbach, M., Koller, M., 2013. Biodegradable latexes from animal-derived waste: Biosynthesis and characterization of mcl-PHA accumulated by *Ps. citronellolis*. React. Funct. Polym. 73, 1391–1398.

Næs, T., Isaksson, T., Fearn, T., Davies, T., 2002. A User-Friendly Guide to Multivariate Calibration and Classification. NIR Publications, Chichester.

Nanda MR, Yuan Z, Qin W, Poirier MA, Chunbao X. 2015. Purification of Crude Glycerol using Acidification : Effects of Acid Types and Product Characterization. Austin J Chem Eng;1:1–7.

Navrátil, M., Norberg, A., Lembren, L., Mandenius, C.F., 2005. On-line multi-analyzer monitoring of biomass, glucose and acetate for growth rate control of a Vibrio cholerae fed-batch cultivation. J. Biotechnol. 115, 67-79.

Nerkar, M., Ramsay, J. A.,Ramsay, B. A.,Vasileiou, A. A., Kontopoulou, M.,2015. Improvements in the melt and solid-state properties of poly(lactic acid), poly-3-hydroxyoctanoate and their blends through reactive modification. Polymer64(1),51-61.

Ng, K.S., Ooi, W.Y., Goh, L.K., Shenbagarathai, R., Sudesh, K., 2010 Evaluation of jatropha oil to produce poly(3-hydroxybutyrate) by *Cupriavidus necator* H16. Polym. Degrad. Stabil. 95, 1365-1369.

Noda, I., Lindsey S.B., Caraway D., 2010. Nodax™ Class PHA Copolymers: Their Properties and Applications. G.-Q. Chen (ed.), Plastics from Bacteria: Natural Functions and Applications, Microbiology Monographs, Vol. 14.

Noureddini, H., Teoh, B.C., Davis Clements, L., 1992. Viscosities of vegetable oils and fatty acids. J. Am. Oil Chem. Soc. 69, 1189–1191.

Obruca S., Marova I., Snajdar O., Mravcova L., Svoboda Z., 2010.Production of poly(3-hydroxybutyrate-co-3-hydroxyvalerate) by *Cupriavidus necator* from waste rapeseed oil using propanol as a precursor of 3-hydroxyvalerate.Biotechnol. Lett. 32, 1925–1932.

Obruca, S., 2015. Use of Lignocellulosic Materials for PHA Production. Chem. Biochem. Eng. Q. 29, 135–144.

Obruca, S., Benesova, P., Oborna, J., Marova, I., 2014a. Application of protease-hydrolyzed whey as a complex nitrogen source to increase poly(3-hydroxybutyrate) production from oils by *Cupriavidus necator* 775–781.

Obruca, S., Petrik, S., Benesova, P., Svoboda, Z., Eremka, L., Marova, I., 2014b. Utilization of oil extracted from spent coffee grounds for sustainable production of polyhydroxyalkanoates. Appl. Microbiol. Biotechnol. 98, 5883–5890.

Ostle, A.G., Holt, J.G., 1982. Fluorescent Stain for Poly-3- Hydroxybutyrate. Appl. Environ. Microbiol. 44, 238–241.

Pandey, J., 2015. Bioplastics : Need for the future 2, 6–11.

Park, D.H., Kim, B.S., 2011. Production of poly(3-hydroxybutyrate) and poly(3-hydroxybutyrate-co-4-hydroxybutyrate) by *Ralstonia eutropha* from soybean oil. New Biotechnol. 28 (6), 719-724.

Park, S.J., Jang, Y.-A., Noh, W., Oh, Y.H., Lee, H., David, Y., Baylon, M.G., Shin, J., Yang, J.E., Choi, S.Y., Lee, S.H., Lee, S.Y., 2015. Metabolic engineering of *Ralstonia eutropha* for the production of polyhydroxyalkanoates from sucrose. Biotechnol. Bioeng. 112, 638–643.

Partovi, M., Lotfabad, T.B., Roostaazad, R., Bahmaei M.,Tayyeby, S., 2013. Management of soybean oil refinery wastes through recycling them for producing biosurfactant using *Pseudomonas aeruginosa* MR01. World J. Microbiol. Biotechnol, 29, 1039-1047.

Peña, C., Castillo, T., García, a., Millán, M., Segura, D., 2014. Biotechnological strategies to improve production of microbial poly-(3-hydroxybutyrate): A review of recent research work. Microb. Biotechnol. 7, 278–293.

Philip, S.; Keshavarz, T.; Roy, I., 2007. Polyhydroxyalkanoates: Biodegradable polymers with a range of applications. J. Chem. Technol. Biotechnol., 82, 233–247.

Rai, R., Keshavarz, T., Roether, J. A, Boccaccini, A. R., Roy, I., 2011a. Medium chain length polyhydroxyalkanoates, promising new biomedical materials for the future. Mater. Sci. Eng. R Reports 72, 29–47.

Rai, R., Yunos, D.M., Boccaccini, A.R., Knowles, J.C., Barker, I. A., Howdle, S.M., Tredwell, G.D., Keshavarz, T., Roy, I., 2011b. Poly-3-hydroxyoctanoate P(3HO), a medium chain length polyhydroxyalkanoate homopolymer from *Pseudomonas mendocina*. Biomacromolecules 12, 2126–2136.

Ramsay, J. A., Berger, E., Voyer, R., Chavarie, C., Ramsay, B. A., 1994. Extraction of poly-3-hydroxybutyrate using chlorinated solvents. Biotechnol. Tech. 8, 589–594.

Rao, U., Sridhar, R., Sehgal, P.K., 2010. Biosynthesis and biocompatibility of poly(3-hydroxybutyrate-co-4-hydroxybutyrate) produced by *Cupriavidus necator* from spent palm oil. Biochem. Eng. J. 49, 13-20.

Rathinasabapathy, A., Ramsay, B. a, Ramsay, J. a, Pérez-Guevara, F., 2014. A feeding strategy for incorporation of canola derived medium-chain-length monomers into the PHA produced by wild-type *Cupriavidus necator*. World J. Microbiol. Biotechnol. 30, 1409–16.

Reddy, R.L., Reddy, V.S., Gupta, G.A., 2013. Study of Bio-plastics As Green & Sustainable Alternative to Plastics. Int. J. Emerg. Technol. Adv. Eng. 3, 82–89.

Rocha, Â., Lourenço, N.M.T., Vidinha, P., Simões, P., Paiva, A., 2014. Separation of free fatty acids from deodorizer distillates using choline hydrogen carbonate and supercritical carbon dioxide. Sep. Purif. Technol. 131, 14–18.

Roychoudhury, P., O'Kennedy, R., McNeil, B., Harvey, L.M., 2007. Multiplexing fibre optic near infrared (NIR) spectroscopy as an emerging technology to monitor industrial bioprocesses. Anal. Chim. Acta 590, 110-117.

Rydz, J., Sikorska, W., Kyulavska, M., Christova, D., 2014. Polyester-Based (Bio)degradable Polymers as Environmentally Friendly Materials for Sustainable Development. Int. J. Mol. Sci. 16, 564–596.

Rydz, J.; Zawidlak-Węgrzyńska, B.; Christova D. Degradable polymers. 2015. In *Encyclopedia of Biomedical Polymers and Polymeric Biomaterials*; Mishra, M.K., Ed.; CRC Press: Boca Ratón,FL, USA.

Sathiyanarayanan, G., Saibaba, G., Seghal Kiran, G., Selvin, J., 2013. A statistical approach for optimization of polyhydroxybutyrate production by marine *Bacillus subtilis* MSBN17. Int. J. Biol. Macromol. 59, 170–177.

Savitzky, A., Golay, M.J.E., 1964. Smoothing Differentiation of Data by Simplified Least Squares Procedures. Anal. Chem. 36, 1627-&.

Shamala, T.R., Vijayendra, S.V.N., Joshi, G.J., 2012. Agro-industrial residues and starch for growth and co-production of polyhydroxyalkanoate copolymer and a-amylase by bacillus SP. CFR-67. Brazilian J. Microbiol. 43, 1094–1102.

Shawaphun, S., Manangan, T., 2009. Study of extraction process and characterization of poly-3-hydroxyalkanoate produced from *Alcaligenes latus*. 3rd Int. Conf. Ferment. Technol. Value Added Agric. Prod. 1–9.

Siracusa, V., Rocculi, P., Romani, S., Rosa, M.D., 2008. Biodegradable polymers for food packaging: a review. Trends Food Sci. Technol. 19, 634–643. doi:10.1016/j.tifs.2008.07.003

Srivastava, S.K., Tripathi, A.D., 2013. Effect of saturated and unsaturated fatty acid supplementation on bio-plastic production under submerged fermentation. Biotech 3, 389–397.

Strayer, D., 2006. Institute of Shortening and Edible Oils (ISEO). Food fats and oils. 9th edition. New York: 44.

Sudesh, K., Abe, H., Doi, Y., 2000. Synthesis, structure and properties of polyhydroxyalkanoates: Biological polyesters. Prog. Polym. Sci. 25, 1503–1555.

Suehara, K.I., Yano, T., 2004. Bioprocess monitoring using near-infrared spectroscopy. Recent Progress of Biochemical and Biomedical Engineering in Japan I, 173-198.

Sukan, A., Roy, I., Keshavarz, T., 2014. Agro-Industrial Waste Materials as Substrates for the Production of Poly (3-Hydroxybutyric Acid) 229–240.

Sun, Z., Ramsay, J. a., Guay, M., Ramsay, B. a., 2006. Automated feeding strategies for high-cell-density fed-batch cultivation of *Pseudomonas putida* KT2440. Appl. Microbiol. Biotechnol. 71, 423–431.

Sun, Z., Ramsay, J. A., Guay, M., Ramsay, B. A., 2007. Carbon-limited fed-batch production of medium-chain-length polyhydroxyalkanoates from nonanoic acid by *Pseudomonas putida* KT2440. Appl. Microbiol. Biotechnol. 74, 69–77.

Tamburini, E., Vaccari, G., Tosi, S., Trilli, A., 2003. Near-infrared spectroscopy: A tool for monitoring submerged fermentation processes using an immersion optical-fiber probe. Appl. Spectrosc. 57, 132-138.

Tan, G.Y.A., Chen, C.L., Li, L., Ge, L., Wang, L., Razaad, I.M.N., Li, Y., Zhao, L., Mo, Y., Wang, J.Y., 2014. Start a research on biopolymer polyhydroxyalkanoate (PHA): A review. Polymers (Basel). 6, 706–754.

Taniguchi, I., Kagotani, K., Kimura, Y., 2003. Microbial production of poly(hydroxyalkanoate)s from waste edible oils. Presented at The First International Conference on Green & Sustainable Chemistry, Tokyo, Japan. Green Chem. 5, 545.

Teixeira, A.R.S., Santos, J.L.C., Crespo, J.G., 2011. Production of Steryl Esters from Vegetable Oil Deodorizer Distillates by Enzymatic Esterification 2865–2875.

Thakor N, Trivedi U, Patel KC., 2005. Biosynthesis of medium chain length poly(3-hydroxyalkanoates) (mcl-PHAs) by *Comamonas testosteroni* during cultivation on vegetable oils. Bioresour Technol, 96:1843–50.

Tian, J., Sinskey, A.J., Stubbe, J., 2005. Kinetic Studies of Polyhydroxybutyrate Granule Formation in Wautersia eutropha H16 by Transmission Electron Microscopy Kinetic Studies of Polyhydroxybutyrate Granule Formation in Wautersia eutropha H16 by Transmission Electron Microscopy. Society 187, 3814–3824. doi:10.1128/JB.187.11.3814

Tokimoto T., Kawasaki N., Nakamura T., Akutagawa J., Tanada S.,2005. Removal of lead ions in drinking water by coffee grounds as vegetable biomass.J. Coll.Interface Sci. 281, 56–61.

Toop, G., Alberici, S., Spoettle, M., van Steen, H., 2013. Trends in the UCO market Trends 31.

Top A.G.M., 2010, Production and utilization of palm fatty acid distillate (PFAD). Lipid Technol, 22:11–3.

Torró-Palau, A. M., Fernández-García, J. C., Orgilés-Barceló, A. C., Martín-Martínez, J. M., 2001. Characterization of polyurethanes containing different silicas, Int. J. Adhesion Adhesives 21(1), Pages 1-9

Tosi, S., Rossi, M., Tamburini, E., Vaccari, G., Amaretti, A., Matteuzzi, D., 2003 Assessment of in-line near-infrared spectroscopy for continuous monitoring of fermentation processes. Biotechnol. Prog. 19, 1816-1821.

Tripathi, A.D., Srivastava, S.K., Singh, R.P., 2013. Statistical optimization of physical process variables for bio-plastic (PHB) production by *Alcaligenes sp*. Biomass and Bioenergy 55, 243–250. doi:10.1016/j.biombioe.2013.02.017

Verleyen, T., Verhe, R., Garcia, L., Dewettinck, K., Huyghebaert, A., De Greyt, W., 2001. Gas chromatographic characterization of vegetable oil deodorization distillate. J. Chromatogr. A 921, 277–285.

Verlinden RA, Hill DJ, Kenward M A, Williams CD, Piotrowska-Seget Z, Radecka IK., 2011. Production of polyhydroxyalkanoates from waste frying oil by *Cupriavidus necator*. AMB Express, 1:11.

Verlinden, R.A. J., Hill, D.J., Kenward, M. A., Williams, C.D., Radecka, I., 2007. Bacterial synthesis of biodegradable polyhydroxyalkanoates. J. Appl. Microbiol. 102, 1437–1449.

Volova, T.G., Zhila, N.O., Kalacheva, G.S., Brigham, C.J., Sinskey, A.J., 2013. Effects of intracellular poly(3-hydroxybutyrate) reserves on physiological-biochemical properties and growth of Ralstonia eutropha. Res. Microbiol. 164, 164–171.

Wang, F., Lee, S.Y., 1997. Poly (3-Hydroxybutyrate) Production with High Productivity and High Polymer Content by a Fed-Batch Culture of *Alcaligenes latus* under Nitrogen Limitation . Poly(3-Hydroxybutyrate) Production with High Productivity and High Polymer Content by a Fed-Ba 63, 3703–3706.

Wong, Y.M., Brigham, C.J., Rha, C., Sinskey, A.J., Sudesh, K., 2012. Biosynthesis and characterization of polyhydroxyalkanoate containing high 3-hydroxyhexanoate monomer fraction from crude palm kernel oil by recombinant *Cupriavidus necator*. Bioresour. Technol. 121, 320–327.

Yamane, T., Chen, X.F., Ueda, S., 1996. Polyhydroxyalkanoate synthesis from alcohols during the growth of Paracoccus denitrificans. FEMS Microbiol. Lett. 135, 207–211.

Zinn, M., Witholt, B., Egli, T., 2001. Occurrence, synthesis and medical application of bacterial polyhydroxyalkanoate. Adv. Drug Deliv. Rev. 53, 5–21.